

A STUDY OF THE STABILITIES
OF NEGATIVE IONS

BY

GILLIAN C. GOODE

A thesis submitted for the
degree of Doctor of Philosophy
in the Department of Chemistry
of the University of Aston in
Birmingham. August, 1969.

THE UNIVERSITY
OF ASTON IN
BIRMINGHAM.
LIBRARY

19 DEC 1969

124042

541.132

900

SUMMARY

The Magnetron technique, which had been developed for the measurement of electron affinities from observations on the equilibrium between neutrals, electrons and ions at a heated metal surface, was applied to the measurement of electron affinities of both radicals and molecules.

A series of metal hexafluorides was studied, which showed that they captured electrons directly to form negative ions of the type MF_6^- . The relative electron affinities of these compounds were shown to be consistent with their relative oxidising powers.

Electron capture by the radicals $C_2H.$, $CF_3.$, $SiF_3.$, $R_1R_2N.$ and $R_1R_2P.$, (where R_1 and R_2 can be phenyl (Ph), methyl (Me) or hydrogen (H)), was studied to determine the effect the nature of the centre of acceptance and substitution at this centre had upon the electron affinity of the radical. The additional electron was shown to be localised as a lone pair on the atomic centre where the free valence lay, and the experimental electron affinity was compared to the calculated electron affinity of the atomic centre, in the same valence state, as given by the method of Hinze and Jaffe.

The disadvantage of the Magnetron technique lay in the fact that the identification of the ions was only indirect and, therefore complex reactions, which gave rise to similar numbers of ions of differing mass, could have been misinterpreted in terms of a simple reaction. To overcome this a surface ionisation source was attached to an Atlas AMP 3 Quadrupole Mass Filter, which enabled direct identification of the ions to be made along with the usual Magnetron type measurements.

This work was carried out between November 1965 and October 1968 at the University of Aston in Birmingham. It has been done independently, and has not been submitted for any other degree.

G. C. Goode.

G. C. GOODE.

ACKNOWLEDGEMENTS

I wish to express my gratitude to Professor F.M. Page for his supervision and encouragement during the past three years.

I would also like to thank Mr. R.E.K. Rackwitz for his valuable advice, and the United States Army and the Central Electricity Generating Board for financial support of this research.

"The Road goes ever on and on
Down from the door where it began.
Now far ahead the Road has gone,
And I must follow if I can,
Pursuing it with eager feet,
Until it joins some larger way
Where many paths and errands meet
And whither then? I cannot say."

J.R.R. Tolkien
"The Lord of the Rings."

C O N T E N T S

	<u>Page</u>
1. Introduction	
1.1. Introduction	1
1.2. The occurrence of Negative Ions	2
1.3. The determination of the Stability of Negative Ions	5
2. The Apparatus	
2.1. The Theory of the Magnetron	22
2.2. The design of the Apparatus	24
2.3. The measurement of temperature	26
2.4. Operation of the Apparatus	27
3. Theoretical considerations of electron and negative ion emission	
3.1. Introduction	29
3.2. The Application of the Theory of Rate Processes to the thermal emission of electrons and negative ions.	
3.2.1. Introduction	30
3.2.2. The emission of electrons	31
3.2.3. The emission of negative ions	34
3.2.4. Evaluation of Q/Q_i and temperature correction to 0°K	37
3.2.5. Evaluation of the Electron Affinity from log-log plots	42
3.2.6. The Entropy of the reaction	42
4. Polarisation Capture Affinities	
4.1. Introduction	44
4.2. Experimental	45
4.3. Discussion	46
5. σ Capture Affinities	
5.1. Introduction	55
5.2. Electron Capture by Acetylene	
5.2.1. Introduction	60
5.2.2. Experimental	60
5.2.3. Discussion	61

5.3.	Electron Capture by CF_3 and SiF_3 .							
5.3.1.	Introduction..	68	
5.3.2.	Experimental	69	
5.3.3.	Discussion	71	
5.4.	Electron Capture by NH_2 , PH_2 , R_1R_2N and R_1R_2P .							
5.4.1.	Introduction	78	
5.4.2.	Experimental	81	
5.4.3.	Discussion							
	5.4.3.1.	Electron Capture by R_1R_2N	86	
	5.4.3.2.	Electron Capture by R_1R_2P	96	
5.5.	Experimental and Predicted electron affinities							97
6.	The identification of negative ions using a Quadrupole Mass Filter							
6.1.	Introduction	105	
6.2.	Experimental	106	
6.3.	Results	111	
6.4.	Discussion	112	
6.5.	Conclusions	114	
References	115	

<u>Figure</u>	<u>Between Pages</u>
1. The forces acting upon an electron in a cylindrical magnetron	22-23
2. Effect of magnet current on anode current	24-25
3. Magnetron and Grid Assembly	24-25
4. Layout of the Apparatus	25-26
5. Circuit Diagram	25-26
6. Filament temperature calibration	26-27
7. Potential energy diagram for reaction	30-31
8. Potential energy barrier to electron emission	31-32
9. Electron capture by TeF_6/Pt	45-46
10. Electron capture by WF_6/Pt	46-47
11. Electron capture by UF_6/Pt	46-47
12. Resonance states of CCl_4^-	47-48
13. Interaction between Cl^- and the C-Cl bond in CCl_4^-	48
14. Electron work function for W and $\text{C}_2\text{H}_2/\text{W}$	60-61
15. Electron capture by $\text{C}_2\text{H}_2/\text{W}$	61-62
16. Electron capture by $\text{CF}_3\text{H}/\text{Pt}$	69-70
17. Electron capture by $\text{C}_2\text{F}_6/\text{Ir}$	70-71
18. Electron capture by CF_4/Pt	70-71
19. Electron capture by $\text{CF}_3\text{Br}/\text{Pt}$	71-72
20. Electron capture by $\text{CF}_3\text{Cl}/\text{Ir}$	71-72
21. Electron capture by SiF_4/Pt	71-72
22. Electron capture by $(\text{Ph} \text{---} \text{N})_2/\text{W}$	81-82
23. Electron capture by $(\text{Ph} \text{---} \text{N})_2/\text{W}$	82-83

<u>Figure</u>		<u>Between Pages</u>
24	Electron Capture by $(\begin{smallmatrix} \text{Ph} \\ \text{Me} \end{smallmatrix} \text{N-N})_2/\text{W}$	82-83
25.	Electron Capture by $(\begin{smallmatrix} \text{Me} \\ \text{Me} \end{smallmatrix} \text{N-N})_2/\text{W}$	83-84
26a.	Electron Capture by PhNH_2/Ir	83-84
26b.	Electron work function for PhNH_2/Ir	83-84
27.	Electron capture by $\text{C}_6\text{F}_5\text{NH}_2/\text{Ir}$	83-84
28a.	Electron capture by $\text{Ph}_2\text{NH}/\text{Ir}$	84-85
28b.	Electron work function for $\text{Ph}_2\text{NH}/\text{Ir}$	84-85
29.	Electron capture by PhMeNH/Ir	84-85
30.	Electron capture by $\text{Me}_2\text{NH}/\text{W}$	84-85
31.	Electron capture by $\text{P}_2\text{H}_4/\text{Pt}$	85-86
32.	Electron capture by PH_3/W	86-87
33.	Electron capture by $\text{Ph}_2\text{PH}/\text{Ir}$	86-87
34.	Promotion energies for various valence states of C and C^-	101-102
35.	Promotion energies for various valence states of Si and Si^-	101-102
36.	Promotion energies for various valence states of N and N^-	101-102
37.	Promotion energies for various valence states of P and P^-	101-102
38.	Quadrupole Mass Filter	106-107
39.	Ion source and filament circuit	107-108
40.	x,y,z axes of the quadrupole field	109-110
41.	Stability diagram for ion motion in the quadrupole field	109-110
42.	Electron capture by Br_2/W	112-113
43.	Electron capture by T.C.NE/Ir	112-113

<u>Table</u>		<u>Page</u>
1.	Electron Affinities of Atoms	10
2.	Comparison of calculated and experimental polarisation capture electron affinities	49
3.	Reaction products of MF ₆ with O ₂ , NO and ONF	52
4.	Summary of fluorocarbon results	77
5.	Electron Affinities of the amino radicals	89
6.	Bond dissociation energies of the first N-H bond in some substituted amines	90
7.	Electron Affinities and Base Strengths of some amines	91
8.	N-H bond dissociation energies of some amines from the literature	94
9.	Promotion Energies for various valence states of C, C ⁻ , Si and Si ⁻	99
10.	Promotion Energies for various valence states of N, N ⁻ , P and P ⁻	100
11.	Ground state electron affinities of C, N, Si, and P	101
12.	Comparison of predicted and experimental electron affinities	104

1. INTRODUCTION

1.1 Introduction

The conception of a negatively charged ion dates back to the ionic theory of electrolysis. In this theory a molecule XY is supposed to dissociate in solution to give ions X^+ and Y^- . The application of a potential difference then produces a drift of the positive ions X^+ to the cathode and of negative ions Y^- to the anode. The drift velocity of these ions in the field direction is so small however that the ions must be regarded as forming clusters of considerable size by solvation.

The study of the passage of electricity through gases showed that in this case also the carriers of negative charge were not by any means exclusively electrons, but often particles of molecular mass¹. Although the opportunities for cluster formation in a gaseous medium are much less than for electrolysis the negative-charge carriers in a gas, at not too low pressures ($> 10^{-2}$ Torr), may be complex. Hence when quantitative measurements are carried out the working pressure ^{must be} is low ($< 10^{-4}$ Torr,) where simple reactions predominate. The most fruitful source of knowledge at first was the mass spectrograph used by J. J. Thomson² to identify a number of simple negatively charged molecules and atoms, and the study of the diffusion of ions in gases, carried out by Townsend et al¹, provided further information of a semi-quantitative nature. The recent spectroscopic techniques of Branscomb et al^{3,4,5,6}, and Berry et al⁷ have given very accurate quantitative information about negative ions but have in the main been applied to atomic ions. Also various calculations and extrapolation methods have successfully given values for the stabilities of negative ions

but again have been almost exclusively carried out for atomic ions.

Recently a great deal of qualitative work has been done on molecular ions by mainly mass spectrometric techniques, but quantitative measurements are still very meagre and often contradictory.

1.2 The occurrence of Negative Ions

An understanding of the stability of negative ions is important in many fields of research, particularly in flame chemistry, astrophysics and studies of the ionosphere.

Since the discovery of the ionized layers in the upper atmosphere physicists have been interested in their properties and composition. The proportion of negative charge in an ionized layer, which is present in the form of negative ions, depends on the balance between the rates of formation and destruction of these ions. During the daytime photo-detachment by the sun's radiation causes the concentration of negative ions to be very small. However at night this source of detachment is absent and particularly in the E layer, where the rate of attachment is high⁸, negative ions are present in quite large concentrations. The chief chemical constituents of the D and E layers are N_2 , O_2 and N_2 , O and possibly O_2 , respectively, resulting in the formation of O_2^- at the lowest layers and O^- , NO_2^- and NO_3^- at higher altitudes⁸. This has led to many experimental attempts to measure both the stability and the rate of formation of these ions^{4,9,10,11}.

One of the instances in which negative ions have played a decisive role in determining the nature of an observable phenomenon is that of the solar continuous spectrum. It has been shown that the absorption of negative hydrogen ions present in the solar photosphere determines

the spectral distribution in the visible region¹² and hence the apparent colour temperature of many of the stars¹³. In the atmospheres of certain cooler stars there appears to be a rather greater proportion of carbon than in other stars and it is possible that CN^- and C_2^- might be important in determining certain features of the emission spectra of these stars¹⁴, but it is difficult to make any estimate due to the uncertainty in the electron affinities.

One of the fields where a knowledge of the stability of negative ions is important is that of flame ionisation², due mainly to the interest in rocket propulsion and magnetohydrodynamic generation.

In rocket propulsion problems arise in the control of the rocket due to attenuation of the electro-magnetic signals by the electrons in the rocket flame. When an electro-magnetic wave passes through a partially ionised medium the electrons, due to their small mass, are excited into sympathetic oscillation; this directed momentum is rapidly lost by the electrons colliding with the gas molecules, hence the energy of the wave is degraded into the thermal energy of the gas. The attenuation may easily be controlled if the electrons are removed, which is done by introducing species into the flame that readily capture electrons, that is molecules with a high electron affinity.

The inverse of this problem occurs in magnetohydrodynamic generators where electricity is generated directly from a high velocity flame burning between the poles of a magnet. The flame can be thought of as being equivalent to the armature of a dynamo, where the electrical energy output is obtained at the expense of the thermal and kinetic energy of the flame gases, and it is essential that the conductivity of the

flame is high, that is a high concentration of free electrons must be present. Hence it is important to know the value of the electron affinities of all species present in the flame to assess the efficiency of an M.H.D. generator.

A knowledge of electron affinities is essential in the discussion of ionic-covalent resonance, for example if a molecule is considered to be a hybrid between covalent A-B and ionic A^+B^- , whilst it is possible to construct potential energy curves for both species the separation between the two curves, which is the important criterion in ionic-covalent resonance, depends directly on the values of the ionisation potential of A and the electron affinity of B.

Another case where the lack of electron affinity data is unfortunate is when the strengths of chemical bonds are considered in relation to the electronegativities of the bonded species. This arises as electronegativity is defined as a function of $\frac{1}{2} [I + E]$ where I and E are the ionisation potential and the electron affinity of the particle being considered¹⁵.

In the study of electro-chemical reactions both at ordinary and highly polarised electrodes, such as the polarograph^{16,17}, a knowledge of the stabilities of the negatively charged species produced is desirable. For example a quantitative study of the reduction potentials of neutral species in the polarograph gives a value for the change in energy, ΔE , for the overall reaction. As the reaction is carried out in solution ΔE contains solvation terms which are not in general known for negative ions. Hence a comparison of ΔE with the heat of the same reaction carried out in the gaseous phase, based upon measurements of

electron affinities in the gaseous phase, will give information about the heats of solvation of the ions concerned and ultimately a better understanding of electrode processes.

Finally a considerable amount of work has been done by Lovelock et al¹⁸ on the formation of negative ions by biologically active materials. The electron capture detector developed by this school was used, in conjunction with a gas chromatograph, to determine the relative reduction, produced by various materials, in the electron concentration of a radioactively generated plasma. The relative reduction in the electron concentration was found as expected to depend upon the electronegativity of the material, with a few exceptions, where anomalously high reductions occurred; these were almost always with compounds that had a high biological activity. Although it is not implied that the ability to capture electrons is a direct cause of biological activity, the results suggest that there is a close link between the two.

1.3 The determination of the Stability of Negative Ions

A measure of the stability of a negative ion X^- is given by the quantity known as the electron affinity of the parent molecule, radical or atom, X, which is defined to be,

$$E(X) = E_0 - E_- \quad 1.1$$

where E_0 and E_- are the energies of the ground states of the molecule, radical or atom and the negative ion, respectively; for a stable negative ion the electron affinity must be positive.

The static field of a neutral atom is by itself insufficient to bind an additional electron. However, as an electron approaches an atom the coulomb field of the electron induces dipole, quadr^uipole and

higher multipole moments in the atom, which results in an attractive potential having the asymptotic behaviour $\propto 1/r^4$ for large distances¹⁹, r , of the electron from the atomic nucleus, α being the dipole polarizability of the atom. In many cases, provided allowance is made for the effect of the Pauli exclusion principle, this polarization potential is sufficiently strong to bind the extra electron to the atom to produce a stable negative ion.

The Pauli exclusion principle states that two electrons with the same spin quantum numbers cannot have identical quantum numbers, so in the case of the inert gas atoms He, Ne, Ar, with completely filled 1s, 2p, 3p shells, respectively, any additional electron must go into a shell with a higher principal quantum number. Since the polarization field is not sufficiently strong to bind the extra electron in such an orbital, the resulting negative ion will be unstable. Whereas atoms like H, the alkali metals and the halogens, with a single electron absent from their outer s and p shells, respectively, will form stable negative ions.

If two electrons have the same spin quantum numbers they will tend to stay apart due to the exclusion principle. This results in the effective polarizability of the atom being increased, which results in a stronger binding than would have been expected. It follows that the greater the number of electrons in the outermost shell of the parent neutral atom having the same spin quantum number as the additional electron, the greater will be the energy of binding of the extra electron. For example, consider the negative ions Be^- , B^- , C^- , N^- , O^- , and F^- , where the ground energy state of the negative ions are taken

to be the same as for the neutral atoms B, C, N, O, F and Ne, that is $2p$, $2p^2$, $2p^3$, $2p^4$, $2p^5$, and $2p^6$, respectively, (Inner $1s^2$ and $2s^2$ shells have been omitted). As the ground state of the parent Be atom has completely filled $1s^2 2s^2$ shells but no $2p$ electron it seems probable that Be^- in the $2p$ state is unstable. In B there is a single $2p$ electron with the same spin quantum number as the additional $2p$ electron, while in C there are two such electrons, and therefore the electron affinity of C would be expected to be greater than that of B. However for N there are ~~no~~ electrons with the same spin quantum number as the extra electron, and so the probability of a stable negative ion of N is reduced. For O there is a single electron with the same spin quantum number as the additional electron and in F there are two such electrons, which suggests that both O and F form stable negative ions with F having the greater electron affinity.

A similar trend is postulated for the negative ions of Mg, Al, Si, P and S, which have partly filled $3p$ shells and Cl, whose $3p$ shell is completely filled.

These qualitative considerations are in agreement with experimental observations, but are insufficient to lead to any quantitative information on the stability of negative ions.

The earliest attempts to evaluate electron affinities followed the development of the Born-Haber cycle²⁰ and were confined to a refinement of the calculation of lattice energies on which this cycle is based. The lattice energy, U , of a crystal consisting of M^+ and X^- is related to the heat of sublimation, S , per molecule MX , the dissociation energy, $D(MX)$, of the molecule MX , the ionisation energy, $I(M)$ of the atom M ,

and the electron affinity $E(X)$ of the atom X by the formula.

$$E(X) = I(M) + D(MX) + S - U \quad 1.2$$

Therefore if all the quantities on the right hand side are known, the electron affinity can be derived.

Calculations of the lattice energies of the alkali halides have been carried out by Born and Heisenberg²¹, Mayer and Helmholtz⁽²²⁾, Verwey and de Boer²³, Huggins²⁴, Kapustinsky²⁵ and Löwdin²⁶, all in good agreement. More recent calculations on the lattice energies of the alkali halides have been performed by Cubicciotti²⁷, who using the best available data for the quantities D , S and I gave the values of the electron affinities for F , Cl , Br and I as 3.45 eV, 3.62 eV, 3.49 eV and 3.19 eV in satisfactory agreement with those obtained from photo-detachment studies^{6,7}.

The lattice energy of the crystal LiH , calculated by Hylleraas²⁸ and by Bichowsky and Rossini²⁹ gave the electron affinity for H as 0.78 eV in good agreement with quantum mechanical calculations.

Lattice energy calculations have also been performed on the alkali oxides by Morris³⁰ and on the alkaline earth oxides and sulphides by Sherman³¹, Mayer and Maltbie³², Kapustinsky²⁵ and Baughan³³. Since these crystals contain the doubly charged negative ions O^{2-} and S^{2-} equation 1.2 gave the electron affinities of O and S for the attachment of two electrons as -6.2 eV and -3.9 eV respectively³³.

The electron affinities of various molecular systems have also been calculated by the application of equation 1.2. The determination of the lattice energies of the alkali hydroxides by Born and Kornfeld³⁴, Kapustinsky³⁵ and Juza³⁶ gave the electron affinity of OH as 2.3 eV,

while the determination of the lattice energy of KO_3 by Nikolskii et al gave the electron affinity of O_3 as 2.9 eV^{37} .

Sherman³¹ calculated the lattice energies of the alkali cyanides which led to an electron affinity for CN of 3.69 eV , which may be in error due to the uncertainty in the value for the heat of formation of CN.

Yatsimirskii³⁸ from lattice energy calculations on the hydrosulphides, alkali nitrites and alkali nitrates derived electron affinities for respectively SH, NO_2 and NO_3 of 2.6 eV , 1.6 eV and 3.9 eV , the value for NO_2 is much lower than those derived from electron impact³⁹, and surface ionisation techniques⁹.

Pritchard⁴⁰ calculated the electron affinity of NH_2 to be 1.2 eV from lattice energy calculations on the alkali amines, in good agreement with recent mass spectrometric values⁴¹, and Evans et al⁴² from lattice energy calculations on the alkali oxides gave the electron affinity of O_2^- as 0.7 eV , which is rather high when compared with the value given by photodetachment studies⁴³.

A second useful technique for calculating electron affinities was suggested by Glockler⁴⁴, and later improved by Edlén⁴⁵.

The ionization energies of the members of an isoelectronic series of atoms and ions are represented to a good approximation by the quadratic expression

$$I(Z) = a_2 Z^2 + a_1 Z + a_0 \quad 1.3.$$

where $I(Z)$ is the ionization energy of the ground state of the member of the sequence with the atomic number Z and a_0 , a_1 and a_2 are constants, which may be determined empirically. Glockler⁴⁴ suggested that it should

be valid to extend this relation to the negative ion member of the isoelectronic sequence for which $Z = Z^-$. He expressed the electron affinity of the parent atom as:

$$E(Z) = I(Z^-) = 3I(Z_0) - 3I(Z_1) + I(Z_2) \quad 1.4.$$

where Z_0 , Z_1 and Z_2 are the atomic numbers of the neutral atom and the singly and doubly charged positive ions of the isoelectronic sequence.

Table 1 gives the values of the electron affinities of atoms obtained using Glockler's formula, Edlén's formula, those obtained experimentally, and the theoretical values.

Table 1

Atom	Glockler ⁽⁴⁴⁾	Edlén ⁽⁴⁵⁾	Experiment	Theory ⁽⁴⁷⁾
H	0.74	0.63	0.77 ± 0.02 ⁽⁴⁶⁾	0.75415 ⁽⁴⁸⁾
He	-0.53	0.19	-	-
Li*	0.42	0.82	-	0.58
Be*	0.22	-	-	-
B	-0.10	0.33	-	0.30
C	0.92	1.24	1.25 ± 0.03 ⁽⁵⁾	1.17
N	-0.56	0.05	-	-0.27
O	1.01	1.47	1.465 ± 0.005 ⁽⁴⁾	1.22
F	3.04	3.50	3.448 ± 0.005 ⁽⁷⁾	3.37
Ne	-1.24	-0.57	-	-
Na*	-0.05	0.47	-	0.78
Mg*	-0.58	-	-	-
Al	0.03	0.52	-	0.49
Si	1.07	1.46	-	1.39
P	0.38	0.77	-	0.78
S	1.79	2.15	2.07 ± 0.07 ⁽³⁾	2.12
Cl	3.39	3.70	3.613 ± 0.003 ⁽⁷⁾	3.56

All Electron Affinities are given in eV.

*The values correspond to the $3s^2S$ and $4s^2S$ states of Be^- , Mg^- respectively.

In general, the extrapolation methods support the qualitative conclusions regarding the stability of negative ions inferred by using

the Pauli exclusion principle. On applying equation 1.4 to Be^- it was found that the $2p^2P$ state of Be^- was unstable, as predicted on qualitative arguments, but the $3s^2S$ state was stable by 0.22 eV. This was attributed to an s electron, under certain conditions, being more readily attracted to a neutral atom than a p electron, due to the short range character of the potential field and the greater penetrating power of an s orbital⁴⁹. The same arguments were applied to Mg^- but both the $3p^2P$ and $4s^2S$ states were found to be unstable.

Comparison with experimental results showed that Glockler's formula works very well for atomic hydrogen but tends to slightly underestimate the value of the electron affinity for other atoms.

Edlén⁴⁵ attempted to improve Glockler's formula by introducing additional terms into equation 1.3., to allow for the screening effect of the inner electrons. He gave the binding energy $I(Z)$ of an electron with principal quantum number n , belonging to an atomic system of nuclear charge Z , effective nuclear charge $Z - S$, and containing N electrons as

$$I(Z)/(R/n^2) = \sigma^2 + 2a\sigma - b + c(\sigma + a)^{-1} \quad 1.5.$$

where $\sigma = Z - (N - 1)$, a is the asymptotic value for a penetration parameter p defined by $\sigma + p = Z - S$ and b, c are constants which are determined using known ionisation potentials.

Using equation 1.5. Edlén gave the electron affinity as

$$E(Z) = I(Z^-) = 3I(Z_0) - 3I(Z_1) + I(Z_2) + Q \quad 1.6.$$

where $Q = 3\{I(Z_0) - 2I(Z_1) + I(Z_2) - 2R/n^2\} \{-I(Z_0) + 2I(Z_1) - I(Z_2) + 6R/n^2\} / \{I(Z_0) - 4I(Z_1) + 3I(Z_2) - 12R/n^2\}$

Using equation 1.6. Edlén obtained electron affinities in good

agreement with experimental results, except for negative ions with small Z numbers. For example he found a small positive electron affinity for He, implying that the ground state negative ion of He is stable which is unlikely, and his value for H is in poor agreement with the theoretical value, the experimental value and that calculated using Glocker's method.

In a few cases quantum mechanical methods have been applied to the calculation of binding energies of negative ions. The negative hydrogen ion has been extensively studied by a number of variational treatments of differing degrees of approximation, which gave values for the electron affinity in very good agreement. The most accurate is that given by Pekeris⁴⁸ of 0.75415 eV in excellent agreement with photodetachment results⁴⁶. The variational method has also been applied to He^- and Li^- by Wu⁵⁰ who showed that He^- was unstable and gave $E(\text{Li}) = 0.54$ eV. More recent values for Li have been given by Strotskite and Iutis⁵¹ of $E(\text{Li}) = 0.54$ eV and Weiss⁵² of $E(\text{Li}) = 0.48$ eV. As the extension of the variational method to more complicated atoms is impracticable, due to computational difficulties, all other determinations have used the Hartree-Fock method. Clementi et al⁴⁷ have calculated the values for the electron affinities of B, C, N, O, F, Na, Al, Si, P, S and Cl: the values are given in table 1 and are in good agreement with both the extrapolation techniques and the photodetachment results.

The stability of a negative molecular ion is difficult to determine accurately by calculation and the only system that has been investigated is H_2^- . The earliest calculations were carried out by Eyring et al⁵³ who showed that H_2 has a negative electron affinity, since the energy of the

ground electronic state of H_2^- in its equilibrium configuration was found to be greater than the corresponding energy for H_2 . This was followed by the more elaborate calculations of McDowell and Dalgarno⁵⁴ and Fischer-Hjalmars⁵⁵, using the valence bond technique, both of which gave negative values for the electron affinity of H_2 of + 3.6 eV and - 0.28 eV, respectively.

A recent method of calculating the electron affinity of a molecular system is that due to Hinze and Jaffe⁵⁶. They have produced tables of promotion energies for all possible valence states of atoms with no open d shells from which, provided the valence state of the ion-precursor and the ion are known along with the ground state electron affinity, the valence state electron affinity E_v may be calculated since

$$E_v = \left(P_o - P_- \right) + E_g \quad 1.7.$$

where E_v , E_g are the valence state and ground state electron affinities respectively and P_o , P_- are the promotion energies of the ion precursor and ion, respectively. This method is discussed in greater detail in Chapter 5 of this dissertation.

Although lattice energy, quantum mechanical and extrapolation methods give satisfactory results for the electron affinities of atoms they are either invalid or involve too complicated mathematics to be generally applied to molecular ions. In general the stabilities of molecular ions are of greatest interest, hence many experimental techniques have been developed to measure this quantity.

The majority of experimental methods fall into one of three groups, determination of the energy threshold for destruction of the ion, determination of the energy threshold for formation of the ion and the study

of the equilibrium between atoms, electrons and negative ions.

Typical of the first group are the photodetachment studies of Branscomb et al^{3,4,5,6} and Berry et al⁷. In the technique used by Branscomb et al the negative ions were generated in a medium pressure discharge and isolated by a mass filter. They then passed into a reaction chamber where they were crossed by a high intensity monochromatic, photon beam of sufficient energy to detach the electron. By varying the wavelength of the photon~~beam~~ they determined the photodetachment spectrum and hence the stability of the ion from the threshold for photodetachment. The results obtained by Branscomb et al are $E(C) = 1.25 \pm 0.03 \text{ eV}^{(5)}$, $E(O) = 1.465 \pm 0.005 \text{ eV}^{(4)}$, $E(S) = 2.07 \pm 0.07 \text{ eV}^{(3)}$ and $E(I) = 3.076 \pm 0.005 \text{ eV}^{(6)}$.

Photodetachment experiments on the halogens F, Cl, Br and I have been carried out by Berry et al⁽⁷⁾. They produced the negative ions in sufficiently high concentration, by shock heating either rubidium or cesium halides, that the absorption spectra could be determined directly, leading to electron affinities of $E(F) = 3.448 \pm 0.005 \text{ eV}$, $E(Cl) = 3.163 \pm 0.003 \text{ eV}$, $E(Br) = 3.363 \pm 0.003 \text{ eV}$ and $E(I) = 3.063 \pm 0.003 \text{ eV}$, the value for the electron affinity of I being in close agreement with that obtained by Branscomb. Photodetachment techniques being spectroscopic give very accurate values for electron affinities but are restricted to negative ions that can be produced in reasonably high concentrations.

Typical of the second group are electron impact studies carried out in a mass spectrometer. In this technique a beam of almost monoenergetic electrons is passed through the gas, resulting in the forma-

tion of negative or positive ions, depending upon the electron energy. Then from the appearance potential $A(A^-)$ of the process $AB + e \rightarrow A^- + B$. The electron affinity of A is given as

$$A(A^-) = D(A - B) - E(A) + K.E. (B + A^-) \quad 1.8.$$

where $D(A - B)$ is the bond dissociation energy of A - B and K.E. is the kinetic energy of the products, A^- and B.

A considerable amount of the information on the existence of negative ions is derived from electron impact studies, but relatively few quantitative measurements have been made, due mainly to the lack of information on the kinetic energy term and to some extent on bond dissociation energies.

The earliest studies were made by Knipping⁵⁷, who studied the energy required to produce the dissociation of HX into H^+ and X^- , giving the values $E(Cl) = 4.25$ eV, $E(Br) = 2.95$ eV and $E(I) = 2.65$ eV, in reasonable agreement with later studies. Further information on the halogens was obtained by Hogness and Harkness⁵⁸ who, from a study of iodine showed that I^- , I_2^- and I_3^- were stable ions: they gave the appearance potential of I^- as approximately 0eV resulting in $E(I) > D(I_2)$. Baker and Tate⁵⁹ observed Cl_2^- in the mass spectrum of carbon tetrachloride and Blewett⁶⁰ identified Br_2^- as a stable ion.

Tilxen⁶¹ using a mass spectrometer demonstrated the existence of the ions O^- , O_2^- , NO_2^- , NO_3^- , OH^- and H^- in discharges in air, oxygen, hydrogen, water vapour and the inert gases although he did not detect the ions N^- , N_2^- , He^- , Ne^- or Ar

Dukelskii and Ionov⁶² from studies on the vapours of selenium,

tellurium, antimony and bismuth established the existence of the ions Se^- , Se_2^- , Se_3^- , Se_4^- , Te^- , Te_2^- , Sb^- , Sb_2^- , Sb_3^- , Bi^- , Bi_2^- , Bi_3^- and Bi_4^- . In all cases they showed that the appearance potential of the monoatomic ion was less than 1 eV and deduced that $E(\text{Se}) > 1.74$ eV, $E(\text{Sb}) > 2.04$ eV, $E(\text{Bi}) > 0.74$ eV and $E(\text{Te}) > 2.39$ eV.

Neuert et al from mass spectrometric studies identified the ions C_2H^- , C_2^- , H^- , C^- and CH^- from acetylene⁶³, PH_2^- , PH^- , P^- and H^- from phosphine⁶⁴, AsH_2^- , AsH^- , As^- and H^- from arsine⁶⁴, SiH_3^- , SiH_2^- , SiH^- , Si^- and H^- from silane⁶⁴, HSe^- from hydrogen selenide⁶⁵, S^- , SO^- , O^- and SO_2^- from sulphur dioxide^{65,66} and HS^- from hydrogen sulphide⁶⁵; from the appearance potentials, without consideration of the kinetic energy term, they determined the electron affinities $E(\text{C}_2\text{H}) > 2.8$ eV⁶³, $E(\text{PH}_2) > 1$ eV⁶⁴, $E(\text{HSe}) > 1.08$ eV⁶⁵, $E(\text{S}) > 2.3$ eV⁶⁵, $E(\text{SO}) > 2.56$ eV⁶⁵, $E(\text{O}) > 2.04$ eV⁶⁵, $E(\text{SO}_2) \leq 1.2$ eV⁶⁶ and $E(\text{HS}) > 1.65$ eV⁶⁵.

Studies of the ionisation by electron impact of the molecular gases O_2 , CO , CO_2 , NO , N_2O , NO_2 and SO_2 have been made by many investigators, giving values for the electron affinity of monatomic oxygen from 1.2 to 2.3 eV. A study of CO was carried out by Lagergren⁶⁷ and by Fineman and Petrocelli⁶⁸. From analysis of the appearance potentials for positive and negative ions of C and O Lagergren concluded that $E(\text{O}) = 1.45$ eV and $E(\text{C}) = 1.12 \pm 0.2$ eV, whereas Petrocelli et al obtained $E(\text{O}) = 1.70 \pm 0.2$ eV and found different values for $E(\text{C})$ depending on whether they based their analysis on the appearance potentials of O^+ or C^- . From their positive ion data they found $E(\text{C})$ to be between 1.32 and 1.36 eV, in agreement with the photo-detachment results, while from their negative ion data they found $E(\text{C})$

to lie between 1.71 and 1.76 eV. Other investigations include the electron impact studies on CO₂ by Craggs and Tozer⁶⁹ which gave $E(0) = 1.2 \pm 0.3$ eV, on NO₂ by Collin and Lossing⁷⁰ and Fox⁷¹ which gave, respectively, $E(0) = 2.3 \pm 0.2$ eV and $E(0) = 1.35 \pm 0.05$ eV and on O₂ by Randolph and Geballe⁷² who obtained $E(0) = 1.52 \pm 0.1$ eV. In general the electron impact results give an average value of $E(0) = 1.44$ eV which is in reasonable agreement with photodetachment studies.

Provided the electrons have only a small energy spread mass spectrometry readily yields accurate information about the appearance potentials of negative ions, although it is often difficult to extract electron affinity data due to unknown kinetic energy terms and bond dissociation energies. In addition Schultz⁷³ has recently shown that the appearance potential of a negative ion is temperature dependent, and to determine realistic electron affinities the appearance potential must be measured at temperatures where the ion is not formed in a vibrationally excited state.

Typical of the last group are the studies of equilibria in flames and at metal surfaces. The idea of measuring the equilibrium between atoms, electrons and ions was first used by Rolla and Piccardi⁷⁴. In their experiment a fine metallic thread was placed in a flame and heated to red heat which caused electrons to be emitted and, in the presence of certain atoms or molecules, reactions of the type, $X + e \rightleftharpoons X^-$ were possible. A thin metal plate at a positive potential with respect to the wire was held a short distance away, which attracted the electrons giving rise to a small electric current. The introduction of a substance such as methyl iodide caused a reduction in

the current due to the formation of I^- by the reaction $I + e \rightleftharpoons I^-$, since the iodide ions have a much smaller mobility than the free electrons. Hence from the reduction in electron current together with a knowledge of the rate at which iodine atoms were entering the system, they calculated the equilibrium constant, from which, knowing the temperature of the flame, T , they calculated the electron affinity of iodine.

$$\text{i.e. } \log K = \log \frac{(I^-)}{e(I)} = -E/RT + C \quad 1.9.$$

Using methyl iodide and ethyl bromide Piccardi⁷⁵ determined $E(I) = 3.56$ eV and $E(\text{Br}) = 3.76$ eV, respectively, and using sulphur dioxide (SO_2), selenium dioxide (SeO_2) and molybdenum oxide (MO_3) Rolla and Piccardi^{76,77} determined $E(\text{SO}_2) = 2.80$ eV, $E(\text{SeO}_2) = 2.30$ eV and $E(\text{MO}_3) = 2.73$ eV respectively.

Equilibrium studies involving dissociation of molecular beams of alkali halides at hot tungsten surfaces, were investigated by Dukelskii and Ionov⁷⁸. At the hot surface the alkali halides dissociated, with the alkali metal atoms evaporating partly as positive ions and the halogen atoms as negative ions. The resulting positive and negative ions were collected alternately by a Faraday cylinder: the negative ions were separated from the electrons by application of a magnetic field. The ionization of the positive and negative ions is described by the Saha-Langmuir⁷⁹ relation as

$$i^+/i^- = (1 + 4 \exp(\chi - E/kT)e)/(1 + 2 \exp(I - \chi/kT)e) \quad 1.10$$

where e is the electronic charge, i^+ , i^- are the observed positive ion and negative ion currents. E is the electron affinity of the halogen atom, I is the ionization potential of the alkali metal atom, χ is the work function of the surface and T is its temperature.

Hence from the observed positive and negative ion currents, provided I , T and χ are known the electron affinity is readily calculated. Using potassium fluoride as substrate Dukelskii and Ionov determined $E(F) = 3.62$ eV; with sodium, potassium, rubidium and cesium chlorides they determined an average value of $E(Cl) = 3.77$ eV; using sodium, potassium and rubidium bromides they gave an average value $E(Br) = 3.64$ eV and from potassium iodide they determined $E(I) = 3.30$ eV, in reasonable agreement with the results of Rolla and Piccardi. However in view of the recent photodetachment values all the results are 5-16% too high.

Another method in this group is the 'Magnetron' technique of Sutton and Mayer⁸⁰, in which the negative ion current formed at a hot metallic filament is compared with the corresponding thermionic current. The negative ions and electrons are separated using a triode, filament - grid - anode, assembly mounted in a solenoid with the axis parallel to the filament. In the absence of the magnetic field the current due to the electrons and negative ions can be measured and in the presence of the magnetic field the electrons are constrained into helical paths and are captured by the grid whereas the heavier negative ions are virtually unaffected and pass through to the anode. Then knowing the current due to the electrons and negative ions, the pressure of the substrate and the filament temperature, the equilibrium constant and, therefore, the free energy change for the reaction at the filament temperature can be calculated. The combination of this with the entropies and specific heats of the reaction, gives the electron affinity of the reactant. Mayer et al from the study of iodine determined $E(I) = 3.14 \pm 0.07$ eV⁸⁰, from the study of bromine they gave $E(Br) =$

$3.49 \pm 0.02 \text{ eV}^{80}$ and from the study of chlorine and stannic chloride they determined an average value of $E(\text{Cl}) = 3.72 \pm 0.04 \text{ eV}^{81}$. Bernstein and Metlay⁸² used fluorine as the substrate and determined $E(\text{F}) = 3.57 \pm 0.17 \text{ eV}$. All these results are in good agreement with the latest spectroscopic results⁷. However, both Mayer and Vier⁸³ and Metlay and Kimball⁸⁴ attempted, unsuccessfully in view of later results, to determine the electron affinity of the oxygen atom, using molecular oxygen, by the magnetron technique. The results they obtained were, respectively, $3.07 \pm 0.09 \text{ eV}$ and $2.84 \pm 0.11 \text{ eV}$, which are considerably higher than the now accepted photodetachment value of $1.465 \pm 0.005 \text{ eV}^4$. This discrepancy is probably due to either the failure to accurately calculate the degree of dissociation of oxygen at the hot filament, or failure to account for the reaction of oxygen with the filament.

The Magnetron technique was chosen by Page⁸⁶ for use as a general method for the determination of the stabilities of negative ions. He found that negative ions were formed by two processes, firstly by the simple direct-capture process, that is $\text{AB} + \text{e} \rightarrow \text{AB}^-$; an extensive study of direct capture reactions has been undertaken by Farragher⁸⁷ and Burdett⁸⁸, and secondly by the dissociative-capture process, that is, $\text{AB} + \text{e} \rightarrow \text{A}^- + \text{B}$.

This dissertation represents a study of negative ions formed by dissociative-capture processes and, in particular, the effect of the valence state of the accepting centre and the effect of substitution at this accepting centre upon the stability of the negative ion is investigated.

The disadvantage of the Magnetron technique is that identification of the ions is not direct but done on energetic grounds, and complex reactions, which give rise to similar numbers of ions of different mass, may be misinterpreted in terms of a simple reaction. To overcome this disadvantage the last chapter of this dissertation is concerned with the replacement of the ion source of a Varian Quadrupole Mass Filter by a surface ionisation source, enabling direct identification of the ions formed at the hot surface to be made, in conjunction with the usual Magnetron type measurements of negative-ion current, electron current and filament temperature.

2. THE APPARATUS

2.1. The Theory of the Magnetron³⁹.

Figure 1 shows a cylindrical diode placed in a uniform magnetic field, with direction parallel to the common axis of the filament and anode. As the electron, e , moves from the filament to the anode the electromagnetic force deflects it, the curvature of its path depending upon the flux density B , for a given anode potential; at the critical flux density B_c the electron is shown to just graze the anode.

The electrostatic and electromagnetic forces acting on the electron are, respectively:

$$F = -\epsilon E = \epsilon dV/dr$$

$$\text{and } f = B\epsilon v$$

where ϵ is the electronic charge, V is the potential at a distance r from the filament, and v is the electron velocity at this point.

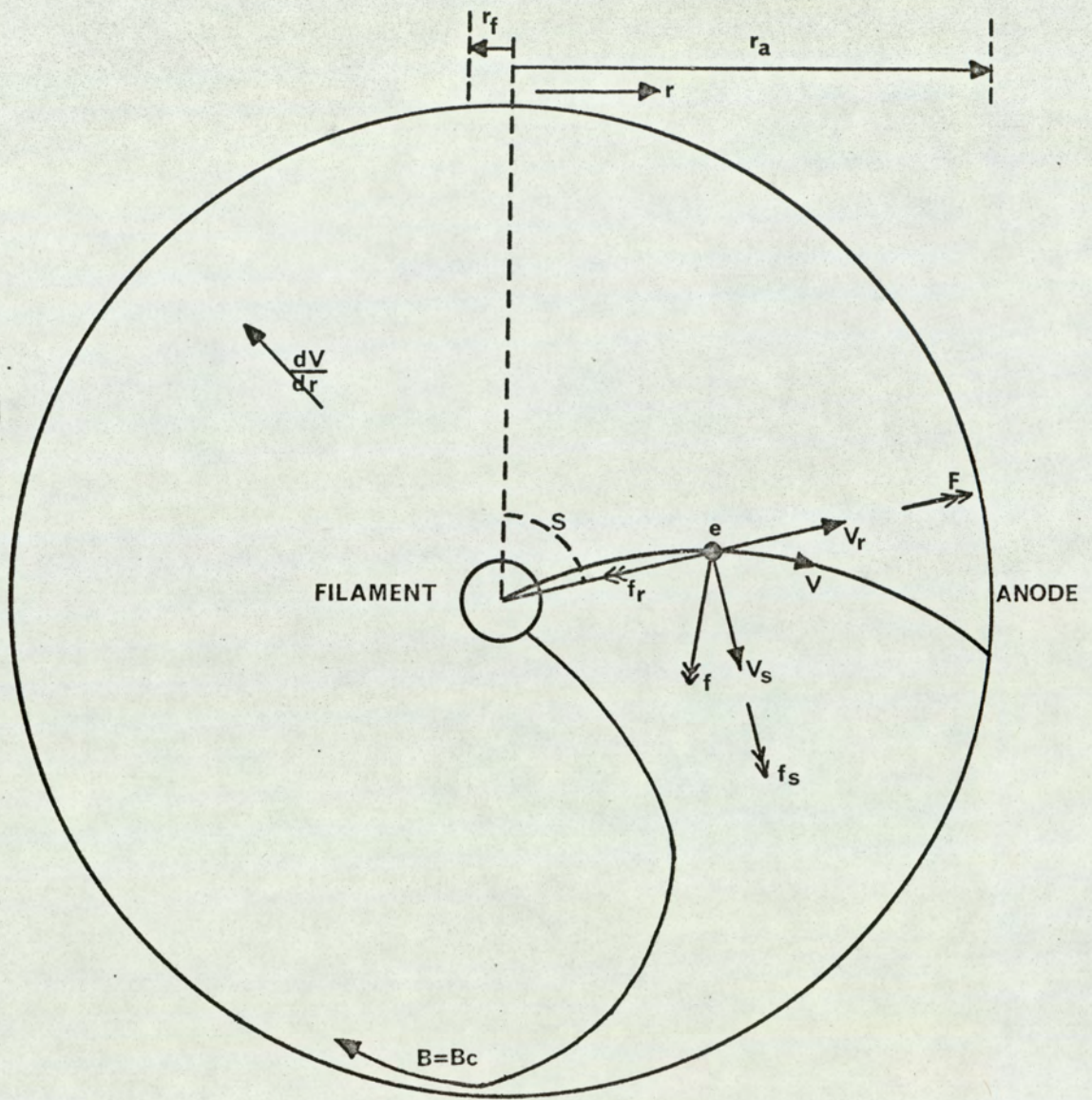
If v is resolved into components v_r and v_s , along and perpendicular to the radius vector, then the components of f will be:

$$f_r = B\epsilon v_s \quad \text{and} \quad f_s = B\epsilon v_r$$

If S is the angle made by the radius vector, r , with an arbitrary line in the azimuthal plane, the angular velocity of the electron, ω , is:

$$\omega = dS/dt = v_s/r$$

If m_e is the mass of the electron the equation of radial motion



THE FORCES ACTING UPON AN ELECTRON IN A CYLINDRICAL MAGNETRON.

FIG. 1.

becomes:

$$\begin{aligned} (d(m_e dr/dt))/dt &= F - f_r \\ &= \epsilon dV/dr - B_e r dS/dt \end{aligned} \quad 2.1.$$

The equation of azimuthal motion is found by equating the moment of the impressed force to the rate of change of angular momentum, thus:

$$r f_s = (d(m_e r^2 dS/dt))/dt$$

or substituting:

$$r B_e dr/dt = (d(m_e r^2 \omega))/dt$$

Integrating each side with respect to time and with initial conditions of $\omega = 0$ at the moment the electron leaves the filament, i.e. when $r = r_f$, gives:

$$\omega = (B_e/2m_e) (1 - r_f^2/r^2) \quad 2.2.$$

Since the velocities with which the electrons leave the cathode are negligible, the velocity v at a point where the potential is V is given by:

$$v = (2\epsilon V/m_e)^{1/2}$$

At the critical flux density B_c the anode current is just cut off and $V = V_a$, $v_r = 0$, $v_s = v$, $r = r_a$, and:

$$\omega = v_s/r_a = (2\epsilon V_a/m_e)^{1/2}/r_a \quad 2.3.$$

Equating 2.2 and 2.3. and noting that $B = B_c$ gives:

$$B_c = (8V_a)^{1/2} / (r_a (e/m_e)^{1/2} (1 - r_f^2/r_a^2)^{1/2}) \quad 2.4.$$

In the magnetron $r_a \gg r_f$ hence:

$$B_c = (8V_a)^{1/2} / r_a (e/m_e)^{1/2} \quad 2.5.$$

Equation 2.5 shows that the value of B_c is independent of the potential distribution, so that the presence of any other grid-electrodes, or of space-charge between the cathode and anode should not affect the

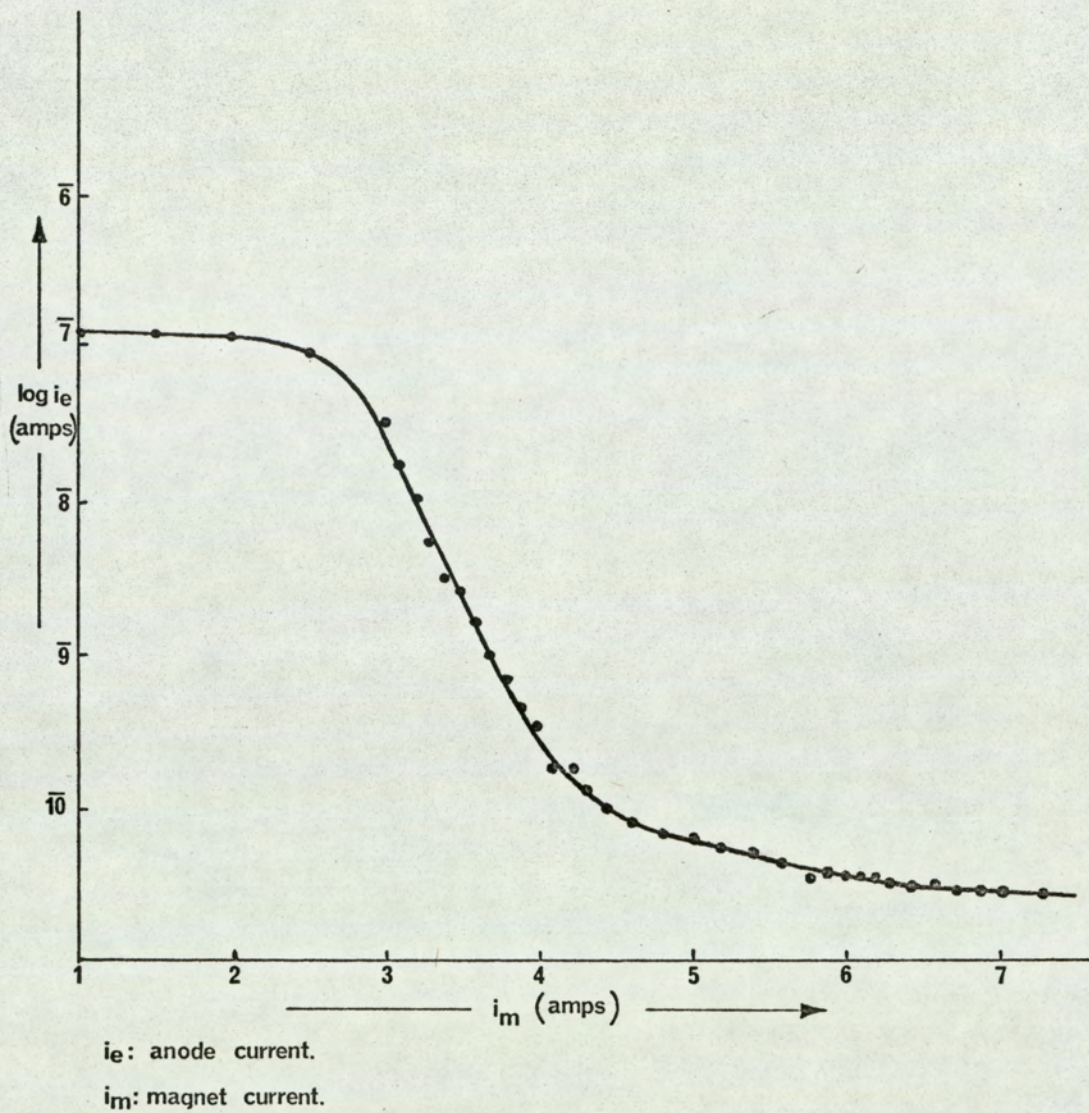
cut-off conditions.

The magnetron assembly used in this work was a tetrode, consisting of a filament, two grids, at slightly different potentials and an anode; the grids were present to collect electrons and so prevent a large space charge being created near the filament, which would have affected the emission of negative ions. Under these conditions the cut-off is not sharp, as shown in figure 2, probably due to asymmetry of the grids, causing the electrons to move out of the azimuthal plane, producing an electron velocity component along the axis, which has been ignored in the above treatment.

2.2. The design of the apparatus.

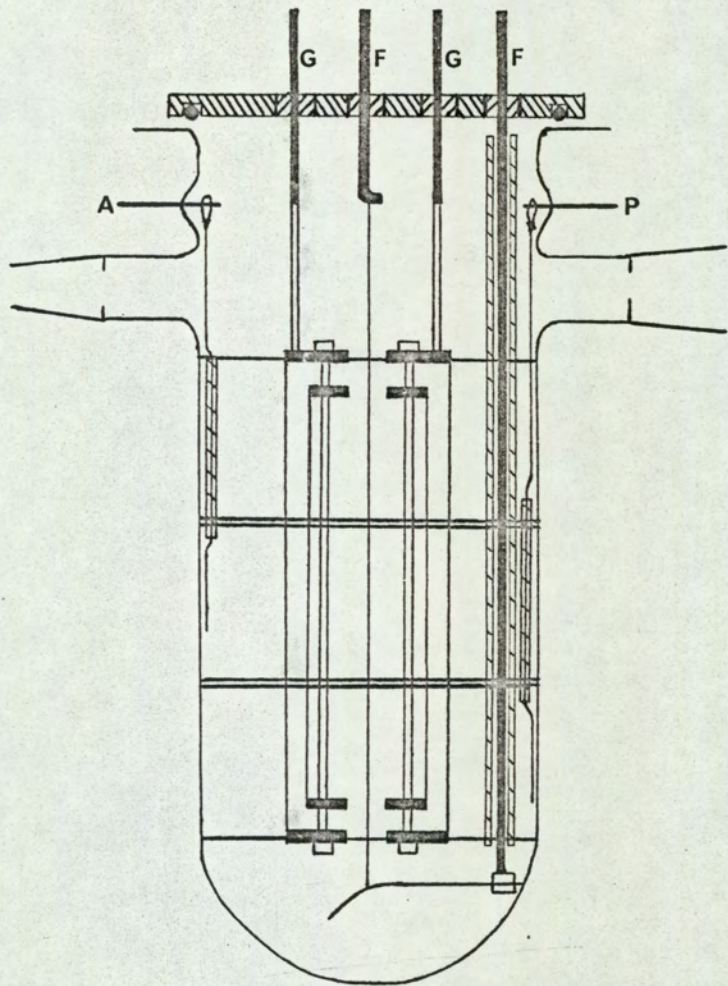
The apparatus consisted essentially of a central filament, F, surrounded by two co-axial grids, G, and an anode A with associated guard plates, P, as shown in figure 3a and 3b. This arrangement ensured that the electron and ion currents were collected only from the central portion of the filament, where the temperature gradient is negligible and distortion of the electrostatic field, due to the finite length of the cylindrical anode, was reduced to a minimum by the guard rings.

The grid and filament assemblies were mounted directly onto metal to glass seals which were soldered into a 0.25" thick brass plate; this was sealed onto the ground glass lip of the magnetron bottle by means of a rubber 'O' ring, lightly coated in Edwards silicone, high vacuum grease. The grid assembly shown in 3b was wound with 40 swg nickel wire, the anode and guard plates were molybdenum and sprung



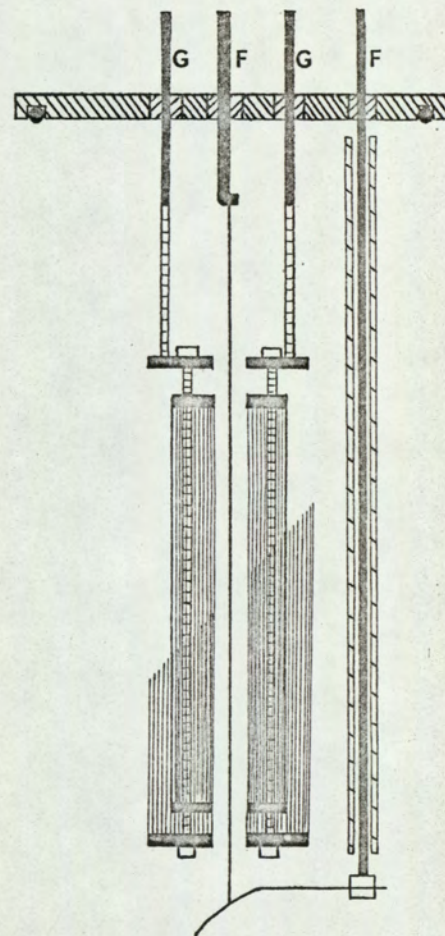
EFFECT OF MAGNET CURRENT ON ANODE CURRENT.

FIG.2.



MAGNETRON ASSEMBLY.

FIG. 3a.



GRID ASSEMBLY.

FIG. 3b.

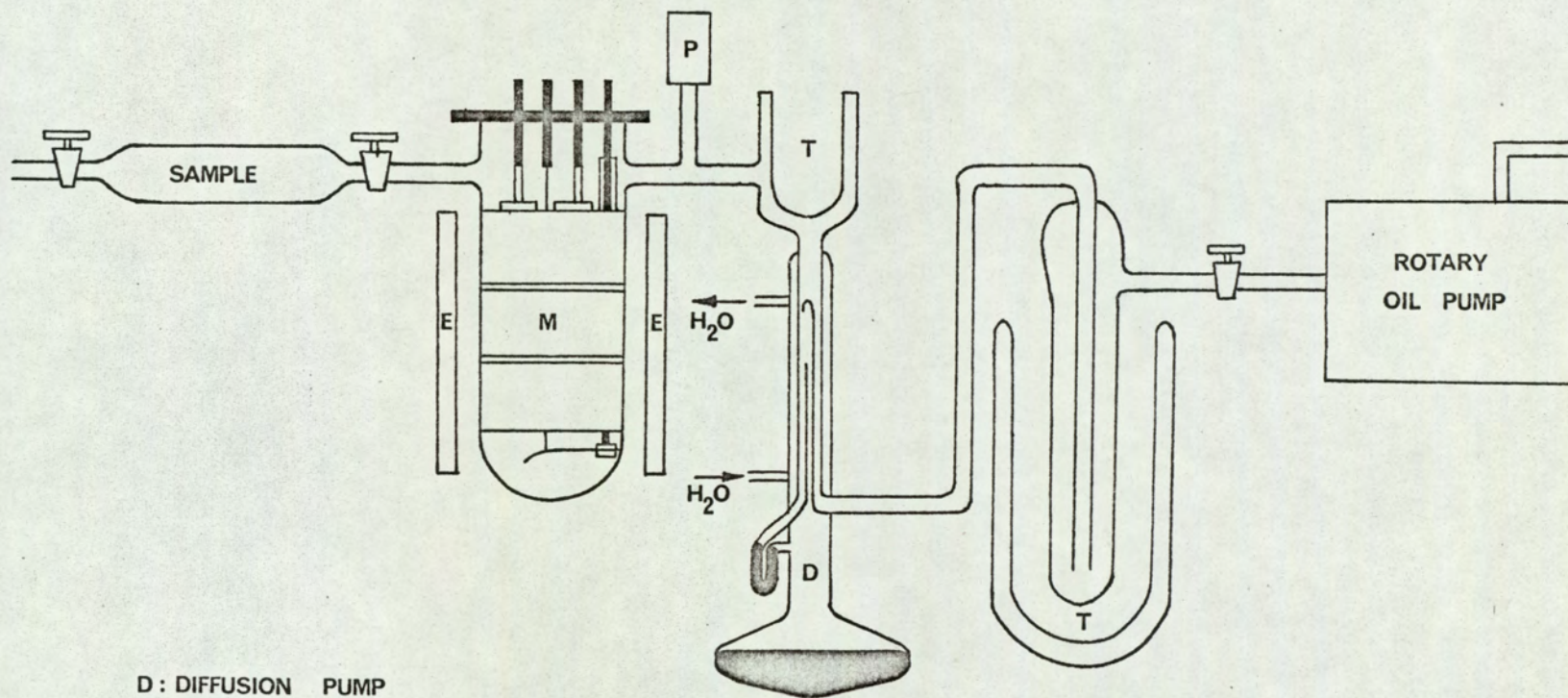
into position, and tension was retained on the filament by means of a 0.01" tungsten wire spring.

The magnetron bottle was mounted in a solenoid, consisting of a brass, water cooled former on which was wound about 1000 turns of 20 s.w.g. enamelled copper wire. The operating current of the magnet was between 6 and 7 amps, where from figure 2, it is seen that the residual electron current is small and independent of magnet current.

The complete apparatus as shown in figure 4 was pumped continuously, using a two stage mercury diffusion pump backed by a Genevac rotary oil pump; this system was capable of maintaining a vacuum of about 10^{-5} Torr. Liquid nitrogen traps were introduced at the positions indicated to prevent mercury and substrate residues contaminating the magnetron bottle.

The sample was introduced via a side arm on the magnetron bottle at a pressure of about 10^{-4} Torr; the pressure of gases and volatile liquids was controlled by an Edwards needle valve and the pressure of liquids and volatile solids was controlled by water/ice or ice/salt mixtures. For non-volatile solids the sample and magnetron bottle were heated with a thermostatically ~~controlled~~ ^{brought to a suitable level} Iso-mantle tape.

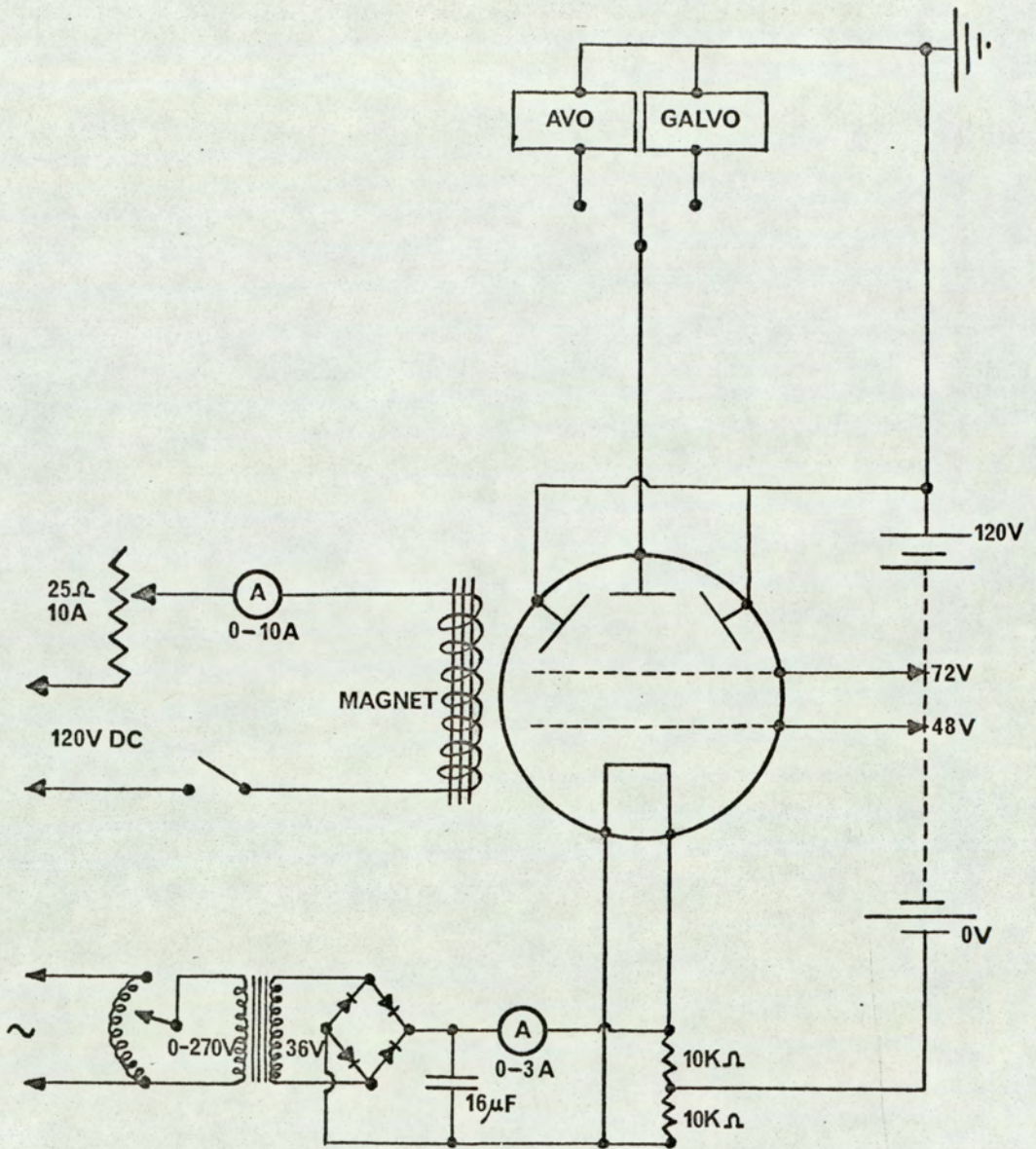
Figure 5 shows the electrical circuits for the complete apparatus. The anode current was measured by an AVO D.C. amplifier in the range 10^{-13} to 10^{-6} amps and by a Pye Scalamp galvanometer in the range 10^{-6} to 10^{-3} amps. The D.C. voltages to the filament, grid and anode assemblies were supplied by an Exide H1006 battery and the magnet current supplied from a continuously charged, 120 volt stack of lead acid accumulators.



D: DIFFUSION PUMP
 E: ELECTRO MAGNET
 M: MAGNETRON
 P: PIRANI GAUGE
 T: LIQUID NITROGEN TRAP

LAYOUT OF THE APPARATUS.

FIG.4.



CIRCUIT DIAGRAM.

FIG. 5.

2.3. The measurement of temperature

The measurement of temperature of the filament is fundamental to the evaluation of Electron Affinities by the magnetron technique and therefore must be determined accurately.

The temperature of the filament was determined using a Leeds and Northrup disappearing filament pyrometer, reading through one thickness of glass. The pyrometer reading will always be lower than the true filament temperature due to the filament having an emissivity less than unity and the absorption of radiation by the glass. In the temperature range 1000 to 2000°K the correction due to absorption by the glass is approximately + 24°K⁸⁹ and the emissivity corrections for the filaments used, Platinum, Iridium and Tungsten are given by:⁹⁰

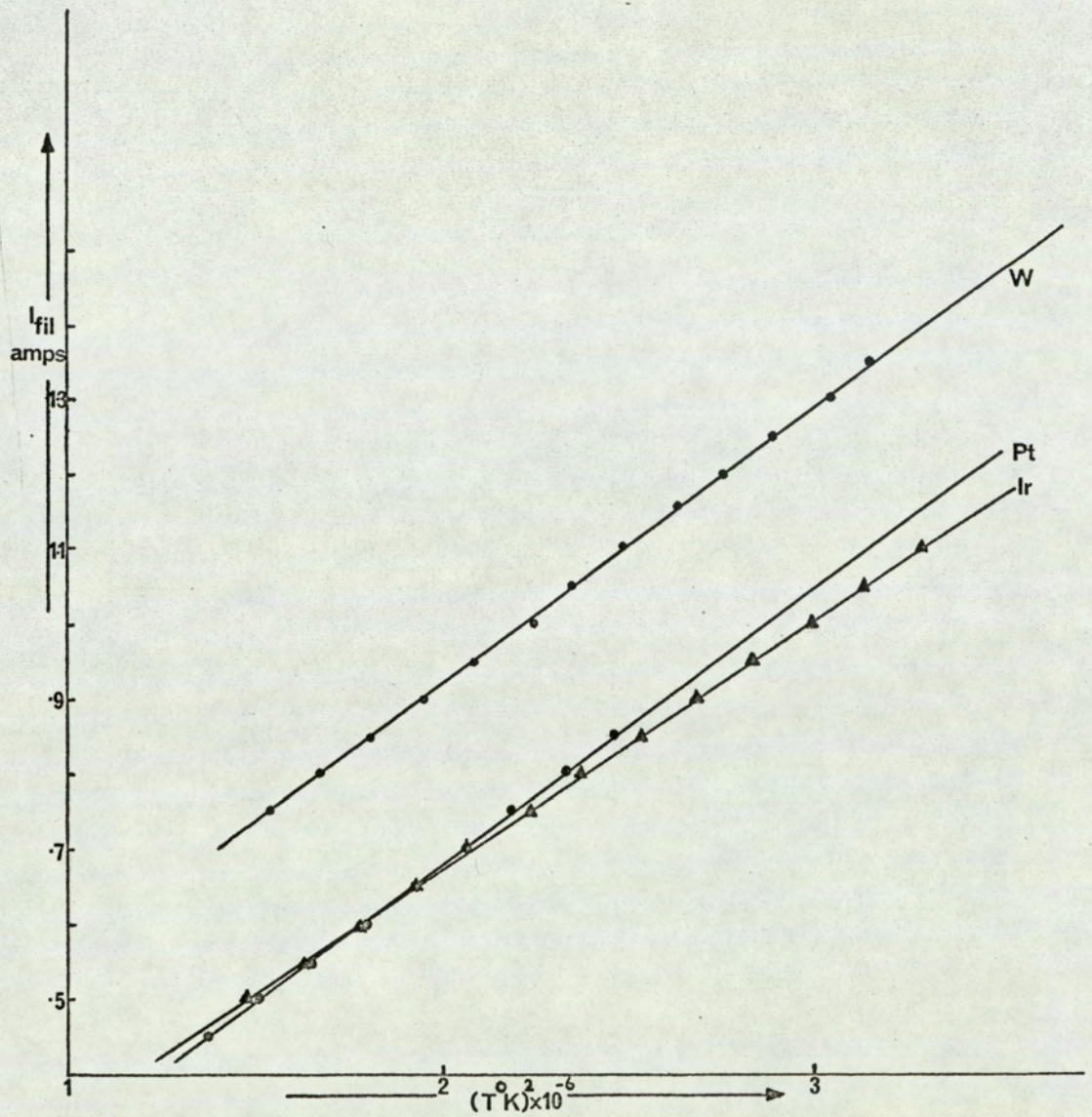
$$\text{For Pt and Ir} \quad (1/T - 1/T_{\text{exp}}) = - .00005481$$

$$\text{and for W} \quad (1/T - 1/T_{\text{exp}}) = - .00003634$$

where T, T_{exp} are the true and experimental filament temperatures, respectively, and the emissivities for Pt, Ir and W taken as 0.3, 0.3 and 0.45⁹¹ respectively.

Having converted the pyrometer temperature into °K and corrected for emissivity and glass absorption effects, the filament current was plotted against the square of the true temperature, as shown in figure 6. Any deviation from the smooth curve was attributed to personal error and hence ~~corrected for~~^{ignored}.

That the plot of filament current against the square of the temperature is a straight line follows directly from ~~Stephans~~^{Stefan's} Law⁹⁰. If the heat lost by conduction at the ends of the filament is neglected, the heat supplied may be set equal to the total radiation emitted E.



FILAMENT TEMPERATURE CALIBRATION.

FIG. 6.

$$\text{i.e.} \quad i_{\text{fil}}^2 R = E = \sigma T^4$$

$$\text{or} \quad i_{\text{fil}} \propto T^2$$

where i_{fil} is the current passing through a filament of resistance R at a temperature T , and σ is Stephan's constant.

2.4. Operation of the Apparatus.

For satisfactory operation of the magnetron the apparatus has to be "outgassed"; the procedure adopted was to maintain the filament at as high a temperature as practicable, this being determined by the melting point of the metal, until the background pressure fell to below 10^{-5} Torr and the 'cut-back' (i.e. the ratio of the electron to ion current in the absence of a substrate) was greater than 10^4 at the maximum operating temperature. The sample was then allowed to flow over the hot filament until electron current and temperature measurements showed the system to have become stabilized.

Having calibrated the filament temperature at set filament current readings, in the presence of the substrate, the total current (i.e. the anode current in the absence of the electromagnetic field) and the negative ion current (i.e. the anode current in the presence of the electromagnetic field) were determined for a range of filament current, hence temperature, readings. In most cases the ion current was a factor of 10^3 less than the electron current, the electron current, therefore, being given by the total current.

Then from the slope of a plot of the logarithm of the ratio of the electron to ion currents against the reciprocal of the corresponding filament temperature the "Apparent Electron Affinity", E_T , of the substrate molecule was determined.

$$\text{i.e. } -d(\log i_e/i_i)/d(1/T) \stackrel{=}{\neq} E_T/R \quad 2.6.$$

If, as in the case of gaseous and very volatile liquids, the sample pressure changed throughout the run the ion current had to be corrected, E_T being given by:

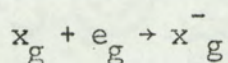
$$-d(\log i_{ep}/i_i)/d(1/T) = E_T/R \quad 2.7.$$

The significance of the value of the "Apparent Electron Affinity" is described in Chapter 3.

3. THEORETICAL CONSIDERATIONS OF ELECTRON AND NEGATIVE ION EMISSION.

3.1 Introduction.

The original interpretation of Magnetron results by Mayer⁸⁰ postulated a complete equilibrium at the filament surface between the atoms, ions and electrons. Since equilibrium exists he was able to determine the equilibrium constant and hence the energy change for the reaction:-



The results obtained for the Electron Affinities of the halogens were satisfactory,^{80,81,82} but extension of the theory to formation of O⁻ from O₂⁸⁴ proved to be unsuccessful. This was possibly due to either incorrect calculation of the degree of dissociation of the gas at the hot surface or interaction of the gas with the filament surface. Failure to explain the oxygen results and lack of suitable substrates caused the method to be abandoned until Page⁸⁶ made a further study of the halogens, using the hydrogen halides as substrates. Page noticed that the total ^{ion} current emitted by the filament was inversely proportional to the gas pressure, in direct opposition with Mayer's theory, where the total current should be independent of pressure, as the ions are postulated to be formed by capture of electrons which have been emitted from the filament. Page interpreted this phenomenon^{on} in terms of an adsorption process which resulted in a raising of the work function of the surface, and using the alternative kinetic approach he was able to extend the theory to successfully^{to} include cases where interaction with the filament occurred. As an extension to the kinetic approach, Farragher⁸⁷ applied the theory

of rate processes⁹² to ion and electron formation; and it is this theory which is discussed in detail and used throughout this work.

3.2. The Application of the Theory of Rate Processes to the thermal emission of electrons and negative ions.

3.2.1. Introduction

The theory of absolute reaction rates⁹² is based upon the idea that a rate process is characterised by an initial configuration, AB, which, by a continuous change of reaction co-ordinates, passes through some intermediate configuration AB* before the final configuration, P, is attained. The intermediate configuration is termed the 'Activated Complex' and is situated at the highest potential energy point of the most favourable reaction path. (Figure 7.) The activated complex is regarded as an ordinary molecule possessing the usual thermodynamic properties, with the exception that motion in the direction along the reaction co-ordinate leads to decomposition at a definite rate. With these assumptions Glasstone et al derived by statistical methods, the concentration and rate at which the activated complex passed through the critical configuration of the activated state, the product of which gives the reaction rate.

$$\text{i.e. Reaction Rate} = (AB^*)\nu \quad 3.1.$$

Where (AB^*) = concentration of the activated complex at the top of the barrier.

ν = frequency of crossing the barrier.

Provided that the rate of the forward reaction is small compared with the rate of the backward reaction the states AB and AB* can be

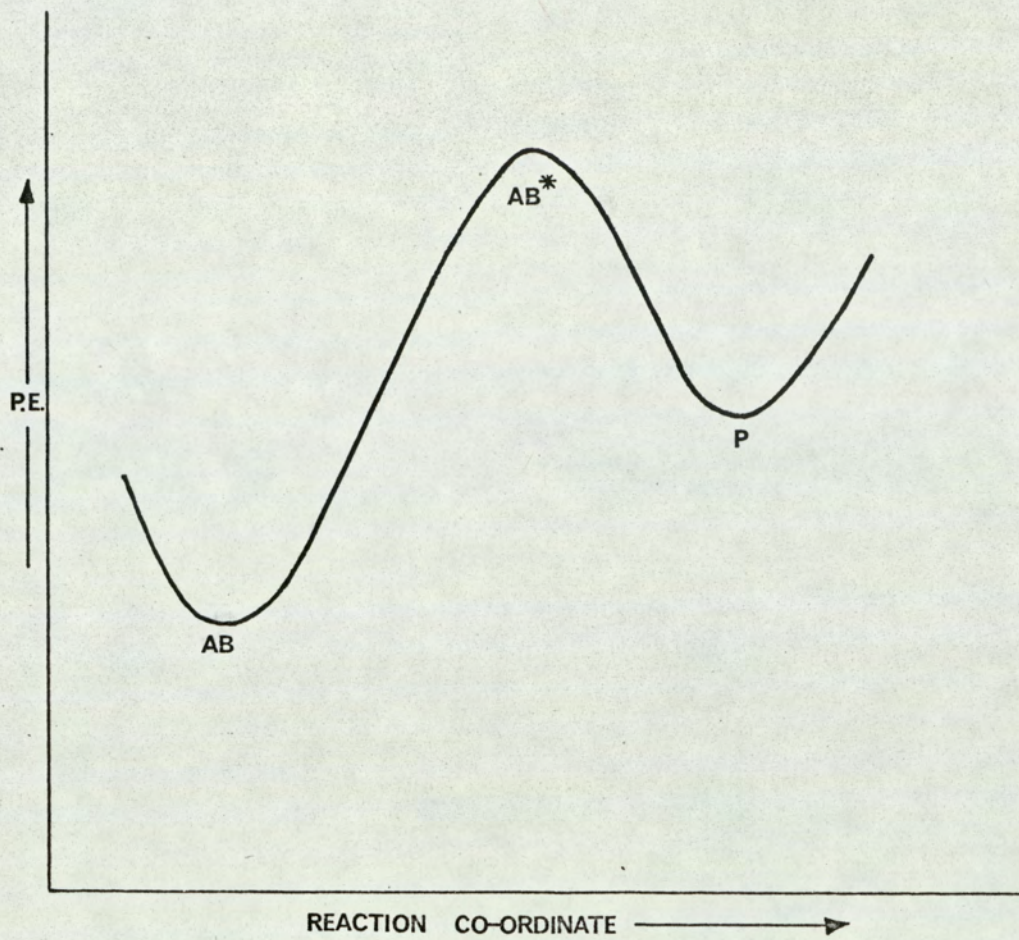


FIG.7.

considered to be in equilibrium, the equilibrium constant, K^* , being given by:

$$K^* = \frac{(AB^*)}{(AB)} = \frac{Q_{AB^*}}{Q_{AB}} \cdot \exp(- (b - a)/kT) \quad 3.2.$$

Where Q_{AB^*} , Q_{AB} are the partition functions of the states AB^* and AB , respectively, and b and a are the corresponding energies.

k is Boltzmann's constant.

T is the temperature in $^{\circ}K$.

$$\text{Hence } (AB^*) = (AB) \frac{Q_{AB^*}}{Q_{AB}} \cdot \exp(- (b - a)/kT) \quad 3.3.$$

Now the partition function of the activated complex is postulated to contain one term which represents translational motion along the reaction co-ordinate; this term arises from a weak vibration of frequency ν and contributes $kT/h\nu$ to the partition function, i.e.

$$Q_{AB^*} = Q'_{AB^*} \frac{kT}{h\nu} \quad 3.4.$$

$$\text{Hence } (AB^*) = \left(\frac{kT}{h\nu}\right) (AB) \left(\frac{Q'_{AB^*}}{Q_{AB}}\right) \exp(- (b - a)/kT) \quad 3.5.$$

Combining equations 3.1 and 3.5 gives:

$$\text{Reaction Rate} = \left(\frac{kT}{h}\right) (AB) \left(\frac{Q'_{AB^*}}{Q_{AB}}\right) \cdot \exp(- (b - a)/kT) \quad 3.6.$$

3.2.2. The Emission of Electrons.

An electron emitted from the hot filament in the magnetron is subjected to two opposing forces, the potential gradient within the magnetron and its own image force. Combination of these two forces leads to a point of maximum potential at an energy barrier, termed the Schottky barrier.⁹³ See figure 8.

If the methods of absolute rate theory are applied to electron emission the potential energy maximum at the Schottky barrier should

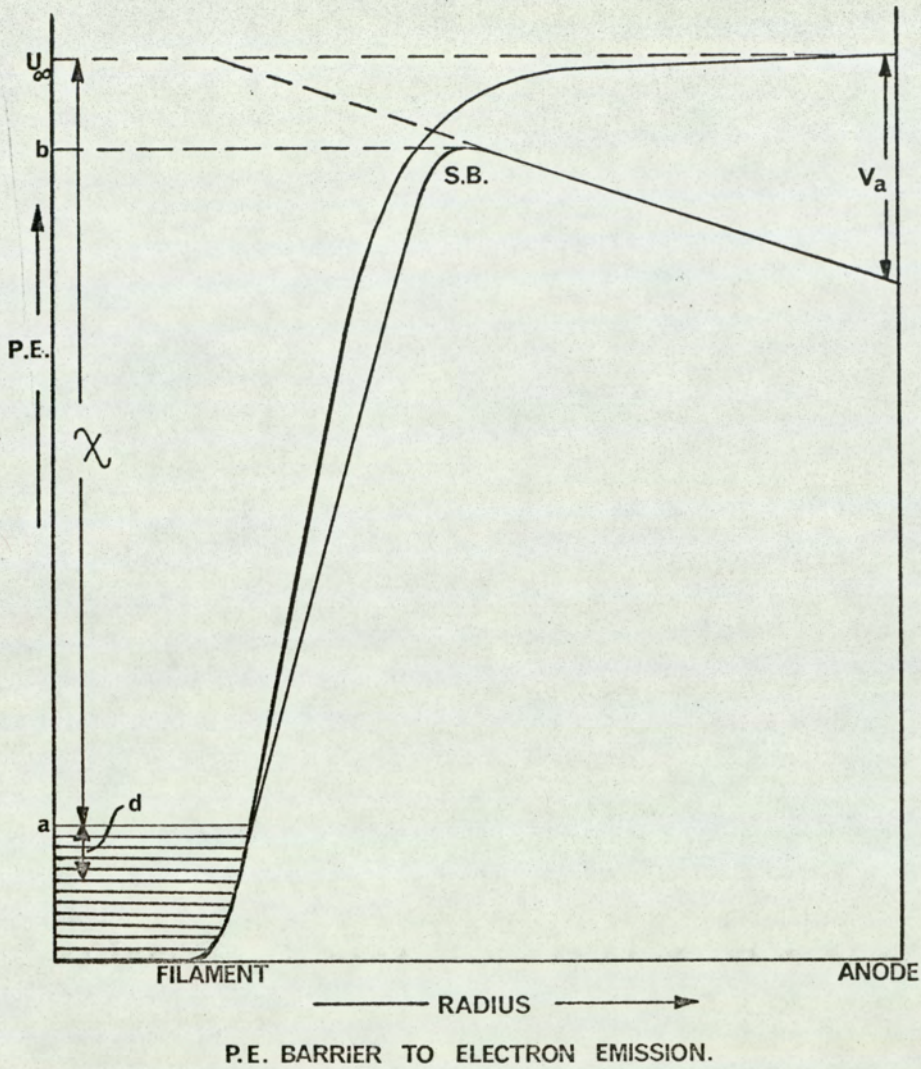


FIG. 8.

define the energy and position of the activated state for the emission reaction.

If the electrons in the activated state, e^* , are assumed to be in equilibrium with those in the metal, e_m , then the equilibrium constant for formation of the activated complex, K^* , is given by 3.2.

$$\text{i.e. } K^* = (C^*)/(C_m) = (Q^*/Q_m) \exp(- (b - a)/kT) \quad 3.7.$$

Where (C^*) , (C_m) represent the concentration of electrons in the activated state and in the metal, respectively.

Q^* , Q_m represent the partition function per unit area for the electrons in the activated state and the partition function per unit volume for the electrons in the metal, respectively.

a , b represent the zero point energy of the electrons in the metal and the ground state energy of the electrons in the activated state, respectively.

$$\text{From 3.4 } Q^* = Q^* \nu kT/h\nu \quad 3.8.$$

Where ν is the frequency of the rate determining motion

Substituting 3.7 and 3.8 into 3.6 gives:-

Reaction Rate for Electron Emission

$$= (kT/h) (C_m) (Q^* \nu / Q_m) \exp(- (b - a)/kT) \quad 3.9.$$

$$\text{But } (C_m) \text{ is given by: } (C_m) = Q_m \exp(d/kT) \quad 3.10.$$

where d is the average kinetic energy of the electrons in the metal and is given by $d = 3F/5 + \pi^2 k^2 T^2 / 4F$,⁹³ where F is the Fermi energy and equal to $h^2 / 8m_e (3n/\pi)^{2/3}$, m_e is the mass of the electron, and n is the number of free electrons per unit volume.

$$\text{Hence Reaction Rate} = (kT/h)Q^{*'} \cdot \exp(- (b - a - d)/kT) \quad 3.11.$$

The electron in the transition state has three translational degrees of freedom; one of which has been accounted for in the rate determining motion and two which may be treated classically, i.e. $Q^{*'} = 2(2\pi m_e kT)/h^2$, the factor 2 being introduced to allow for the spin degeneracy of the electron.

$$\text{Hence Reaction Rate} = 4k^2 \pi m_e T^2 / h^3 \cdot \exp(- (b - a - d)/kT) \quad 3.12.$$

Since electron current per unit area of surface, i_e , is given by the product of the rate of electron emission and the electronic charge, e .

$$i_e = e 4k^2 \pi m_e T^2 / h^3 \cdot \exp(- (b - a - d)/kT) \quad 3.13.$$

From diagram 8, the work function χ is given by $N(U_\infty - (a + d))$, hence the change in work function due to the applied field, $(U_\infty - b)$, must be evaluated.

The resultant force, at the Schottky barrier, on the electron is zero, therefore if x is the distance of the Schottky barrier from the surface of the metal

$$\epsilon^2 / 4x^2 = eV_a / r_f \cdot \log(r_a / r_f) \quad 3.14.$$

$$\text{and } (U_\infty - b) = \epsilon^2 / 4x + eV_a x / r_f \log(r_a / r_f) \quad 3.15.$$

In the Magnetron V_a is 120 volts, r_a is 2.25 cm, r_f is 1.25×10^{-2} cm and ϵ is 4.803×10^{-10} esu. Substituting these values into 3.14 and 3.15 gives $x = 4.42 \times 10^{-6}$ cm. and $(U_\infty - b) = 1.63 \times 10^{-2}$ electron volts.

As $(U_\infty - b)$ is only 1.63×10^{-2} ev., the ground state energy of the electron in the activated complex may be equated to that of an electron at infinity.

$$\text{Hence } N (b - (a + d)) = \chi \quad 3.16.$$

Substituting 3.16 into 3.13, introducing the transmission coefficient, \bar{d} , and noting that the gas constant $R = Nk$ gives

$$i_e = (\bar{d}\epsilon_0 k^2 m_e / h^3) T^2 \exp^{-\chi/RT} \quad 3.17.$$

which is the Dushman-Richardson⁹³ equation for electron emission.

3.2.3. Emission of Negative Ions

In applying the theory of rate processes to the formation of negative ions it is convenient to consider the problem in two parts, firstly to discuss the rate of emission of ions from a surface fully covered by the ion precursors and secondly to discuss the influence of temperature and pressure upon the number of ion precursors present on the surface. Although the model used describes a hypothetical fully covered surface, the following derivation is only intended to apply to sparsely covered surfaces, where interactions between the adsorbed precursors and desorbing ions and between the surface layers and the energy levels of the metal may be neglected.

Ions are presumed to be formed by the interaction of electrons in the metal with adsorbed ion precursors, either atoms or molecules, resulting in the formation of an activated state which may be irreversibly desorbed as an ion.

From 3.2 the equilibrium constant associated with the formation of the activated complex is

$$\begin{aligned} K^* &= (C_{AB^*}) / (C_{AB}) (C_m) \\ &= (Q_{AB^*} / Q_{AB} Q_m) \exp(- (b - a - f) / kT) \end{aligned} \quad 3.18.$$

$$\text{Hence } (C_{Ae^*}) = (C_{AB}) (C_m) Q_{AB^*} / Q_{AB} Q_m \cdot \exp(- (b - a - f) / kT) \quad 3.19.$$

where the activated complex, the adsorbate and the electrons in the metal are denoted by AB^* , AB and n , respectively, and a , b , f are the zero point energy of the electrons in the metal, the ground state energy of the system (ion precursor and electron in the activated state) and the ground state energy of the adsorbed ion precursor respectively.

Noting that $(C_m) = Q_m \cdot \exp(d/kT)$ and $Q_{AB^*} = (kT/h\nu)Q'_{AB^*}$ and introducing the transmission coefficient, \bar{d} , the rate of ion formation is given by:

$$\text{Rate} = (\bar{d}kT/h) \left((C_{AB}) \cdot Q'_{AB^*}/Q_{AB} \right) \exp(- (b - a - f - d)/kT) \quad 3.20.$$

If, as before, the energy zero at infinity is taken as the energy of the activated state, the algebraic sum of the energy terms may be equated to the sum of the work function, χ , the heat of desorption, E_d , and the Electron Affinity E of the ion precursor.

$$\text{i.e. } N(b - a - f - d) = E_d + \chi + E$$

And rate of ion emission

$$= (\bar{d}kT/h) \left((C_{AB}) \cdot Q'_{AB^*}/Q_{AB} \right) \exp(- (E_d + \chi - E)/RT) \quad 3.21.$$

or the ion current per unit area, i_i , is

$$i_i = (\epsilon \bar{d}kT/h) \left((C_{AB}) \cdot Q'_{AB^*}/Q_{AB} \right) \exp((E - \chi - E_d)/RT) \quad 3.22.$$

If the adsorption centres on the surface are regarded as reactants, and every adsorbed molecule uses up one active centre, the theory of rate processes defines the rate of adsorption, U_a , as

$$U_a = (C_s) (C_g) kT_g/h (Q'_{ab^*}/Q_g Q_s) \exp(-E_a/RT_g) \quad 3.23.$$

where (C_g) is the gas phase concentration of the adsorbate.

(C_s) is the concentration of adsorption sites.

Q_g is the gas phase partition function per unit volume

Q_s is the partition function per unit area for the adsorption sites

Q'_{ab*} is the partition function per unit area for the activated complex for adsorption.

E_a is the activation energy for adsorption

T_g is the gas temperature

and the rate of desorption, U_d , as

$$U_d = ((C_{AB})kT/h) (Q^*_d/Q_{AB}) \exp(-E_d/RT) \quad 3.24.$$

where Q^*_d is the partition function per unit area for the activated complex for desorption

E_d is the activation energy for desorption

T is the filament temperature.

Provided that ion formation represents only a minor perturbation of the adsorption-desorption equilibrium, the rates of adsorption and desorption may be equated to give:

$$\begin{aligned} (C_{AB})/Q_{AB} = & ((C_s)(C_g)T_g/T) (Q'_{ab*}/Q_g Q^*_d Q_s) \exp(-E_a/RT_g) \\ & \cdot \exp(E_d/RT) \end{aligned} \quad 3.25.$$

Substituting 3.25 into 3.22 gives

$$\begin{aligned} i_i = & (\epsilon dkT_g/h) ((C_s)(C_g)) (Q'_{ab*} Q'_{AB*}/Q_g Q^*_d Q_s) \exp(-E_a/RT_g) \\ & \cdot \exp(E - \chi/RT) \end{aligned} \quad 3.26.$$

As the adsorption centres are atoms of the metal, which have vibrational energy only, the partition functions Q_s may be taken as unity, hence $(C_s)/Q_s = f(1 - \theta)$, where θ is the fraction of surface covered by the adsorbate.

Hence substituting $(C_s)/Q_s = f(1 - \theta)$, $C_g = p/kT_g$ and noting that for most adsorption processes at low surface coverage the activation energy for adsorption, E_a , is zero and $(1 - \theta)$ will approxi-

mate to unity, the ion current is given by:

$$i_i = (\epsilon \bar{d} p / h) (Q'_{ab*} Q'_{AB*} / Q_g Q_d^*) \exp (E - \chi / RT) \quad 3.27.$$

As Q'_{ab*} contains only two translational degrees of freedom, (since one has been allowed for in the rate determining motion) and assuming the internal contributions to be equal Q'_{ab*} / Q_g is given by:

$$Q'_{ab*} / Q_g = h / (2\pi M_{AB} k T_g)^{1/2} \quad 3.28.$$

As Q'_{AB*} and Q_d^* each possess two translational degrees of freedom they can be replaced by the internal partition functions Q_i and Q , which represent the vibrational, rotational and electronic contributions for the activated state ion and the gas phase molecule, respectively, assuming that the latter is identical to those for the activated state for adsorption and the activated state for desorption.

$$\text{i.e. } Q'_{AB*} / Q_d^* = Q_i / Q \quad 3.29.$$

Substituting 3.28 and 3.29 into 3.27 gives

$$i_i = (\epsilon \bar{d} p / 2\pi M_{AB} k T_g)^{1/2} (Q_i / Q) \exp ((E - \chi) / RT) \quad 3.30$$

Hence combining 3.17 with 3.30, assuming that the transmission coefficients are identical, gives the basic equation governing negative ion emission in the magnetron.

$$\text{i.e. } i_e / i_i = (A T^2 Q / Q_i) \exp (-E / RT) \quad 3.31.$$

$$\text{where } A = 4\sqrt{2}\pi^{3/2} k^{5/2} m_e M_{AB}^{1/2} T_g^{1/2} / h^3 p.$$

3.2.4. Evaluation of Q/Q_i and temperature correction to 0°K .

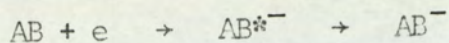
From magnetron results the apparent electron affinity, E_T , is determined, which is given by:

$$d(\log i_e / i_i) / d(1/T) = -E_T / R \quad 2.6.$$

Hence to calculate the true electron affinity of the ion precursor, E , in equation 3.31 the contribution of Q/Q_i must be evaluated

and a temperature correction applied due to the ~~pre~~-exponential factor being temperature dependent. Q/Q_i will be dependent upon the mode of formation of the ion: there are four modes of ion formation possible and these will be discussed in turn.

(i) Type 1 (Direct Capture)



In this case the molecular ion is formed ^{so} that is there is no dissociation of the substrate molecule, and the internal partition function for the activated state ion and the gas phase molecule are identical, except for the electronic contribution. The ground state of the ion will probably be a singlet and the molecule a doublet.

Hence $Q/Q_i = 2$ and 3.31 becomes:

$$i_e/i_i = 2(AT^2/\Delta) \exp(-E/RT) \quad 3.32.$$

Since $E_T = -Rd(\log i_e/i_i)/d(1/T)$ taking logarithms of 3.32 and differentiating with respect to $1/T$ gives

$$E_T = E + 2RT \quad 3.33.$$

(ii) Type 2.

This case refers to substrate molecules where fission occurs through a weak bond prior to any ion producing reaction. Energetically this is identical to a Type 1 process and the true electron affinity is given by 3.33.

(iii) Type 3. (Dissociation without Adsorption)

In this case the substrate molecule dissociates during ion formation and the dissociation energy of the bond broken, D , must be included in the exponential term in 3.31.

If it is postulated that the dissociation is caused by electron capture the only process which is affected by dissociation is the

ion forming reaction, since adsorption, desorption and electron emission precede capture or are not dependent upon it. Hence the activated state ion is of the same form as for direct capture reactions,



and only the three vibrations associated with the bond which breaks are considered, all others are presumed to be the same in the activated state ion as in the adsorbed molecule. In the activated state ion the vibrations associated with the bond which eventually breaks must be almost fully excited, that is the vibrational frequencies are approximately 100 cm^{-1} ⁹². Under these circumstances the ratio Q/Q_i in 3.31 is given by:

$$Q/Q_i = \prod_1^3 (1 - \exp(-h\nu_1^*/kT)) / \prod_1^3 (1 - \exp(-h\nu/kT)) \quad 3.34.$$

where ν_1^* , ν are the frequencies of the vibration in the activated state ion and the normal molecule, respectively.

T is the vibrational temperature of the adsorbed species in $^{\circ}\text{K}$, and assumed to be equal to the filament temperature.

h, k have their usual meanings.

Since ν_1^* approximates to 100 cm^{-1} 3.34 becomes:

$$Q/Q_i = (h\nu_1^*/kT)^3 / \prod_1^3 (1 - \exp(-h\nu/kT))$$

and the equation governing ion emission is:

$$i_e/i_i = AT^2 (h\nu_1^*/kT)^3 \prod_1^3 (1 - \exp(-h\nu/kT))^{-1} \exp(-(E - D)/RT) \quad 3.35.$$

Since $E_T = -Rd(\log i_e/i_i)d(1/T)$ taking logarithms of 3.35 and differentiating with respect to $1/T$ gives

$$E_T = E - D - RT + R \sum_1^3 h\nu/k (\exp(h\nu/kT) - 1) \quad 3.36.$$

If T and ν are taken to be 1500°K and 1000 cm^{-1} respectively

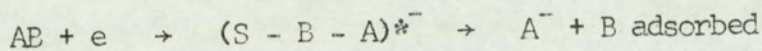
3.36 approximates to:

$$\begin{aligned} E_T &\approx E - D - RT + 3RT \\ \therefore E_T &\approx E - D + 2RT \end{aligned} \quad 3.37.$$

(iv) Type 4 (Dissociation with Adsorption)

In this case the substrate molecule dissociates during ion formation to give a negative ion, A^- , and a residue B , which is chemically adsorbed on the filament surface, S . This results in the bond dissociation energy, D , and the heat of adsorption of B on the filament surface, Q , being included in the exponential term in 3.31.

In this case the activated state for ion formation is planar and the overall ion-forming reaction is,



with the rate determining step now assumed to be the stretching of the $B - A^-$ bond instead of translation of the whole complex normally to the surface. Due to the activated state for ion formation being attached to the surface by the atom B , it must lose two rotational degrees of freedom and Q/Q_i is given by:

$$\begin{aligned} Q/Q_i &= ((8\pi^2 kT(I_x I_y)^{\frac{1}{2}})/(\sigma_g h^2/\sigma^*)) \\ &\cdot \prod_{i=1}^3 (1 - \exp(-h\nu_i^*/kT)) / \prod_{i=1}^3 (1 - \exp(-h\nu_i/kT)) \end{aligned} \quad 3.38.$$

Of the three vibrations associated with the bond that breaks, one is rate determining and the other two are assumed, as in the previous case, to have a frequency of 100 cm^{-1} . Hence:

$$\begin{aligned} Q/Q_i &= ((8\pi^2 kT(I_x I_y)^{\frac{1}{2}})/\sigma_g h^2/\sigma^*) (h\nu_1^*/kT)^2 \cdot (1 - \exp(-h\nu_1/kT)) \\ &\quad \prod_{i=1}^3 (1 - \exp(-h\nu_i/kT)) \end{aligned} \quad 3.39.$$

where ν_1 is the frequency of the surface - B vibration

σ_g, σ^* are the symmetry factors for the gas phase molecule and activated state complex, respectively.

I_x, I_y are the moments of inertia associated with the two rotational degrees of freedom lost by the activated state complex, I_z being the moment of inertia about the S - B - A* axis.

And the equation governing ion formation is:

$$i_e/i_i = BT(1 - \exp(-h\nu_1/KT)) \prod_{i=1}^3 (1 - \exp(-h\nu_i/KT))^{-1} \cdot \exp(-(E - D + Q)/RT) \quad 3.40.$$

Where $B = A \cdot (h\nu_1/k)^2 (8\pi^2k (I_x I_y)^{1/2} / \sigma_g h^2 / \sigma^*)$

$$\text{And } E_T = E - D + Q + RT + R \sum_{i=1}^3 \ln \exp(h\nu_i/KT) - 1 - R h \nu_1 / k (\exp(h\nu_1/KT) - 1) \quad 3.41.$$

If as before $T \approx 1500^\circ\text{K}$ and $\nu = \nu_1 \approx 1000 \text{ cm}^{-1}$, 3.41 approximates to

$$\begin{aligned} E_T &\approx E - D + Q + RT + 3RT - RT \\ \therefore E_T &\approx E - D + Q + 3RT \end{aligned} \quad 3.42.$$

The validity of expressions 3.37 and 3.42 depends upon the vibrational frequencies in the molecule, hence expressions 3.36 and 3.41 are more correct. Also vibrational energy transfer is a slow process and the vibrational temperature could lie anywhere between gas temperature and filament temperature. This implies that the correction to E for dissociative capture and dissociative capture with adsorption could lie between -RT and 2RT, and RT and 3RT, respectively.

Since the vibrational temperature is unknown the equations used, in this dissertation, for evaluation of Electron Affinities are 3.33, 3.37, 3.42.

3.2.5. Evaluation of the Electron Affinity from log-log plots

Under circumstances where continuous deposition on or etching of the filament occurs it is difficult to accurately determine the filament temperature. In such cases, provided the experimental work function χ_T is known the 'apparent electron affinity', and hence the true electron affinity can be evaluated from the slope of a plot of the logarithm of the ion current against the logarithm of the electron current.

$$\text{i.e. From 3.17.} \quad R d (\log i_e) / d(1/T) = - \chi - 2RT = - \chi_T$$

$$\text{From 3.27.} \quad R d (\log i_i) / d(1/T) = E - \chi - nRT = E_T - \chi_T$$

$$\text{Hence } d \log i_i / d \log i_e = - (E_T - \chi_T) / \chi_T \quad 3.43.$$

$$\text{And } E_T = E + (2 - n)RT$$

where n depends upon the mode of ion formation and is discussed in 3.2.4.

3.2.6. The Entropy of the Reaction

Combining equations 3.17 and 3.27 and noting that $Q^{*'} = 2(2\pi m_e kT/h^2)$ gives:

$$i_e / i_i = (kT/p) (Q_g / Q'_{ab*}) (Q^*_d Q^{*'} / Q'_{AB*}) \exp (E_a / RT_g) \exp - (E / RT) \quad 3.44.$$

which may be written in the form:

$$i_e / i_i = (kT/p) K_1 K_2 \quad 3.45.$$

where K_1 and K_2 are the concentration equilibrium constants for the reactions:



If ΔG_1 and ΔG_2 are the associated Gibb's Free Energy changes, 3.45 may be written as:

$$i_e/i_i = (kT/p) \exp(-\Delta G_1/RT_g) \exp(-\Delta G_2/RT) \quad 3.48.$$

Since $\Delta G = \Delta H - T\Delta S$ 3.48 becomes:

$$i_e/i_i = (kT/p) \exp(-\Delta H_1/RT_g) \exp(\Delta S_1/R) \exp(-\Delta H_2/RT) \exp(\Delta S_2/R) \quad 3.49.$$

If the adsorption process is non-activated $\Delta H_1 = 0$ and defining $\Delta S = \Delta S_1 + \Delta S_2$ 3.49 becomes:

$$i_e/i_i = (kT/p) \exp(-\Delta H_2/RT) \exp(\Delta S/R) \quad 3.50.$$

Taking logs of 3.50 and differentiating with respect to T and noting that $d(\log i_e/i_i)/dT = E_T/RT^2$ gives $E_T = RT + \Delta H_2$. Hence taking logs of 3.50, re-arranging and substituting for ΔH_2 gives:

$$\Delta S = R(\log(i_e/i_i) - \log(kT/p)) + E_T/T - R \quad 3.51.$$

$$= 4.56(18.98 + \log_{10}(i_e/i_i) - \log_{10}(T/p)) + E_T/T - 1.98 \quad 3.52.$$

Where T is in $^{\circ}\text{K}$, R and E_T are in cal/mole/ $^{\circ}\text{K}$, p is in mm of Hg. and ΔS is the sum of the entropy changes for the reactions of equations 3.46 and 3.47 with all transition states in the standard state of one mole per cm^2 and the gas molecules in the standard state of one mole per cm^3 .

Farragher⁸⁷ found that the value for the change in entropy was characteristic of the mode of ion formation and could, therefore, be used as a diagnostic test for the reaction type.

Type 1 and 2 being given by: $\Delta S = 110 \pm 17$. e.u.

Type 3 " " " $\Delta S = 53 \pm 7$. e.u.

Type 4 " " " $\Delta S = 82 \pm 5$. e.u.

4. POLARISATION CAPTURE AFFINITIES

4.1 Introduction

Experimental evidence shows that species which have a positive electron affinity can be classified into four groups, according to the type of ion formed.

The first group contains ions formed when a free radical accepts an electron to form a singlet ion, where the electron is apparently localized as a lone pair. This type of ion is discussed in chapter 5 of this dissertation.

The second group contains doublet ions which are formed from singlet molecules with a delocalized π electron system. This type of ion has been extensively examined by Farragher⁸⁷ and Burdett⁸⁸.

The third group contains multiplet ions formed from multiplet acceptors; the only examples so far quoted are S^- and O^- .

The last group contains doublet ions which are formed when a singlet molecule containing no delocalized π electron system captures an electron. The existence of these negative ions cannot be described simply in terms of the orbitals of the uncharged acceptor but must include the distortion of the electron distribution within the ion. An example of this type of ion is SF_6^- , which has been identified by Fox and Hickman⁹⁴, using a mass spectrometer and by Herron, Rosenstock and Shields⁹⁵, who showed that SF_6^- was formed at a hot tungsten surface in the presence of SF_6 vapour. Page et al^{96,97,98} found, using the Magnetron technique, evidence that at low temperatures ion formation occurred in the presence of SF_6 , CCl_4 , $CHCl_3$, CH_2Cl_2 , C_2Cl_6 , BF_3 and CBr_4 which they attributed to the formation

of, respectively, SF_6^- , CCl_4^- , CHCl_3^- , CH_2Cl_2^- , C_2Cl_6^- , BF_3^- and CBr_4^- .

In this work, using tellurium hexafluoride, tungsten hexafluoride and uranium hexafluoride as substrate gases, copious negative ion currents were observed over a temperature range 1200-1600°K, which are, similarly, attributed to the formation of, respectively, TeF_6^- , WF_6^- and UF_6^- .

4.2 Experimental

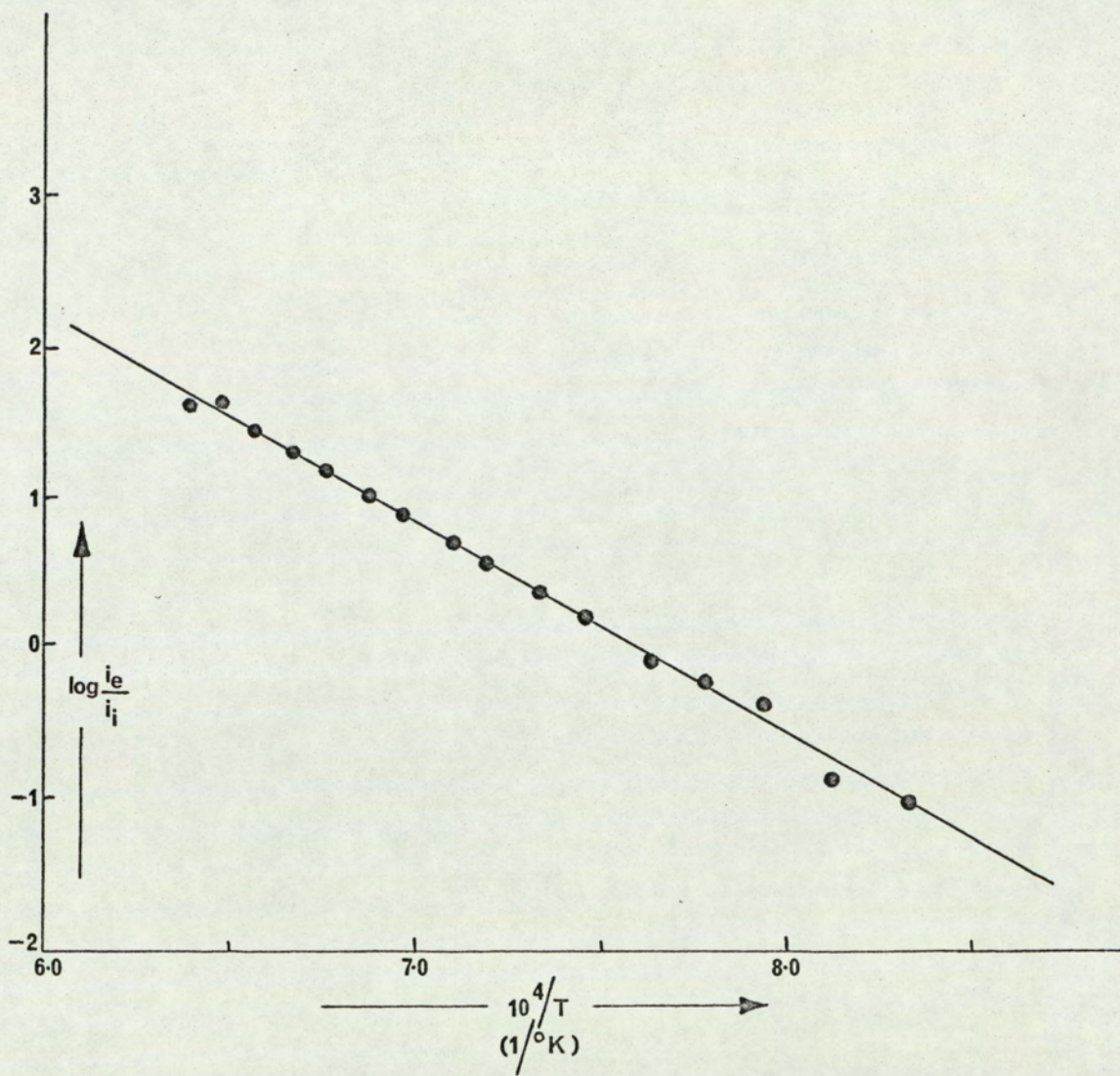
All the three compounds, at low temperatures, gave a negative ion current that was greater than the corresponding electron current; hence to evaluate the electron current, the ion current (the current in the presence of the magnetic field) had to be subtracted from the corresponding total current (current in the absence of the magnetic field).

Tellurium hexafluoride

The sample was obtained from Professor R.D. Peacock, Leicester University, the filament used was platinum and the sample pressure was approximately 1.0×10^{-4} Torr. The values for the apparent electron affinity, at a mean filament temperature of 1400°K, were 64.0, 59.4, 65.8, 67.2, 69.5, 71.8 and 59.5 kcals/mole, which gave a mean value for E_T of 65.3 ± 4.7 kcals/mole. A typical graph is shown in figure 9.

Tungsten hexafluoride

The sample was obtained from Cambrian Chemicals Ltd., the filament used was platinum and the sample pressure was approximately 4.5×10^{-4} Torr. The values for the apparent electron affinity, at



ELECTRON CAPTURE BY TeF_6/Pt

FIG. 9.

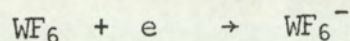
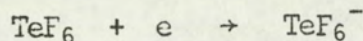
a mean filament temperature of 1437°K were 75.8, 73.1, 74.0, 73.1, 74.5, 71.3 and 75.8 kcal/mole, which gave a mean value for E_T of 73.9 ± 1.6 kcal/mole. A typical graph is shown in figure 10.

Uranium hexafluoride

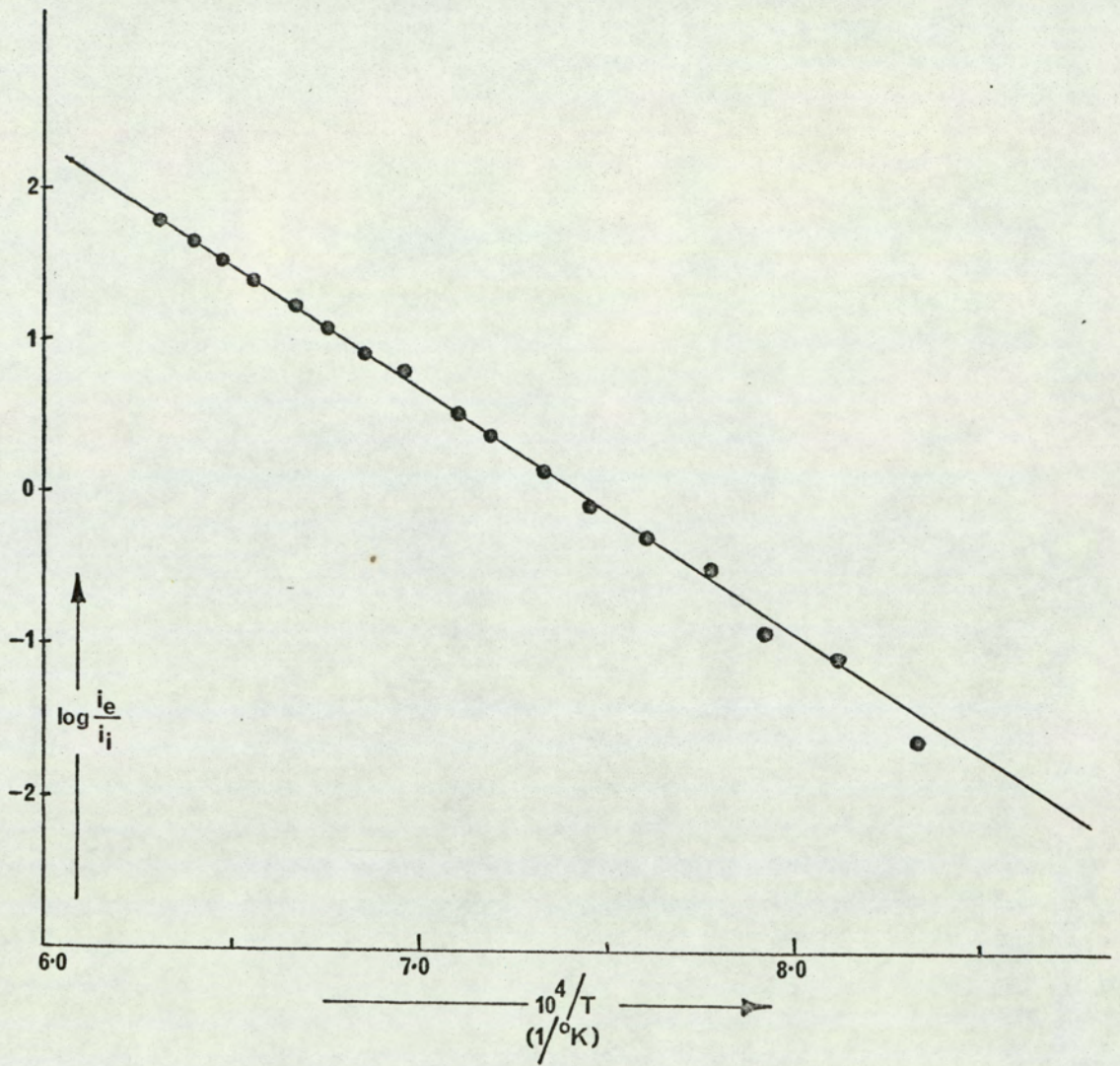
The non-active sample was obtained from the United Kingdom Atomic Energy Authority, the filament used was platinum and the sample pressure was approximately 4.5×10^{-4} Torr. The values obtained for the apparent electron affinity, at a mean filament temperature of 1410°K were 89.6, 86.5, 82.7, 97.4 and 95.6 kcal/mole, which gave a mean value for E_T of 90.2 ± 6.1 kcal/mole. A typical graph is shown in figure 11.

4.3 Discussion

The change in entropy for the overall ion forming reaction is given by equation 3.52 as $\Delta S = 4.56 (18.98 + \log_{10} (i_e/i_i) - \log_{10} (T/P)) + E_T/T - 1.98$. Substituting the appropriate values into the above equation gives ΔS for TeF_6 , WF_6 and UF_6 as 102.0, 109.9 and 124.4 entropy units, respectively, which are typical of a type 1 process, that is direct capture of an electron by the molecular species. Hence the reactions postulated for these compounds are:

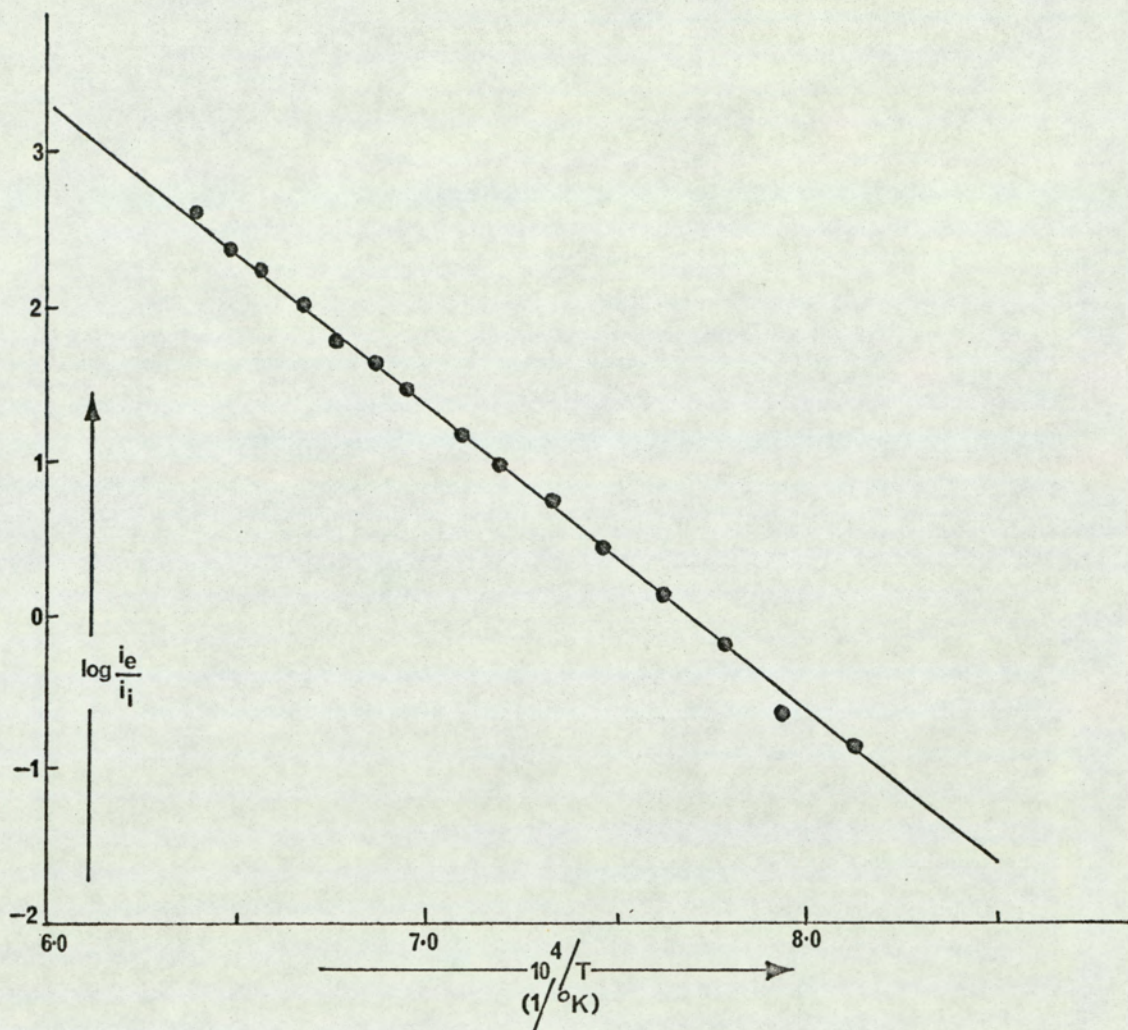


For this type of process the apparent electron affinity is given by equation 3.33 as $E_T = E + 2RT$, where E is the electron affinity of the species and T is the mean filament temperature. Substituting the appropriate values of E_T and T for, respectively, TeF_6 , WF_6 and



ELECTRON CAPTURE BY WF_6/Pt

FIG. 10.



ELECTRON CAPTURE BY UF_6/Pt

FIG. 11.

UF₆ leads to values for the electron affinities of E(TeF₆) = 59.7 ± 4.7, E(WF₆) = 68.2 ± 1.6 and E(UF₆) = 84.6 ± 6.1 kcal/mole.

With polarisation capture ions the negative charge can be thought of as being distributed between the outer atoms in the molecule; Hush and Segal⁹⁹ calculated that for CFH₃⁻ the negative charge distribution is 0.314e and 0.26e for the fluorine and hydrogen atoms respectively, with the central carbon atom bearing a slightly positive charge.

Using this calculation as a basis, a model may be constructed in which a tetrahedral ion, such as CCl₄⁻ is represented as a combination of the four states, as shown in figure 12, where the stability of the ion is mainly due to the electrostatic interaction of the negative charge with the polarizable CCl₃ group, since the next available orbitals in chlorine would require considerable promotion energy.

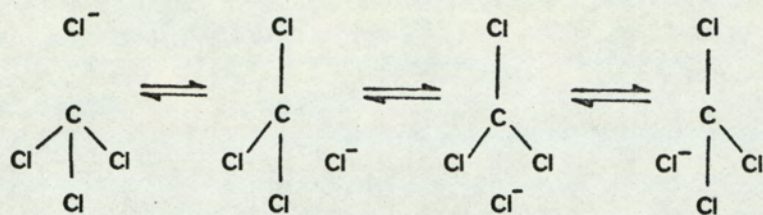
If the polarizability of the CCl₃ group is αCCl₃ and the distance between the negative charge and the centroid of the CCl₃ group is r then the energy due to electrostatic interaction is given by¹⁰⁰

$$W = -\frac{1}{2} \cdot \frac{e^2}{r^4} \cdot \alpha\text{CCl}_3 \quad 4.1$$

The effective values of αCCl₃ and r may be determined approximately by treating the CCl₃ group as three isotropic polarization ellipsoids, each contributing a quarter of the molecular polarizability, α₀, with centroids at the mid-point of the C - Cl bond. Hence

$$W = -\frac{e^2}{2} \sum \frac{\alpha_0}{4r^4} \quad 4.2$$

where r may be calculated in terms of the C - Cl covalent bond length, a, as shown in figure 13.



RESONANCE STATES OF $\cdot\text{CCl}_4^-$.

FIG. 12.

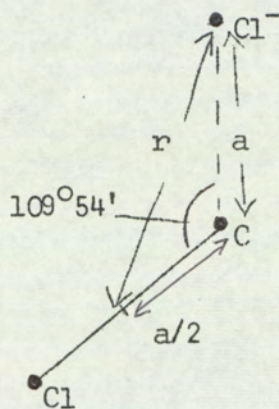


Figure 13

Evaluating for r gives:

$$W = -\frac{1}{2} \cdot \frac{3}{4} \alpha_0 \cdot \frac{1}{2.485 a^4} \cdot e^2 \quad 4.3.$$

$$= -0.1509 \cdot \frac{e^2 \alpha_0}{a^4} \quad 4.4.$$

Similarly for a planar, trigonal ion XY_3^- e.g. BF_3^-

$$W = -0.1088 \cdot \frac{e^2 \alpha_0}{a^4} \quad 4.5.$$

for an octahedral ion XY_6^- e.g. SF_6^-

$$W = -0.2298 \cdot \frac{e^2 \alpha_0}{a^4} \quad 4.6.$$

and for an ion $X_2Y_6^-$ e.g. $C_2Cl_6^-$

$$W = -0.0724 \cdot \frac{e^2 \alpha_0}{a^4} \quad 4.7.$$

or expressing the relationship in terms of the molar refraction, (R) in ccs, gives:

$$\text{Trigonal } XY_3 \quad W = -13.90 \frac{(R)}{a^4} \quad 4.8.$$

$$\text{Tetrahedral } XY_4 \quad W = -19.20 \frac{(R)}{a^4} \quad 4.9.$$

$$\text{Octahedral } XY_6 \quad W = -29.30 \frac{(R)}{a^4} \quad 4.10.$$

$$\text{Ethane-like } X_2Y_6 \quad W = -9.20 \frac{(R)}{a^4} \quad 4.11.$$

Where a is the X-Y covalent bond length in Å, and W is then in kcal/

mole.

Table 2 gives the experimental and calculated electron affinities.

Table 2

Compound	Calculated Electron Affinity (kcal/mole)	Experimental Electron Affinity (kcal/mole)
CCl ₄	52.8	47.4 ⁽⁹⁷⁾
CHCl ₃	61.1	39.2 ⁽⁹⁷⁾
CH ₂ Cl ₂	67.8	30.1 ⁽⁹⁷⁾
C ₂ Cl ₆	38.9	32.8 ⁽⁹⁷⁾
BF ₃	29.7	61.0 ⁽⁹⁸⁾
SF ₆	41.5	33.0 ⁽⁹⁶⁾
CBr ₄	54.7	46.7 ⁽⁹⁸⁾

In all cases the calculated electron affinity will be a maximum value since the Y⁻-X bond will be significantly longer than the covalent bond used in the calculation. Nevertheless, the correlation with the experimental electron affinities is quite good for these molecules, with the exception of BF₃, CHCl₃ and CH₂Cl₂. In calculating the electron affinities of CHCl₃ and CH₂Cl₂ it has been assumed, in the absence of charge distribution data, that the negative charge of the anion is equally distributed between the hydrogen and chlorine atoms. This is unlikely to be true, hence the contribution of the



ionic state is over-estimated, which due to the short C-H bond length leads to a high value for the calculated electron affinities.

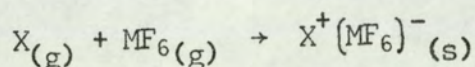
Many compounds of the first and second row elements may be treated in this manner but the extension to the heavy elements such as TeF_6 , WF_6 , and UF_6 is not satisfactory because of the unknown contribution of the inner shell electrons of the heavy atom to the total polarizability. However, an estimate for the electron affinity of the hexafluorides of the heavier elements may be determined semi-quantitatively from a comparative study of the reactions undergone by these compounds.

O'Donnell and Stewart¹⁰¹ have shown that of the three hexafluorides of uranium, tungsten and molybdenum, uranium hexafluoride is the much stronger oxidant. For example they found that tungsten hexafluoride was reduced only with great difficulty by phosphorus trifluoride whereas molybdenum hexafluoride was much more readily reduced by phosphorus trifluoride, although there was some evidence of an equilibrium in the reaction, and uranium hexafluoride was very readily reduced. Similarly, uranium hexafluoride was reduced to some extent by arsenic trifluoride whereas neither molybdenum hexafluoride nor tungsten hexafluoride were reduced. Unequivocal evidence that uranium hexafluoride is a stronger oxidant than molybdenum hexafluoride and tungsten hexafluoride was provided by the fact that uranium hexafluoride readily oxidised tungsten tetrafluoride and molybdenum pentafluoride to the corresponding hexafluorides.

Since oxidation - reduction reactions involve basically the transfer of electrons, where the species that is oxidised loses an electron and conversely, the species that is reduced gains an electron,

then the relative oxidising powers of a series of compounds should give an indication of their relative electron affinities; that is the greater the oxidising power of the species then the greater the value of its electron affinity. Hence from the above experimental evidence the electron affinities of the three hexafluorides should be in the order $UF_6 > MoF_6 > WF_6$.

Recently several workers^{101,102,103} have demonstrated the high oxidising powers of the heavier metal hexafluorides by the preparation of compounds of the type $X^+(MF_6)^-$ from the reaction:



Then, provided the lattice energy of the species $X^+(MF_6)^-$ is known, along with the first ionization potential of X, an estimate for the electron affinity of MF_6 may be made.

It has been shown that molecular oxygen and atomic xenon were spontaneously oxidised by platinum hexafluoride¹⁰³, a reaction that was not undergone by any of the other third transition series hexafluorides. The products of these reactions has been established¹⁰³ as respectively the salts $O_2^+(PtF_6)^-$ and $Xe^+(PtF_6)^-$.

Similarly, the hexafluorides of platinum¹⁰³, iridium¹⁰³, osmium¹⁰³, rhenium¹⁰³, tungsten^{101,102,103}, molybdenum^{101,102}, and uranium^{101,102} were shown, with the exception of tungsten hexafluoride, to oxidise nitric oxide to produce the salt $NO^+(MF_6)^-$. Whereas only osmium, iridium and platinum hexafluorides¹⁰³ reacted with nitrosyl fluoride to produce the ionic product $NO^+(MF_6)^-$. The remaining four hexafluorides, rhenium hexafluoride¹⁰³, tungsten hexafluoride^{101,103}, uranium hexafluoride¹⁰¹ and molybdenum hexafluoride¹⁰¹ reacted with

nitrosyl fluoride to form adducts of the type NOMF_7 and $(\text{NO})_2\text{MF}_8$; this is particularly significant since no reduction of the hexafluorides was necessary to form these adducts. (In all cases the ionic nature of the salts $\text{X}^+(\text{MF}_6)^-$ was deduced from their infra-red absorption spectra and X-ray diffraction data.)

A summary of the reactions of the hexafluorides with, respectively, molecular oxygen, nitric oxide and nitrosyl fluoride is given in table 3 and discussed below in the order i) $\text{O}_2 + \text{MF}_6$ ii) $\text{NO} + \text{MF}_6$ iii) $\text{ONF} + \text{MF}_6$.

Table 3

Compound	Reaction Products		
	$\text{O}_2 + \text{MF}_6$	$\text{NO} + \text{MF}_6$	$\text{ONF} + \text{MF}_6$
WF_6	no reaction	no reaction	$\text{NOWF}_7 + (\text{NO})_2\text{WF}_8$
ReF_6	"	$\text{NO}^+(\text{ReF}_6)^-$	$(\text{NO})_2\text{ReF}_8$
OsF_6	"	$\text{NO}^+(\text{OsF}_6)^-$	$\text{NO}^+(\text{OsF}_6)^- + \text{NOOsF}_7 + \text{ONF}_3\uparrow$
IrF_6	"	$\text{NO}^+(\text{IrF}_6)^-$	$\text{NO}^+(\text{IrF}_6)^- + \text{ONF}_3\uparrow + \text{F}_2\uparrow$
MoF_6	"	$\text{NO}^+(\text{MoF}_6)^-$	NOMoF_7
UF_6	"	$\text{NO}^+(\text{UF}_6)^-$	NOUF_7
PtF_6	$\text{O}_2^+(\text{PtF}_6)^-$	$\text{NO}^+(\text{PtF}_6)^- + \text{F}_2\uparrow$	$\text{NO}^+(\text{PtF}_6)^- + \text{F}_2\uparrow$

i) Since the lattice energy of $O_2^+(MF_6)^-$ is estimated to be about 125 kcal/mole¹⁰³ and the first ionisation potential of molecular oxygen is 281 kcal/mole¹⁰⁴ then the electron affinity of MF_6 must be greater than 156 kcal/mole to account for the observed exothermic reaction $PtF_6(g) + O_2(g) \rightarrow O_2^+(PtF_6)^-(s)$, which suggests that of the hexafluorides, platinum hexafluoride alone has an electron affinity in excess of 156 kcal/mole.

ii) Similarly, the hexafluorides which react with nitric oxide to form salts of the type $NO^+(MF_6)^-$ must have a minimum value for the electron affinity of approximately 90 kcal/mole, since the lattice energy of $NO^+(MF_6)^-$ is estimated as 125 kcal/mole¹⁰³ and the first ionisation potential of nitric oxide is 213 kcal/mole¹⁰⁴; which suggests that the hexafluorides of platinum, iridium, osmium, rhenium, molybdenum and uranium have an electron affinity greater than about 90 kcal/mole.

iii) And lastly, since the enthalpy of dissociation of $ONF(g) \rightarrow NO(g) + F(g)$ has been given as 55 kcal/mole¹⁰⁵, which results in a ΔH for the process $ONF(g) \rightarrow NO^+(g) + F(g) + e$ of 268 kcal/mole, a minimum electron affinity of MF_6 for an exothermic reaction

$ONF(g) + MF_6(g) \rightarrow NO^+(MF_6)^-(s) + F(g)$ would be 143 kcal/mole,

although for the liberation of molecular fluorine this would be reduced to approximately 125 kcal/mole, since the bond dissociation energy of fluorine is 36 kcal/mole¹⁰⁶.

On the basis of the above reactions it is evident that the electron affinity of MF_6 increases regularly in the sequence W, Re, Os, Ir and Pt and also that $E(UF_6) > E(MoF_6) > E(WF_6)$. Where $E(ReF_6)$,

$E(\text{MoF}_6)$ and $E(\text{UF}_6)$ have values greater than 90 kcal/mole but less than 125 kcal/mole, $E(\text{IrF}_6)$ has a value greater than 125 but less than 156 kcal/mole and lastly $E(\text{PtF}_6)$ have a value greater than 156 kcal/mole.

Hence, for the third transition series hexafluorides, the increase in the electron affinity with unit change in atomic number of M appears to be approximately 20 kcal/mole, which suggests that the electron affinity of gold hexafluoride could be greater than 176 kcal/mole and $E(\text{WF}_6)$ should be greater than 70 but less than 90 kcal/mole.

The calculated values for uranium and tungsten hexafluorides of, respectively, >90 kcal/mole and > 70 kcal/mole are in reasonable agreement with the experimentally determined values of $E(\text{UF}_6) = 84.6 \pm 6.1$ kcal/mole and $E(\text{WF}_6) = 68.2 \pm 1.6$ kcal/mole.

Of the hexafluorides of sulphur, selenium and tellurium, SF_6 is extremely inert, whereas SeF_6 and TeF_6 are reduced by NH_3 but not by PF_3 ¹⁰⁷; TeF_6 alone has a weak Lewis acidity¹⁰⁸, combining with F^- in the presence of large cations to form either TeF_7^- or TeF_8^- , and with trialkyl amines to form adducts of the formula $(\text{R}_3\text{N})_2\text{TeF}_6$. The reactions undergone by sulphur, selenium and tellurium hexafluorides, as compared with those for tungsten hexafluoride, show WF_6 to have the higher oxidising power and presumably, therefore, the higher electron affinity, as is found experimentally since $E(\text{SF}_6) = 33$ ⁹⁶ and $E(\text{TeF}_6) = 59.7 \pm 4.7$ kcal/mole.

5. σ CAPTURE AFFINITIES

5.1 Introduction:

In many cases the capture of an electron by a doublet free radical leads to the formation of a stable singlet negative ion⁸⁶, for example



and it is of interest to determine whether the electron added in forming the negative ion is localised on the accepting centre as a lone pair or is delocalised over the whole system. If the electron is localised on the accepting centre as a lone pair then the stability of the ion would be expected to be determined by the nature and valence state of the accepting centre, with substitutional effects acting in a secondary manner.

Experimental evidence shows that the electron affinity of a radical is very sensitive to the nature and valence state of the accepting centre; substitution at this centre has a small effect on the electron affinity causing values for the electron affinity to be approximately 5 kcal/mole above or below the value, depending on the inductive effect of the substituents, found for the hydrogen substituted radical. This is in accordance with the postulate that the additional electron is localised on the central atom at which the free valence lay.

Goddard¹⁰⁹ has recently been successful in giving a quantum mechanical explanation for the stabilities of H^- and Li^- . He showed that the stability of H^- and Li^- arises from an 'exchange term', in particular the nuclear attraction part of this term; the exchange term he describes as being identical to the exchange term in the valence bond wave function of the hydrogen molecule. Extending this idea to the

addition of an electron to a doublet free radical would suggest, in general, that the stability of the resulting ion can be considered to arise from an interaction of the additional electron and the central atom, forming a σ type bond. Radicals forming ions in such a manner are termed to have a σ Electron Affinity.

In order to study the effect that the nature and valence state of the accepting centre, and substitutional effects at this centre, have upon the electron affinity of the radical three approaches have been utilised. Firstly the nature and valence state of the electron accepting centre were kept constant and the effect of substitution at the accepting centre upon the electron affinity of the radical was determined. Secondly the nature of the accepting centre was kept constant but the valence state of the accepting centre was varied and thirdly the nature of the accepting centre was varied but the valence state of the centre was the same in each case. The compounds studied, the results and discussion are given in sections 5.2., 5.3., 5.4., and 5.5.

Then provided the electron affinities of the radical and the atomic centre of acceptance can be equated, the experimental electron affinity can be compared to the theoretical values, deduced from the tables of promotion energies for atoms and their ions given by Hinze and Jaffe⁵⁶.

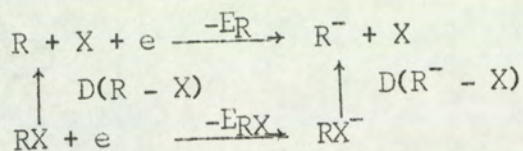
If a radical or molecule $R - X$ is considered, where R is the atomic centre and X is the substituent, then the negative ion may be formed by two processes.

- 1) Form the radical or molecule ion RX^- , which then dissociates

to give the atomic ion R^-

or 2) Dissociate the radical and then form the negative atomic ion.

The two processes can be described by the following energy cycle.



$$\text{Hence } E_R = E_{RX} + (D(R - X) - D(R^- - X)) \quad 5.2.$$

As the term within the brackets will tend to zero, provided there is not a great disparity in the electronegativities of R and X or a change in the hybridisation of R on dissociation, then the σ electron affinity of a radical may be identified with the electron affinity of the acceptor atom in the same valence state. However, if X is very electronegative as in the case of fluorine, considerable errors could be introduced.

The method Hinze & Jaffe⁵⁶ used to evaluate the promotion energies for the various valence states of the atom was to firstly evaluate the Slater equations for all spectroscopic states, arising from configurations composed of s, p and d electrons and then evaluate the Slater Condon parameters by fitting the observed spectroscopic data to the appropriate Slater equations by a least squares method. Since valence state equations are expressed in Slater Condon parameters this allowed the determination of valence state energies. The valence state energies calculated by Hinze are identical with the corresponding valence state promotion energy since he chose the zero of the energy scale to be the spectroscopic ground state.

With negative ions it is impossible to determine the valence state

promotion energies directly as no spectral determinations have been made but Hinze, utilising Kohn's¹¹⁰ extrapolation method, determined the promotion energies for the negative ions of elements, with no open shells, by extrapolating along a series of equivalent valence states of an isoelectronic sequence.

For the evaluation of valence state electron affinities, the electron affinity of the atomic ground state is required beside the promotion energy terms. As the electron affinities of the atomic ground states for negative ions have not in general been determined experimentally, except in the case of carbon, given by Branscomb as $E(C) = 1.25 \pm 0.03 \text{ eV}^5$, the ground state electron affinities are determined using the extrapolation method of Edlen⁴⁵, as described in Chapter 1.

Then provided the bond energy terms in equation 5.2 are negligible, so the electron affinity of the radical can be equated to the electron affinity of the atom in the same valence state, the electron affinity of the radical for a particular valence state, E_v , is given by:

$$E_v = E_g + (P_o - P_-) \quad 5.3.$$

where E_g is the electron affinity of the ground state and P_o and P_- are the promotion energies of the atom and the ion, in the same valence state.

Therefore, if the probable valence state of the radical can be postulated from the known chemical nature and in some cases the known geometry, then from the promotion energy and ground state electron affinity data it is possible to calculate the energy involved in forming the negative ion (i.e. the electron affinity of the ion precursor),

assuming that no rehybridisation takes place in the ion forming process. This can then be compared to the experimental value. Conversely, if the valence state of the radical or ion is difficult to postulate then the comparison of the experimental electron affinity with the theoretical electron affinities for various valence states of the radical will allow prediction of the valence states of both the radical and corresponding negative ion to be made.

As stated earlier, the main aim is to study systems which will indicate the way in which the additional electron is added to the ion precursor and then compare the experimental electron affinities with those calculated using the promotion energy data of Hinze and Jaffe⁵⁶.

To study the effect of substitution at the accepting centre on the stability of the negative ion a series of substituted amines were examined, as the electron affinity of NH_2 is well known^{40,41}. The results are given in section 5.4.

To study the effect upon the electron affinity as one descends a group in the periodic table, where in each case the centre of acceptance is in the same valence state, the systems CF_3 , SiF_3 and NH_2 , PH_2 were studied. The results are given in section 5.3 and 5.4.

And lastly to study how the stability of the negative ion, of a particular centre of acceptance, is affected by the valence state of the centre of acceptance, the electron affinity of the C_2H radical was determined and compared to the values quoted by Smith for $\text{E}(\text{CH})$ ¹¹¹ and Page et. al. for $\text{E}(\text{CH}_3)$ ¹¹² and $\text{E}(\text{C}_6\text{H}_5)$ ¹¹³.

5.2. Electron Capture by Acetylene:

5.2.1. Introduction:

The chemistry of the acetylenes, for example their ability to form fully ionised compounds of the formula $(M^+)(C_2H^-)^{114}$, where M can be any of the alkali metals, and the abundance of C_2H^- found in the mass spectra of hydrocarbons¹¹⁵, aliphatic alcohols¹¹⁶ and flames with hydrocarbon additives¹¹⁷ suggests that C_2H^- has a high stability and is likely to be readily formed at an emitting filament.

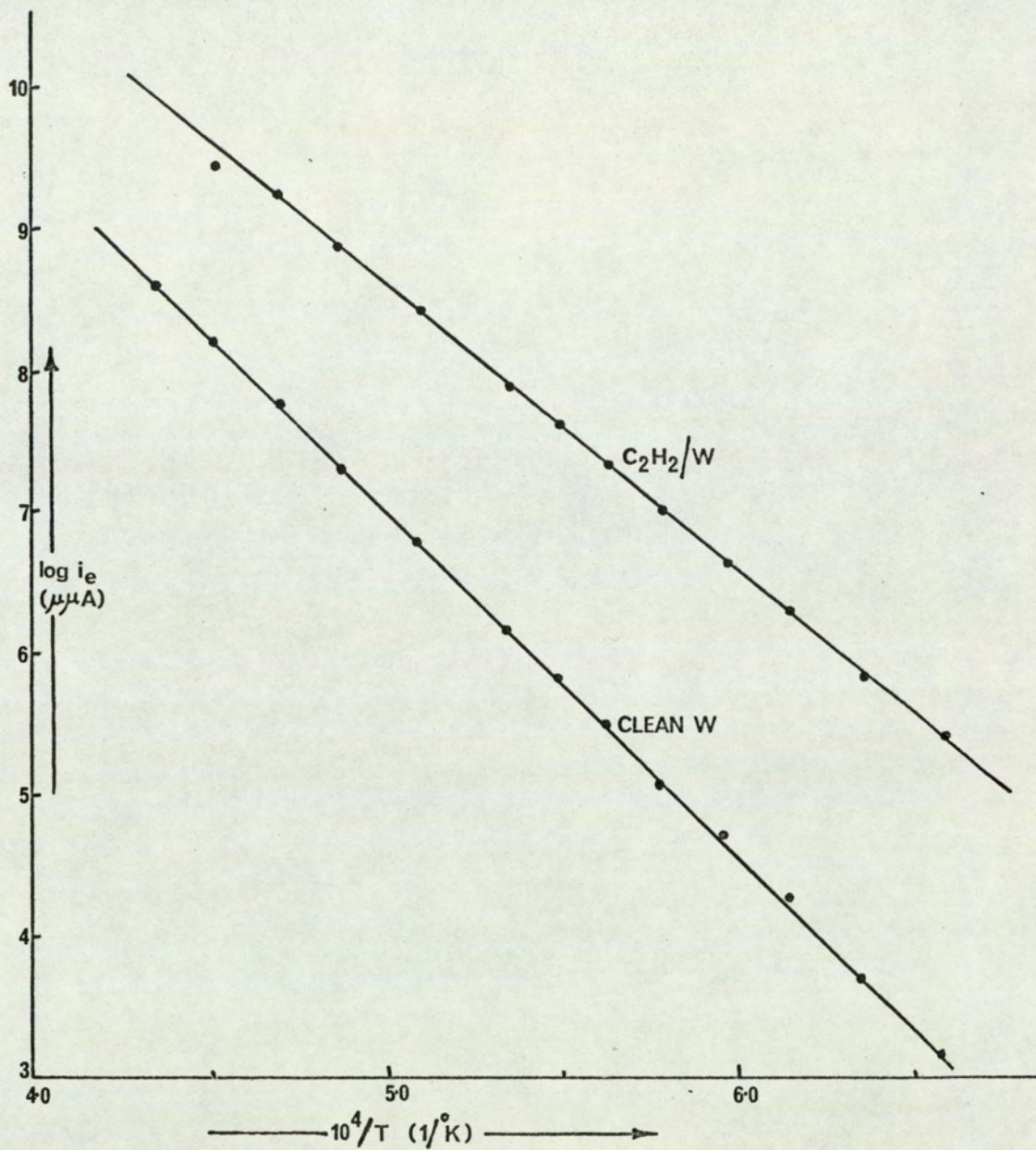
5.2.2. Experimental:

The C_2H_2 was supplied by Cambrian Chemicals Ltd., the filament used was tungsten and the sample pressure was approximately 2×10^{-3} Torr.

The effect of acetylene upon the tungsten filament was to lower the work function from 112.8 ± 2.1 kcal/mole for the 'clean' surface to 90.9 ± 2.4 kcal/mole (the mean filament temperature was $1786^\circ K$), and hence increase the electron emission for a particular temperature. A graph indicating this effect is shown in fig. 14.

To ensure a reproducible filament surface the tungsten filament was kept at $2000^\circ K$, in the presence of acetylene vapour, for fifteen minutes, prior to any measurements being taken. The effect of acetylene vapour upon the filament was very rapid, producing, for any particular temperature, a rapid rise in electron current, which attained a constant value after about ten minutes.

The source of acetylene was disconnected from the Magnetron and the filament was heated at $1800^\circ K$ while the magnetron assembly was continuously pumped. There was not a reduction in the electron emission for a particular filament temperature and the work function of the



ELECTRON WORK FUNCTION FOR W & C_2H_2/W .

FIG. 14.

tungsten surface remained at almost the same value as that given by the tungsten surface in the presence of acetylene, which suggests that there has been a chemical or physical change in the tungsten filament rather than adsorption of a species on the filament surface as the latter is a reversible effect.

The graphs obtained from plotting $\log i_{ep}/i_i$ against I/T gave apparent electron affinities of 32.5, 35.7, 32.0, 26.1, 26.1, 33.6, 24.7, 33.8, 35.0 and 27.9 kcal/mole, giving an average value for E_T of 30.7 ± 4.1 kcal/mole at an average filament temperature of 1670°K . A typical run is shown in figure 15.

5.2.3. Discussion

(1) The Electron Current

The relationship between the experimental work function, χ_T , at a mean temperature T and the work function at 0°K , χ_0 , of the tungsten filament is given as:

$$\chi_T = \chi_0 + 2RT$$

Since from equation 3.17

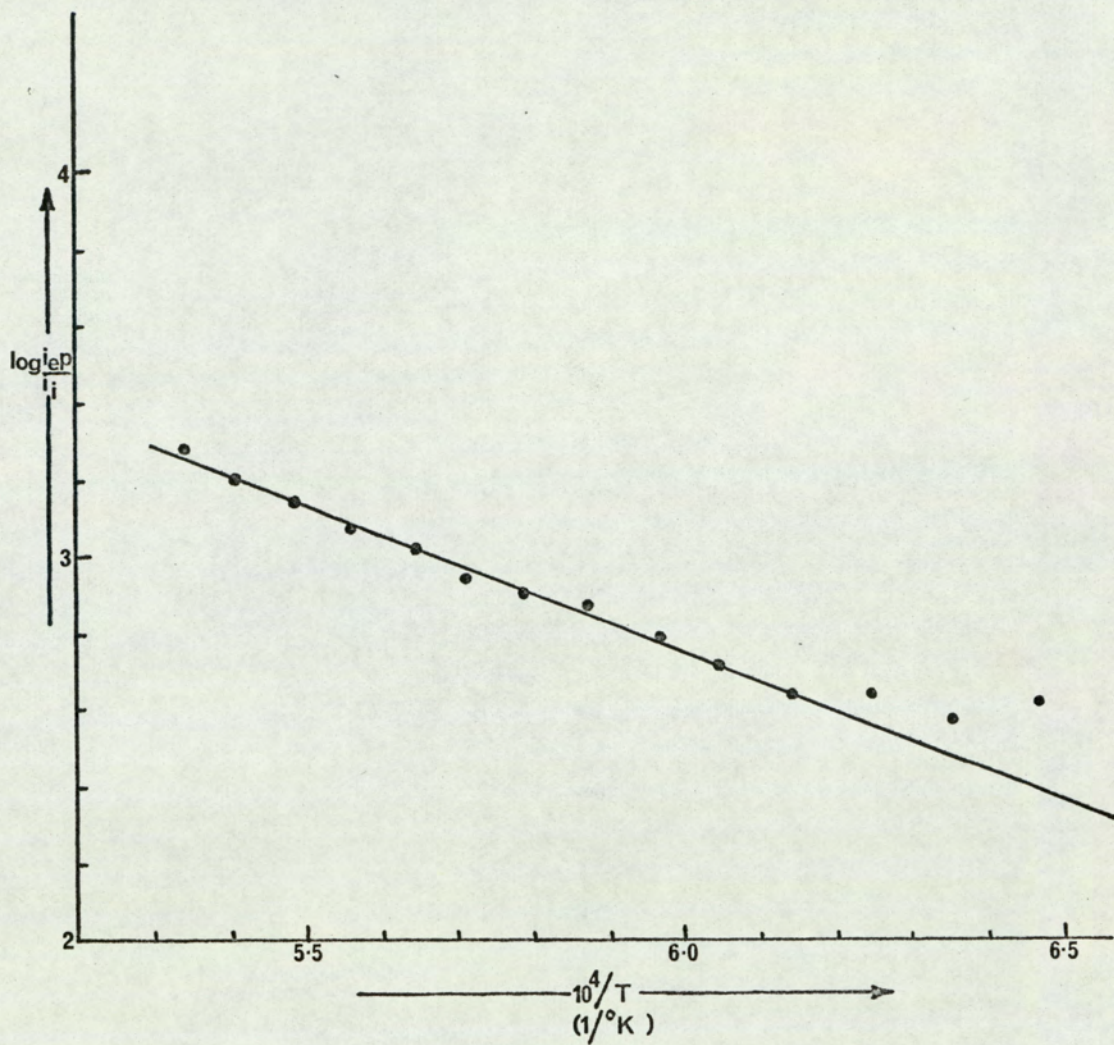
$$i_e = AT^2 \exp - \chi_0/RT$$

and

$$\frac{-Rd \log i_e}{d(I/T)} = \chi_T = \chi_0 + 2RT$$

Hence the work function of the 'clean' tungsten surface, χ_0 , is 105.7 ± 2.1 kcal/mole at 0°K which is in good agreement with the preferred thermionic value of 104.7 kcal/mole.^{117a} Similarly the work function of the tungsten surface in the presence of acetylene gas, χ_c , is 83.8 ± 2.4 kcal/mole at 0°K , resulting in a change in work function, $\Delta\chi$ of 21.9 kcal/mole.

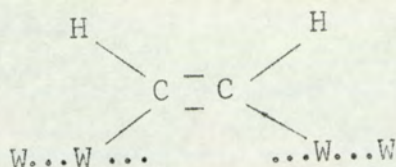
At room temperature acetylene is known to be rapidly, associatively



ELECTRON CAPTURE BY C_2H_2/W .

FIG. 15.

adsorbed onto many metal surfaces including tungsten - the adsorption mechanism postulated is the opening of the first π bond and then the formation of two carbon-tungsten bonds¹¹⁸, as shown below



That the acetylene molecule is adsorbed as shown above is indicated by the fact that in all investigations of the hydrogenation of acetylenic compounds by heterogeneous catalysis the cis olefin is the main product¹¹⁸, although it is often the less stable isomer; the residual unsaturation in the chemi-adsorbed state is shown by the widespread occurrence of polymerisation under such conditions¹¹⁹.

However, unlike ethane which gives ethyl radicals on tungsten¹²⁰, both at room temperature and up to 2000°K, both Robertson¹²⁰ and Le Goff¹²¹ have shown that acetylene and ethylene on hot tungsten filaments are completely decomposed to give carbon and hydrogen. The carbon formed is postulated to diffuse into the tungsten, giving first a solid solution and then a new W_nC phase, where Robertson and Le Goff suggest $n = 2$ and $n = 1$, respectively. The fact that the unsaturated hydrocarbons are completely decomposed is attributed to the close approach their carbon atoms can make to the metal surface.

Le Goff found that when acetylene reacted on a tungsten filament the carbon formed could diffuse into the tungsten, which meant that at any moment a certain fraction of the surface was bare and the rest was covered with carbon. They also found that there was a balance between the deposition of carbon and its diffusion into the tungsten and that

the proportion of bare surface increased with an increase in temperature. Since the probability for reaction increased with an increase in temperature they suggested that all the acetylene molecules striking the bare surface reacted whereas the probability of reaction on the covered surface was zero; hence the temperature variation of the probability for reaction depended on carbon diffusion. They measured the rate of decomposition of acetylene on tungsten at a temperature of about 2000°K and a pressure of 10^{-5} Torr and found that the rate of decomposition of acetylene was large and constant for any amount of carbon in the filament between 0 and 6% by weight, which corresponds to the carbide WC. However around 6% carbon content the rate of decomposition decreased suddenly and above 6% the rate was so small as to be undetectable. From their observations they concluded that the carbon formed, diffused into the tungsten surface and all further reaction occurred at the bare surface. Reaction then proceeded until the carbon content of the filament reached 6% when it ceased, which they attributed to the fact that the rate of diffusion of carbon, in the solid phase, is much lower in the carbide WC than in tungsten containing less than 6% carbon.

In direct opposition to Le Goff's results, Robertson found that the rate of decomposition of acetylene on tungsten at a temperature of about 1850°K increased due to the initial formation of carbon and then became constant when there was enough carbon to just begin to form the W_2C phase, the W_2C layer continues to grow into the tungsten wire as more gas is decomposed. He rejected Le Goff's view of a diffusion controlled process as he found an increase in the gas pressure, and

therefore an increase in the rate of carbon deposition, does not alter the probability for reaction and similar rates are not found for all reactions giving carbon - both results are not consistent with a diffusion controlled process.

From the results of Le Goff and Robertson and the work function values quoted in this dissertation there are three possible reaction mechanisms. In all cases the acetylene decomposes completely and the carbon formed can

- i) Diffuse into the tungsten to produce W_2C , the work function of which is 105.6 kcals/mole.^{117a}
- ii) Diffuse into the tungsten to form WC, the value of the work function is 83.0 kcals/mole.^{117a}
- iii) Not diffuse into the tungsten but form a carbon layer on the filament surface, which should have a work function of 108.4 kcals/mole.^{117a}

The results obtained in this dissertation for the work function of a tungsten surface in the presence of acetylene gas of $\chi_0 = 83.8 \pm 2.4$ kcals/mole is in excellent agreement with that quoted for the work function of WC, and therefore the results advanced by Le Goff.

It is of interest to note that Farragher⁸⁷, when investigating the ionisation of tetracyanoethylene at a W surface, found for temperatures below 1840°K the work function of W in the presence of tetracyanoethylene was 23.0 kcals/mole lower than the 'clean' surface value, and also X-ray examination of the contaminated filament showed the presence of the carbide WC.

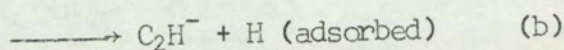
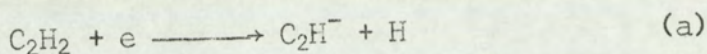
(2) The Ion Current

Initially the ion current was erratic and stabilisation was effected by heating the filament at 2000°K in the presence of acetylene.

The electron current measurements suggest that the emission of negative ions occurs from a WC filament of work function 83.8 ± 2.4 kcal/mole.

A mass spectrum of acetylene, using a surface ionisation source, attached to a Quadrupole Mass Filter showed the predominant negative ion to be $m/e = 25$, identified as C_2H^- .

The possible processes leading to formation of C_2H^- are:



The change in entropy for the overall reaction leading to negative ion formation is determined using equation 3.52 as 89.2 entropy units which is typical of type 4 mechanisms, that is dissociative attachment with adsorption of the uncharged fragment. Hence, reaction (b) is the most probable mechanism.

For reaction (b) the apparent electron affinity of C_2H_2 is given by equation 3.42 as

$$E_{\text{T}} = E_{\text{O}} - D + Q + 3RT$$

where $E_{\text{T}} = 30.7 \pm 4.1$ kcal/mole, $T = 1670^{\circ}\text{K}$, D is the $(\text{H}_1\text{C}_2-\text{H})$ bond dissociation energy given as 113 kcal/mole¹²² and Q is the heat of adsorption of a hydrogen atom on tungsten = 72 kcal/mole⁸⁷. Hence substituting these values into equation 3.42 gives $E_{\text{O}}(\text{C}_2\text{H}) = 62.8 \pm 4.1$ kcal/mole, which is in good agreement with the value of $E_{\text{O}}(\text{C}_2\text{H}) > 64.5$ kcal/mole calculated by Neuert⁶³ from appearance potential data-

and that given by Tiernan and Hughes¹²³ of $71.5 > E(\text{C}_2\text{H}) > 57.7$ kcal/mole. The limits for $E(\text{C}_2\text{H})$ were determined from a study of a series of negative ion - molecule reactions using a Tandem Mass Spectrometer. The magnetron value is, however, considerably lower than the recent value determined by Neuert¹²⁴, from photodetachment studies of $E(\text{C}_2\text{H}) = 85.3$ kcal/mole.

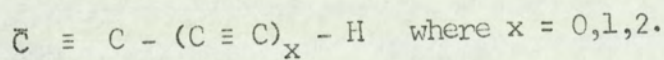
Coulson¹²⁵ showed that an electron in a carbon 2s orbital approaches the nucleus more closely than a 2p electron, which suggests that the effective electronegativity of carbon is greater when exerting a 2s rather than 2p valency. Consequently the greater the s character of the C orbital used in bonding, the greater the electronegativity of the carbon atom. Continuing along these lines Walsh¹²⁶ suggested that the more s character the orbital possesses the more negative the carbon atom will be. Hence in passing from CH_4 , which has a C-H bond moment of $\approx 0.3\text{D}$ in the $\text{C}^{\leftarrow}\text{H}$ sense, to C_2H_4 , which has a C-H bond moment of $\approx 0.4\text{D}$ in the $\text{C}^{\leftarrow}\text{H}$ sense, a reversal of polarity occurs, which is even more pronounced in C_2H_2 where the bond moment is more than 1.0D acting in the $\text{C}^{\leftarrow}\text{H}$ sense. As chemical evidence he cited the acidic nature of acetylene and the high electron attracting character of the $\text{C}\equiv\text{C}$ group as evidenced by the much greater dissociation constant of propiolic acid as compared with acrylic acid. Also on physical evidence his view is supported by the fact that the increase in s character in the C-H bond from the CH radical through CH_4 , C_2H_4 to C_2H_2 is accompanied by a progressive increase in the force constant, bond energy and by a progressive decrease in the internuclear distance.

It follows from Walsh's suggestions that the greater the s character of the carbon orbitals then the greater the electron affinity of

that species, that is the electron affinity should increase along the series CH (pure p), sp^3 , sp^2 and sp hybridized carbon, as is in fact found experimentally. The values obtained are $E(CH) = 21^{111}$, $E(C_{sp}^3) = 24^{112}$, $E(C_{sp}^2) = 51^{113}$ and $E(C_{sp}) = 62.8$ kcal/mole.

Qualitative evidence for the greater stability of acetylenic ions over ethylenic ions is given by Green¹¹⁷ from a study of the negative ions produced in hydrocarbon flames. He showed that in flames containing a small percentage of acetylene the main negative hydrocarbon ions were of the type C_nH^- and C_n^- , both occurring at nearly the same position in the flame. Green found a clearly marked alternation in the relative intensities of the ions, with the C_nH^- type ion, where n was even, being more intense than the C_n^- type ions and the C_nH^- type ions, where n was odd.

In the first case, where n is even, an acetylenic structure may be written for the ion, that is



with the additional electron localized on an sp carbon. Whereas in the second case one is forced to consider an ethylenic structure of the type $\text{>C(=C)}_x = C^- - H$ where $x = 1, 3, 5$, where the electron is now localized on an sp^2 carbon.

Since the Saha equation¹²⁷ equation 5.4., which gives the equilibrium position in the flame for a particular species, defines the equilibrium constant, K_p , in terms of the electron affinity, the flame temperature and in a less sensitive way the spectroscopic multiplicities of the species concerned, it is possible to predict the intensity of a given species in the flame, knowing only the electron

affinity and the flame temperature.

For the reaction $X^- \rightleftharpoons X + e$

$$K_p = \frac{(X)(e)}{(X^-)} = kT^{3/2} \exp^{-5040E/T} \quad 5.4.$$

where E is the electron affinity in electron volts and T is the flame temperature in °K.

Then from the Saha Equation, using the electron affinity of the acetylenic carbon species as 62.8 kcal/mole and the electron affinity of the ethylenic carbon species as 51.0 kcal/mole¹¹³ the acetylenic ions are predicted to be about 25 times as intense as the ethylenic ions, in good agreement with the experimental value of 23.8 as determined from Green's results.

5.3. Electron Capture by CF₃ and SiF₃

5.3.1. Introduction

The high thermal stability, resistance to chemical reaction and high electric strength of certain of the fluorocarbons has led to an interest in these compounds by the Electrical Industry, for use as insulating materials. As it is generally believed that the high electric strengths of such gases, relative to nitrogen, arise from their ability to attach electrons, that is their electron affinity, several workers have investigated the ionisation and dissociation processes resulting from electron impact upon many of the electronegative gases^{128,129}, in particular sulphur hexafluoride^{94,95}. However, with the exception of the electron affinities quoted for the halogen atoms⁷ and Bibby and Carter's¹²⁸ value for the electron affinity of CF₃, little is known about the stability of the negative ions of such gases.

Page et. al. using the Magnetron technique, studied negative ion

formation in sulphur hexafluoride⁹⁶, carbon tetrachloride⁹⁷, chloroform⁹⁷, dichloromethane⁹⁷ and carbon tetrabromide⁹⁸, giving values for the electron affinities of $E(\text{SF}_6) = 33.0$ kcal/mole, $E(\text{SF}_5) = 85.3$ kcal/mole, $E(\text{CCl}_3) = 28.0$ kcal/mole and $E(\text{CBr}_3) = 41.4$ kcal/mole. As an extension of his work, the energetics of negative ion formation in fluoroform, hexafluoroethane carbon tetrafluoride, trifluorobromomethane, trifluorochloromethane and silicon tetrafluoride were investigated.

5.3.2. Experimental

Fluoroform

The CF_3H was supplied by Air Products and Chemical Inc., the filament used was platinum and the sample pressure was approximately 1×10^{-3} torr. A plot of the logarithm of the ratio of the electron and ion current against the reciprocal of the filament temperature yielded three apparent electron affinities in different temperature ranges. In the low temperature range, at a mean temperature of 1342°K , the values for the apparent electron affinity were 25.6, 14.6, 19.2, 11.4, 14.6, 17.5, 16.5 and 17.6 kcal/mole, which omitting the values of 25.6 and 11.4 kcal/mole gave a mean value of 16.7 ± 1.8 kcal/mole. In an intermediate temperature range, at a mean temperature of 1471°K , the values for the apparent electron affinity were -47.1, -48.9, -43.4, -48.9 and -42.0 kcal/mole, giving a mean value of -46.1 ± 3.2 kcal/mole. The high temperature results, at a mean temperature of 1562°K , gave values of 41.6, 52.5, 44.8, 48.5 and 53.9 kcal/mole, which gave a mean value for the apparent electron affinity of 48.3 ± 5.2 kcal/mole. A typical run is illustrated in figure 16.

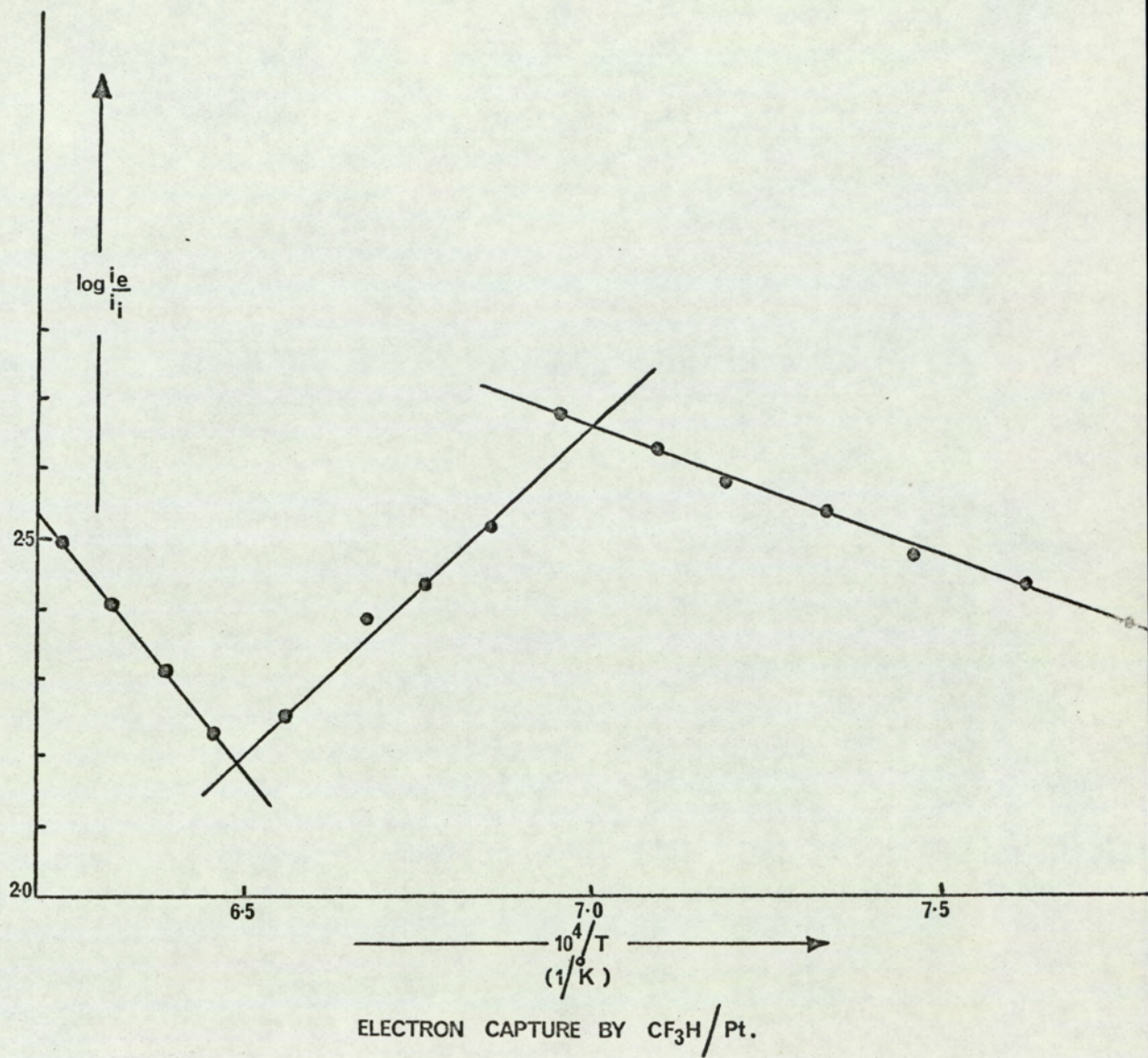


FIG. 16.

Hexafluoroethane

The C_2F_6 was supplied by Cambrian Chemicals Ltd., the filament used was iridium and the sample pressure was approximately 5×10^{-4} Torr. The values obtained for the apparent electron affinity, at a mean filament temperature of $1520^\circ K$ were 1.8, 4.7, 2.7, 1.6 and 6.0 kcal/mole, giving a mean value of 3.3 ± 1.7 kcal/mole. A typical run is illustrated in figure 17.

Carbon tetrafluoride

The CF_4 was supplied by Air Products and Chemicals Inc., the filament used was platinum and the sample pressure was approximately 1.1×10^{-3} Torr. The values obtained for the apparent electron affinity, at a mean temperature of $1390^\circ K$ were -11.4, -17.8, -16.9, -18.7, -17.8, -20.1 and -17.8 kcal/mole, which omitting the value of -11.4 kcal/mole gave a mean value of -18.2 ± 1.1 kcal/mole. A typical run is shown in figure 18.

Trifluorobromomethane

The CF_3Br was supplied by Dr. H. Roberts, Runcorn Laboratories, I.C.I. Ltd., the filament used was platinum and the sample pressure was approximately 1.3×10^{-3} Torr. The values obtained for the apparent electron affinity, at a mean filament temperature of $1408^\circ K$ were -1.1, 0.0, -2.2, -1.8, +5.4, +2.2, -1.4 and +1.1 kcal/mole, which omitting the value of 5.4 kcal/mole, gave a mean value of -0.4 ± 1.6 kcal/mole. A typical run is shown in figure 19.

Trifluorochloromethane

The CF_3Cl was supplied by Dr. H. Roberts, the filament used was iridium, and the sample pressure was approximately 1.0×10^{-3} Torr.

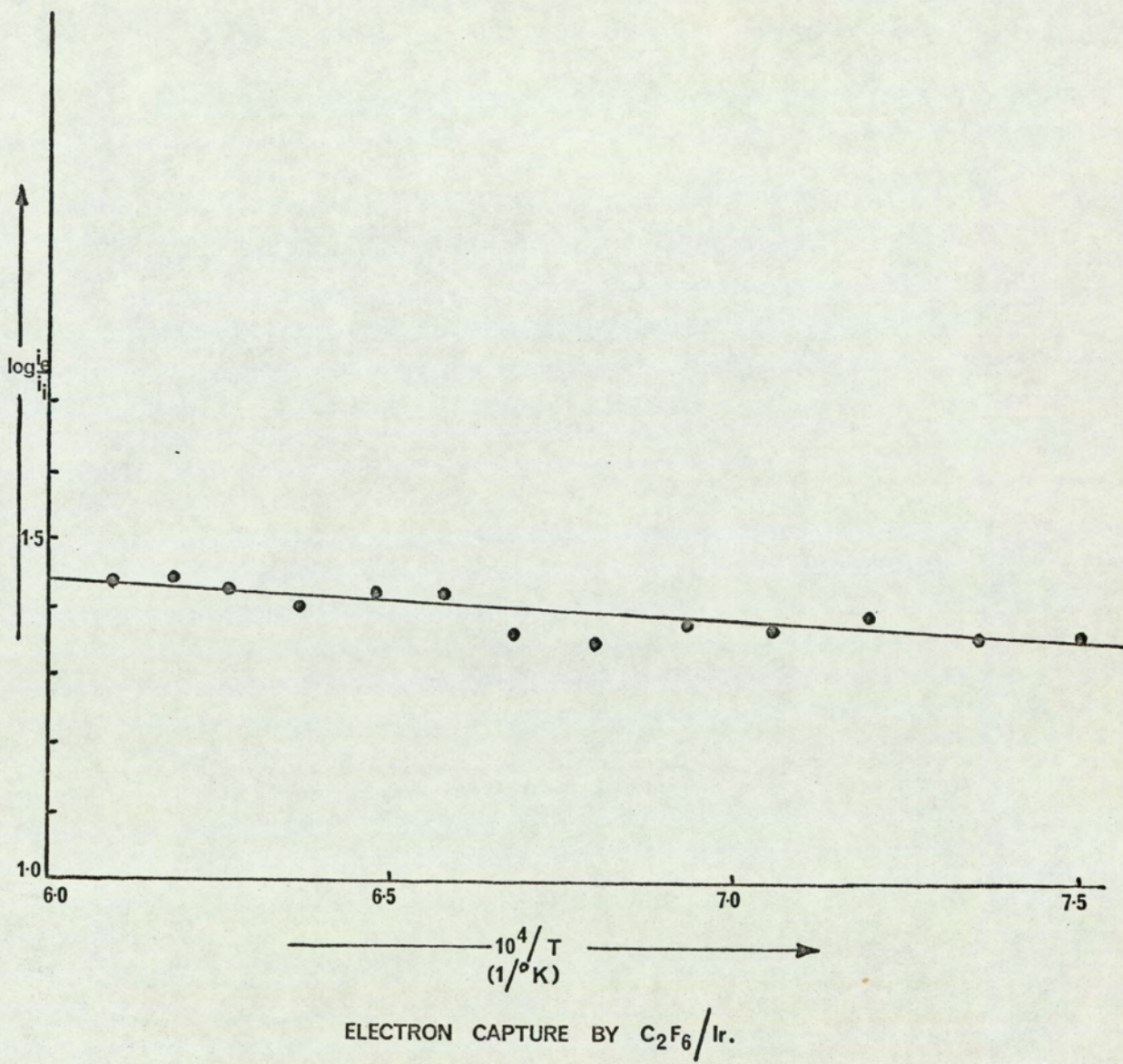


FIG. 17.

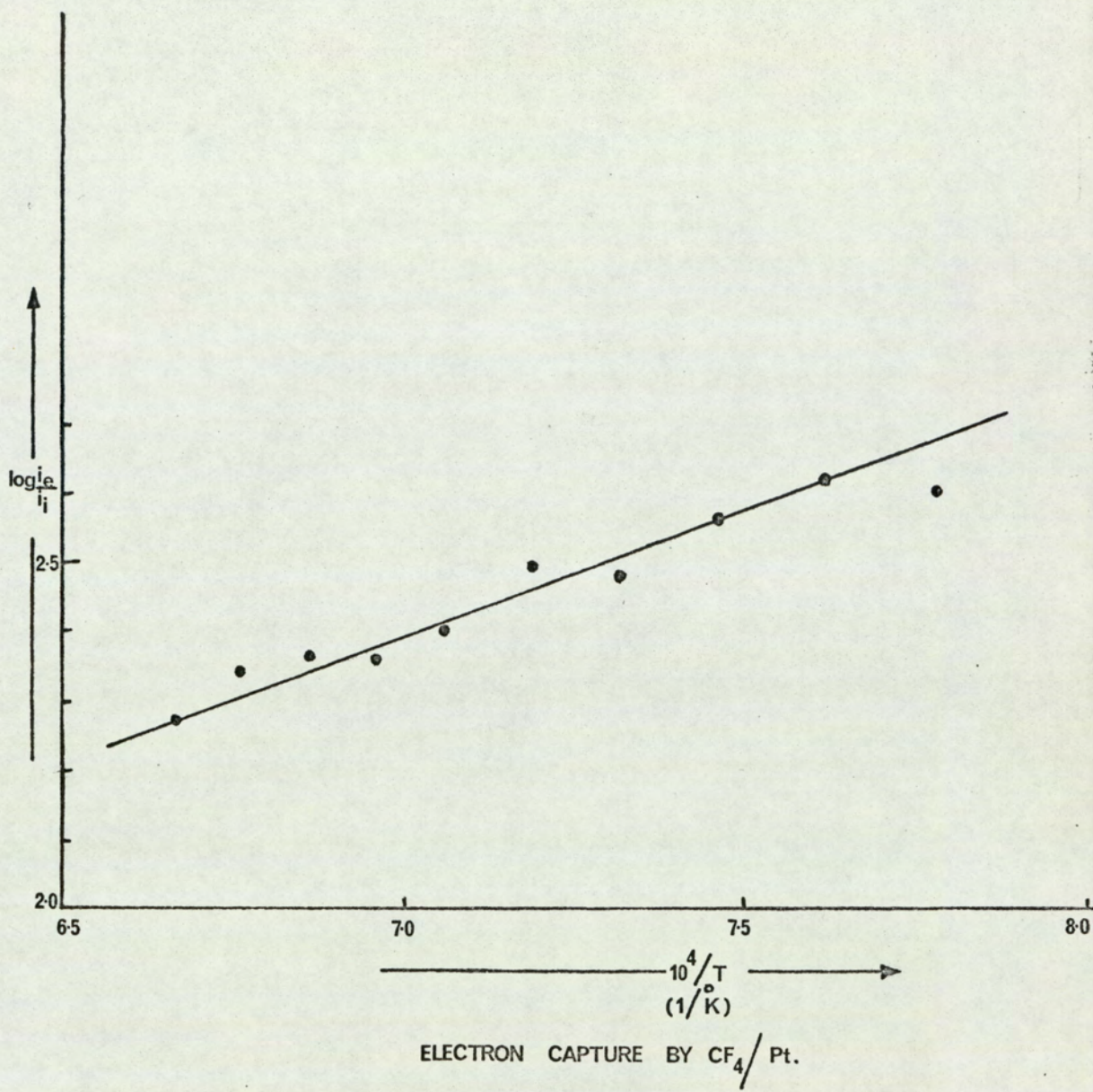


FIG. 18.

The values obtained for the apparent electron affinity, at a mean filament temperature of 1724°K, were -1.0, -2.0, -0.5, +2.5 and +1.6 kcals/mole, which gave a mean value of 0.1 ± 1.9 kcals/mole. A typical run is shown in figure 20.

Silicon tetrafluoride

The SiF₄ was supplied by Air Products and Chemicals Inc., the filament used was platinum and the sample pressure was approximately 1.5×10^{-3} Torr. It was found that during a run the filament temperature increased with time for a particular filament current, causing a corresponding increase in the electron current. This was thought to be due to etching of the filament by the SiF₄ and it was found to be more convenient to plot the logarithm of the ion current against the logarithm of the electron current to determine^e the apparent electron affinity. The slope of such a graph, s , is given by $s = (\chi_T - E_T) / \chi_T$ and hence the apparent electron affinity E_T is given by $E_T = \chi_T(1 - s)$. Where χ_T' is the work function of the surface at the temperature of the filament and obtained from an Arrhenius plot to be 105.6 kcals/mole. The values obtained for the apparent electron affinity at a mean temperature of 1350°K were +1.1, -4.2, +1.3, +4.8, +0.4, +4.5 and -5.3 kcals/mole, which gave a mean value of 0.4 ± 3.9 kcals/mole. A typical run is shown in figure 21.

5.3.3. Discussion

Fluoroform

In the low temperature region the change in entropy for the surface reaction leading to negative ion formation is calculated from equation 3.52 to be 80.6 entropy units (e.U.). This is typical of a

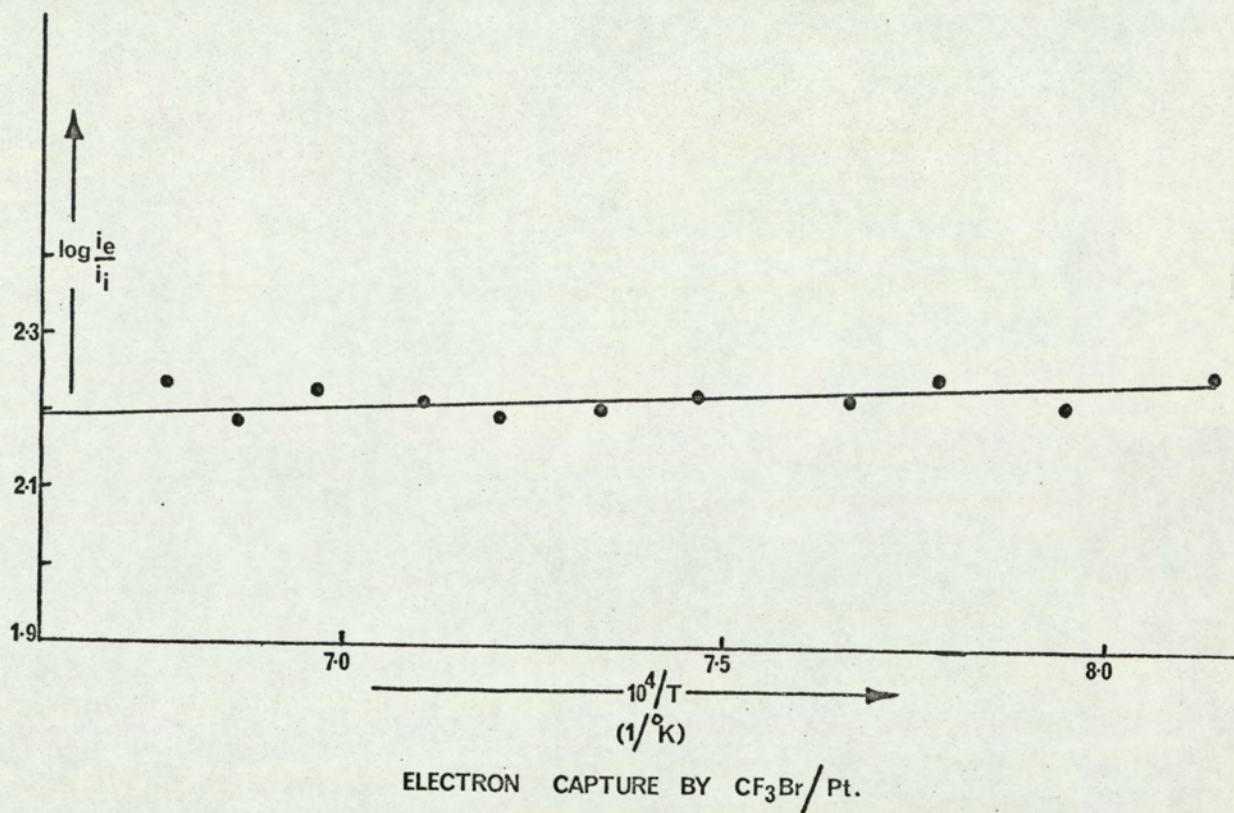


FIG. 19.

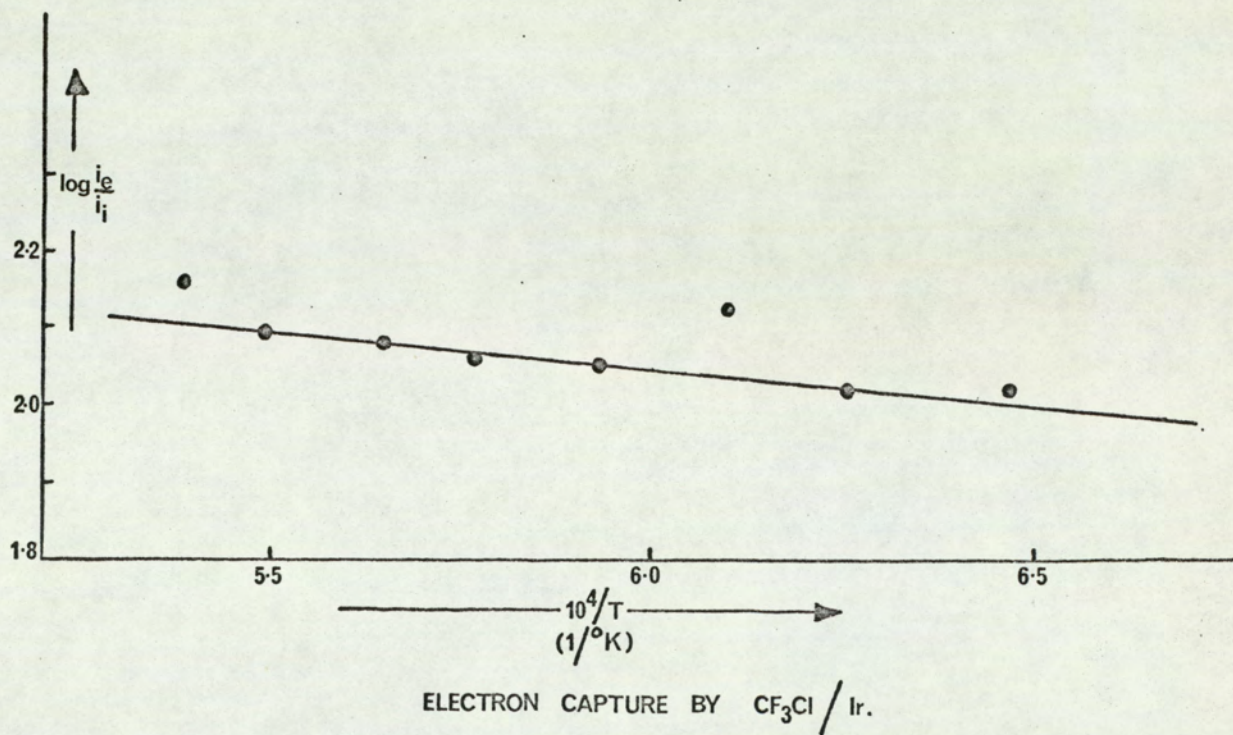
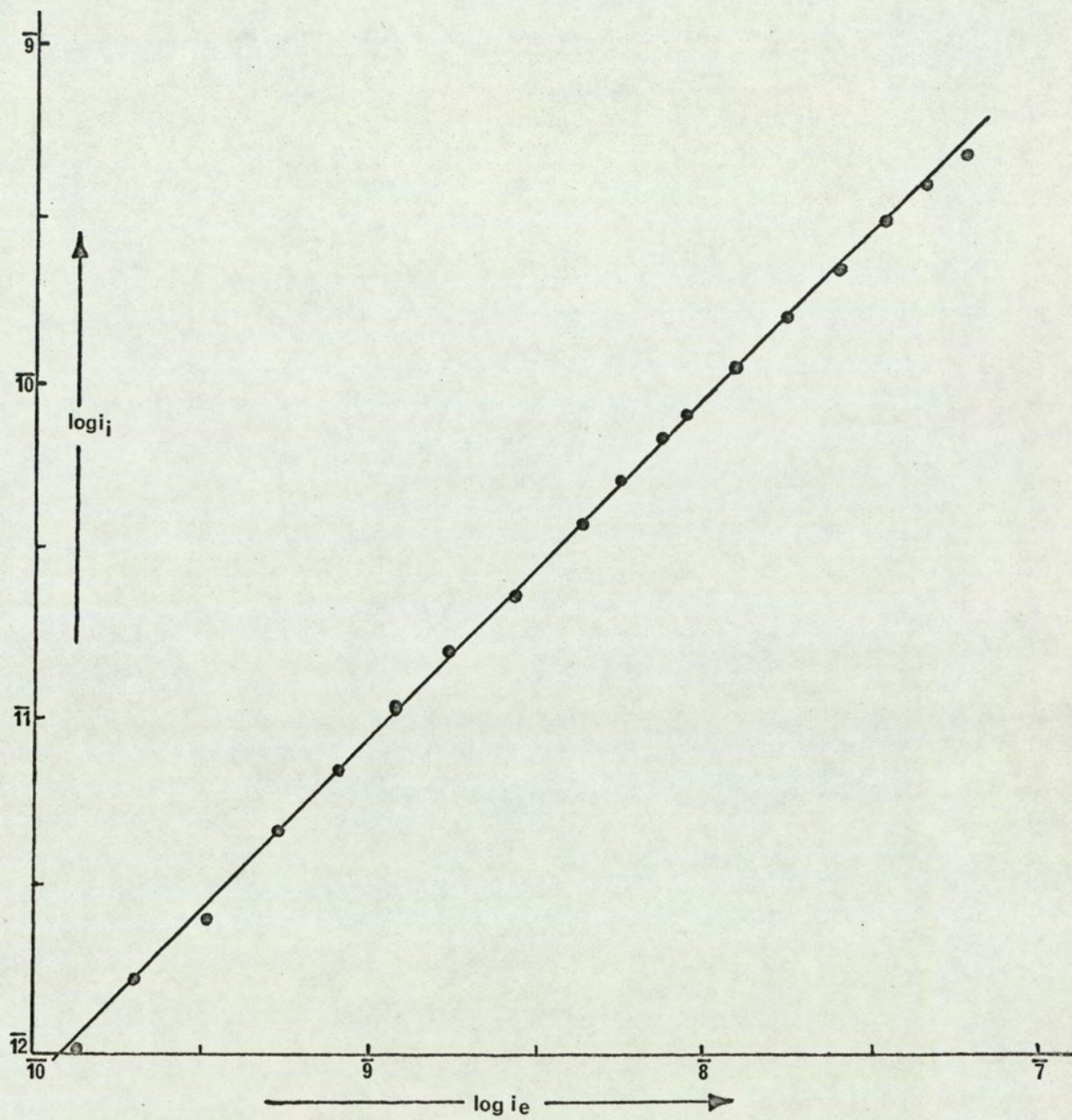


FIG. 20.

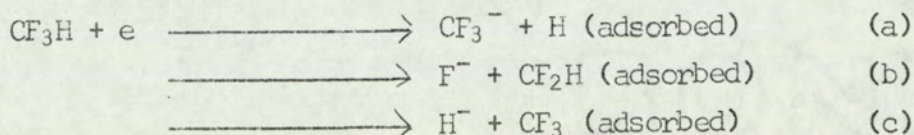


ELECTRON CAPTURE BY SiF_4/Pt .

FIG. 21.

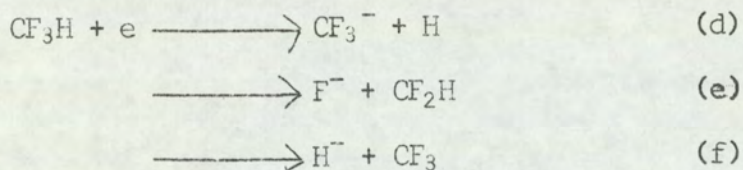
type 4 mechanism, that is dissociative capture, with the uncharged fragment adsorbed on the filament surface. For this type of reaction the apparent electron affinity E_T is given by equation 3.42 as $E_T = E - D + Q + 3RT$ where E is the real electron affinity, D is the bond dissociation energy of the bond broken during ion formation and Q is the heat of adsorption of the neutral fragment on the filament surface.

The possible mechanisms for ion production are



Substituting the appropriate values of $D(\text{CF}_3 - \text{H}) = 103 \text{ kcal/mole}^{106}$, $D(\text{CF}_2\text{H} - \text{F}) = 121 \text{ kcal/mole}^{106}$, $Q_{\text{H}}(\text{Pt}) = 69 \text{ kcal/mole}^{87}$, $E(\text{F}) = 79.6 \text{ kcal/mole}^7$, $E(\text{H}) = 17.8 \text{ kcal/mole}^{46}$, $E_T = 16.7 \pm 1.8 \text{ kcal/mole}$ and $T = 1342^\circ\text{K}$ for reactions (a),(b),(c) gives for reaction (a) $E(\text{CF}_3) = 42.7 \pm 1.8$, for reaction (b) $Q_{\text{CF}_2\text{H}}(\text{Pt}) = 50.1 \pm 1.8 \text{ kcal/mole}$ and for reaction (c) $Q_{\text{CF}_3}(\text{Pt}) = 93.9 \pm 1.8 \text{ kcal/mole}$.

In the mid temperature range ΔS is calculated to be 36.5 eU, which is typical of a type 3 mechanism, that is dissociative capture without adsorption. For this type of mechanism the apparent electron affinity is given by equation 3.37 as $E_T = E - D + 2RT$ and the possible reactions are

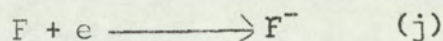
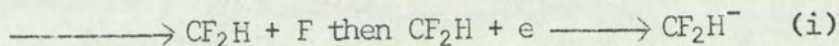
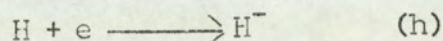
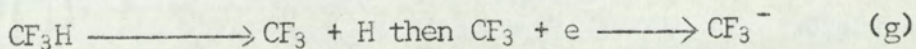


Substituting the appropriate values of D , $E_T = -46.1 \pm 3.2$ and

$T = 1471^{\circ}\text{K}$ into equation 3.37 gives for respectively (d), (e) and (f), $E(\text{CF}_3) = 51.0 \pm 3.2$ kcal/mole, $E(\text{F}) = 69.0 \pm 3.2$ kcal/mole and $E(\text{H}) = 51.0$ kcal/mole.

In the high temperature region $\Delta S = 98.2$ eU, which is typical for a type 1 or 2 mechanism. Since a type 1 mechanism, that is direct capture of an electron by CF_3H to form CF_3H^- , is unlikely under these conditions a type 2 mechanism is postulated, that is the CF_3H dissociates at the hot surface prior to any electron attachment process. For a type 2 mechanism the apparent electron affinity is given by equation 3.33 as $E_T = E + 2RT$.

The possible reactions are



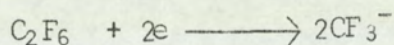
Substituting the values $E_T = 48.3 \pm 5.2$ kcal/mole and $T = 1562^{\circ}\text{K}$ into equation 3.33 gives a value for the electron affinity of 42.0 ± 5.2 kcal/mole.

In the low temperature region the most probable reaction is (a), since it is unlikely that a tetra-atomic molecule will adsorb at these temperatures or have a heat of adsorption as high as 93.9 kcal/mole, which leads to $E(\text{CF}_3) = 42.7 \pm 1.8$ kcal/mole. In the mid temperature region the most probable reaction is (d) giving $E(\text{CF}_3) = 51.0 \pm 3.2$ kcal/mole, since the values for $E(\text{H}) = 51.0$ and $E(\text{F}) = 69.0$ kcal/mole are very different to the well established spectroscopic electron affinities. The high temperature results give the electron affinity

of the ion precursor as 42.0 ± 5.2 kcal/mole, which clearly is not applicable to reaction (h) or (j). The results suggest that either reaction (g) or (i) are the possible reactions, but from a comparison with the low and mid temperature results (g) is the more probable, and the value for $E(\text{CF}_3) = 42.0 \pm 5.2$ kcal/mole is in good agreement with both the low and mid temperature values.

Hexafluoroethane

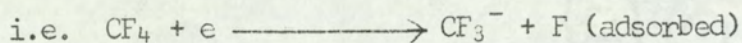
ΔS is calculated to be 63.5 eU which is typical of type 3 reactions. A consideration of the energy terms involved suggests that the most probable reaction leading to negative ion formation is:



In this case the apparent electron affinity is given by $E_T = E - D/2 + 2RT$, where $D = D(\text{F}_3\text{C} - \text{CF}_3) = 96.5 \pm 1.0$ kcal/mole¹³⁰, $T = 1520^\circ\text{K}$ and $E_T = 3.3 \pm 1.7$ kcal/mole. Substituting these values into the above equation gives the electron affinity of CF_3 as 45.5 ± 2.7 kcal/mole, in good agreement with that determined from the fluoroform results.

Carbon tetrafluoride

ΔS is calculated to be 54.6 eU, which suggests a type 3 mechanism. However, for a type 3 mechanism, a consideration of the energetics of all possible ion forming reactions gives unreasonably high values for the electron affinity, and suggests that the most probable reaction is a type 4 mechanism, involving formation of CF_3^- with adsorption of the fluorine atom on the filament.



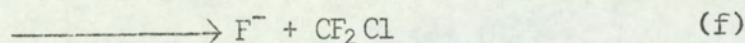
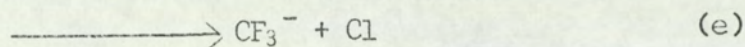
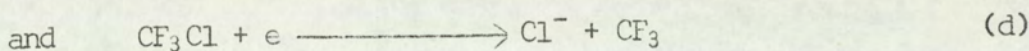
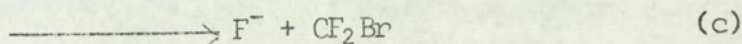
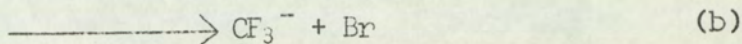
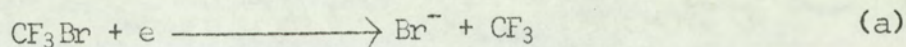
where the apparent electron affinity E_T is given by $E_T = E - D + Q +$

3RT. Substituting the values of $E_T = -18.2 \pm 1.1$ kcal/mole, $T = 1390^\circ\text{K}$ and $D(\text{CF}_3 - \text{F}) = 121$ kcal/mole¹⁰⁶ and an average value for $E(\text{CF}_3)$ of 43.4 ± 2.0 kcal/mole gives a value for the heat of adsorption of a fluorine atom on platinum as 51.1 ± 3.1 kcal/mole. A comparison of $Q_F(\text{Pt})$ with that obtained by Kay and Page for chlorine adsorbed on platinum of $Q_{\text{Cl}}(\text{Pt}) = 35.3$ kcal/mole⁹⁷ and for bromine adsorbed on platinum of $Q_{\text{Br}}(\text{Pt})$ ⁹⁸ = 18.9 kcal/mole, suggests that the value determined for $Q_F(\text{Pt})$ is of the correct order of magnitude, unfortunately no values could be found in the literature for a direct comparison to be made.

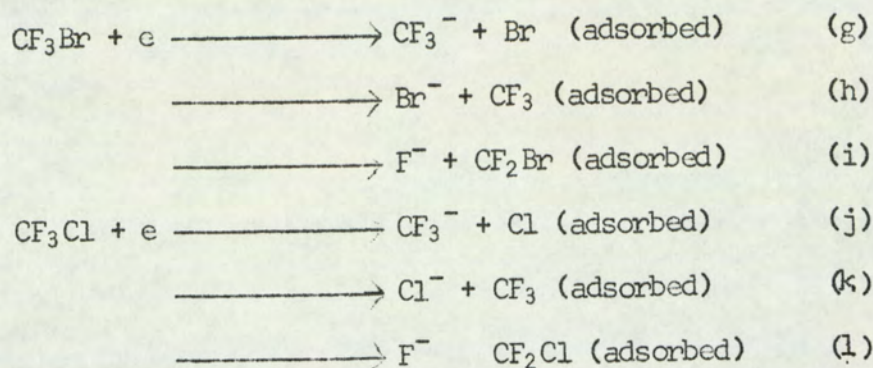
Trifluorobromomethane and Trifluorochloromethane

The change in entropy for the overall ion forming reaction for CF_3Cl and CF_3Br is calculated to be 67.1 and 65.8 eU, respectively. These values for ΔS lie between the values quoted for a type 3 and a type 4 process.

If a type 3 mechanism is considered, the possible reactions for CF_3Br and CF_3Cl are respectively,



where the apparent electron affinity is given by $E_T = E - D + 2RT$ and for a type 4 mechanism:

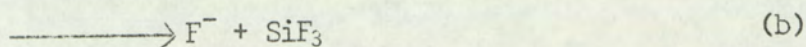
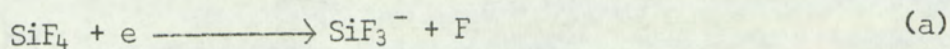


where the apparent electron affinity is given by $E_T = E - D + Q + 3RT$. Where for CF_3Cl $E_T = 0.1 \pm 1.9$ kcal/mole, $T = 1724^\circ\text{K}$, $Q_{\text{Cl}}(\text{Ir}) = 33.5^{97}$, and for CF_3Br $E_T = -0.4 \pm 1.6$, $T = 1408^\circ\text{K}$, $Q_{\text{Br}}(\text{Pt}) = 18.9^{98}$, $E(\text{CF}_3) = 43.4 \pm 2.0$, $E(\text{Br}) = 77.6^7$, $E(\text{Cl}) = 83.4^7$ and $E(\text{F}) = 79.6$ kcal/mole⁷. Then on energetic grounds the most probable reactions for negative ion formation in CF_3Cl and CF_3Br are respectively j and g which gives values for the $(\text{CF}_3 - \text{Cl})$ and $(\text{CF}_3 - \text{Br})$ bond dissociation energies of 87.0 ± 3.9 and 70.7 ± 3.6 kcal/mole respectively, in excellent agreement with the values quoted by Coomber and Whittle of $D(\text{CF}_3 - \text{Cl}) = 86.1 \pm 0.8^{131}$, $D(\text{CF}_3 - \text{Br}) = 69.4 \pm 0.8^{132}$ and by Cottrell¹⁰⁶ of $D(\text{CF}_3 - \text{Cl}) = 83.0$ and $D(\text{CF}_3\text{Br}) = 65.0$ kcal/mole. However, due to Br^- and Cl^- having a greater stability than CF_3^- , reactions (a) and (d) are possible explanations of the experimental results, although the values obtained for the bond energies of $D(\text{CF}_3 - \text{Cl}) = 90.1 \pm 1.9$ and $D(\text{CF}_3 - \text{Br}) = 83.6 \pm 1.6$ kcal/mole are not in agreement with those obtained by other workers.

Silicon Tetrafluoride

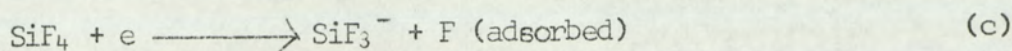
ΔS is calculated as 66.9 eU and, as for CF_3Br and CF_3Cl , lies in between the values quoted for a type 3 and a type 4 process.

If a type 3 process is considered the possible reactions are



where $E_T = E - D + 2RT$, $E_T = 0.4 \pm 3.9$ kcal/mole, $T = 1350^\circ\text{K}$ and D is calculated from the appropriate heats of formation to be 137 kcal/mole¹³³, which leads to an electron affinity value of 132.0 ± 3.9 kcal/mole, which is excessively high for either reaction. Whereas

if a type 4 process is considered, the only possible reaction is:



since the adsorption of a species as large as SiF_3 is unlikely at these temperatures. Since $E_T = E + Q - D + 3RT$ a consideration of the energies involved leads to an electron affinity for SiF_3 of $E(\text{SiF}_3) = 78.3 \pm 7.0$ kcal/mole.

The results for the fluorocarbons are summarized in table 4.

Table 4

Cpd	Information required	Information Derived
CF_3H	$D(\text{CF}_3 - \text{H}), Q_{\text{H}}(\text{Pt})$	$E(\text{CF}_3) = 42.7 \pm 1.8$ kcal/mole
		51.0 ± 3.2 " "
		42.0 ± 5.2 " "
C_2F_6	$D(\text{F}_3\text{C} - \text{CF}_3)$	$E(\text{CF}_3) = 45.5 \pm 1.7$ " "
CF_4	$D(\text{CF}_3 - \text{F}), E(\text{CF}_3)$	$Q_{\text{F}}(\text{Pt}) = 51.1 \pm 3.1$ " "
CF_3Br	$E(\text{CF}_3), Q_{\text{Br}}(\text{Pt})$	$D(\text{CF}_3 - \text{Br}) = 70.7 \pm 3.6$ "
CF_3Cl	$E(\text{CF}_3), Q_{\text{Cl}}(\text{Ir})$	$D(\text{CF}_3 - \text{Cl}) = 87.0 \pm 3.9$ "
SiF_4	$Q_{\text{F}}(\text{Pt}), D(\text{SiF}_3 - \text{F})$	$E(\text{SiF}_3) = 78.3 \pm 7.0$ "

The value for $E(\text{CF}_3)$ determined in the magnetron has to be compared with the value quoted by Bibby and Carter of $E(\text{CF}_3) = 74.4$ kcal/mole¹²⁸

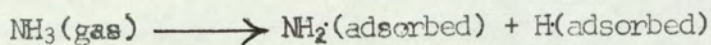
and the values quoted by Page of $E(\text{CCl}_3) = 28.0 \pm 0.7$ ⁹⁷, $E(\text{CBr}_3) = 41.4 \pm 6.0$ ⁹⁸ and $E(\text{CH}_3) = 24.3$ kcal/mole¹¹², although $\text{CH}_3\cdot$ is not strictly comparable since it is planar whereas the other species we thought to be pyramidal.

Since fluorine is more electronegative than either chlorine or bromine, on a simple interpretation, assuming that the additional electron forms a lone pair on the carbon, then $\text{CF}_3\cdot$ would be expected to have a greater electron affinity than $\text{CCl}_3\cdot$, $\text{CBr}_3\cdot$ or $\text{CH}_3\cdot$; as is found experimentally. That the value of $E(\text{CF}_3)$ is as high as Bibby and Carters¹²⁸ value of 74.4 kcal/mole is unlikely since $E(\text{F})$ is only 79.6 kcal/mole⁷; in fact their value may be in considerable error, since it is calculated from the appearance potentials of CF_3^- and CF_3^+ , obtained from the electron impact of C_2F_6 , which, particularly in the case of the appearance potential of CF_3^- , could involve large errors due to kinetic energy terms not having been accounted for and incorrect calibration of the energy scale.

5.4. Electron capture by $\text{NH}_2\cdot$, $\text{PH}_2\cdot$, $\text{R}_1\text{R}_2\text{N}\cdot$ and $\text{R}_1\text{R}_2\text{P}\cdot$.

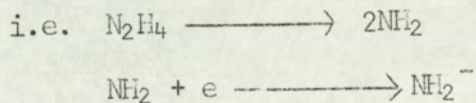
5.4.1. Introduction

Several workers^{134,135, 136} have shown that the decomposition of ammonia, at a pressure of approximately 10^{-4} Torr, on tungsten and platinum filaments gives rise to the formation of the radicals $\text{NH}_2\cdot$, $\text{NH}\cdot$ and N ; with the $\text{NH}_2\cdot$ present in the greatest abundance. The rate controlling step on platinum surfaces at temperatures between 900°C and 1350°C was shown by Apel'baum and Temkin to be¹³⁶



Not surprisingly, the study of negative ions produced in ammonia by both electron impact¹³⁷ and surface ionisation techniques⁸⁶ showed that the predominant ion was NH_2^- ; the values quoted for the electron affinity of the NH_2 radical were 27.9^{41} , 25.7 ± 2.0^{86} in good agreement with Pritchard's⁴⁰ value of 27.7 , determined from lattice energy calculations on the alkali amines.

Page⁸⁶ also investigated the energetics of the formation of negative ions produced in hydrazine at a hot tungsten surface. Szwarc¹³⁸ had shown that hydrazine undergoes homogeneous thermal breakdown to amine radicals and Ramsay¹³⁹ demonstrated that flash photolysis of hydrazine also produced amino radicals, together with some imino radicals at very high energies. The activation energy of the breakdown of hydrazine to radicals is 60 kcal/mole, which Szwarc interpreted as the energy of the N-N bond in hydrazine. Page deduced that if the N-N bond energy is of the order of 60 kcal/mole then hydrazine would be expected to behave as amino radicals when examined in the magnetron, since the N-N bonds would be almost entirely broken at the temperature of the filament. Ion formation should, therefore, take place by a type 2 mechanism.



where the apparent electron affinity is given by $E_T = E + 2RT$.

Page⁸⁶ found that the experimental results were consistent with a type 2 mechanism and determined the electron affinity of NH_2 to be $E(\text{NH}_2) = 25.7$ kcal/mole. A study of ammonia in the magnetron, using a tungsten filament, suggested that negative ion formation went by a

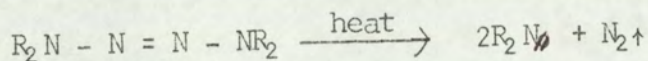
type 4 process that is $\text{NH}_3 + e \longrightarrow \text{NH}_2^- + \text{H}$ adsorbed, consistent with the results from kinetic studies. Using the electron affinity of NH_2 , as determined from the hydrazine studies, Page calculated the first bond dissociation energy in NH_3 to be 104.9 ± 2.0 in satisfactory agreement with the value quoted by Altshuller of 104 ± 2 kcal/mole¹⁴⁰.

As no values for the electron affinities of the substituted amino radicals have been either calculated or determined experimentally, with the exception of MeNH , given as $E(\text{MeNH}) = 36.0$ kcal/mole by Collin¹⁴¹ from mass spectrometric studies, a study of the methyl, phenyl substituted radicals was undertaken to establish the effect of substitution upon the electron affinity of the species.

The compounds studied were diphenylhydrazine, tetraphenylhydrazine, diphenyldimethyl tetrazene, tetramethyl tetrazene, aniline, pent afluoro aniline, diphenylamine, methyl amiline and dimethylamine.

If, as expected, negative ion formation in the substituted hydrazines and amines proceeds by the same mechanism as for respectively hydrazine and ammonia then a study of the above hydrazines and corresponding amines should lead to values for the electron affinity of Ph_2N , PhNH , and $(\text{Ph}_2\text{N} - \text{H})$ and $(\text{PhNH} - \text{H})$ bond dissociation energies.

Gowenlock¹⁴² et. al. have shown that the substituted tetrazenes decompose at a temperature above 120°C by a 3 fragment process, that is



Hence at filament temperatures of approximately 1500°K the tetrazenes would be expected to behave as substituted amino radicals, analogous to the hydrazines. Hence a study of tetramethyl and dimethyl diphenyl

tetrazenes with the corresponding amine should lead to values for $E(\text{PhMeN})$, $E(\text{Me}_2\text{N})$ and $D(\text{Me}_2\text{N} - \text{H})$ and $D(\text{PhMeN} - \text{H})$.

From electron impact studies on phosphine Neuert⁶⁴ has shown that PH_2^- is the predominant negative ion, directly analogous with NH_2^- in ammonia¹³⁷. He gave a lower limit for the electron affinity of PH_2 as 23.0 kcal/mole as compared to 27.9 kcal/mole for $E(\text{NH}_2)$. As a complementary study to electron capture by the amino radical, negative ion formation in phosphine, diphosphine and diphenylphosphine was investigated, with the intention of determining the electron affinity of PH_2 and the first P-H bond dissociation energy of phosphine and diphenyl-phosphine.

5.4.2. Experimental

Samples were obtained commercially unless stated otherwise.

1.2. Diphenyl hydrazine

The filament used was tungsten, the sample pressure was approximately 1.0×10^{-3} Torr and the values obtained for the apparent electron affinity at a mean filament temperature of 1905°K were 39.6, 45.7, 40.0, 45.1, 42.9, 40.4 and 40.1, giving a mean value for E_T of 42.0 ± 2.6 kcal/mole. A typical graph is shown in figure 22.

Tetraphenyl hydrazine

The tetraphenyl hydrazine was prepared following the method of Gattermann¹⁴³, in which diphenylamine is oxidised using potassium permanganate in acetone. The product, tetraphenylhydrazine, was recrystallised from a 5 to 1 mixture of ethanol and chloroform.

The filament used was tungsten and the sample pressure was approximately 5×10^{-4} Torr. Due to the low volatility of the sample the

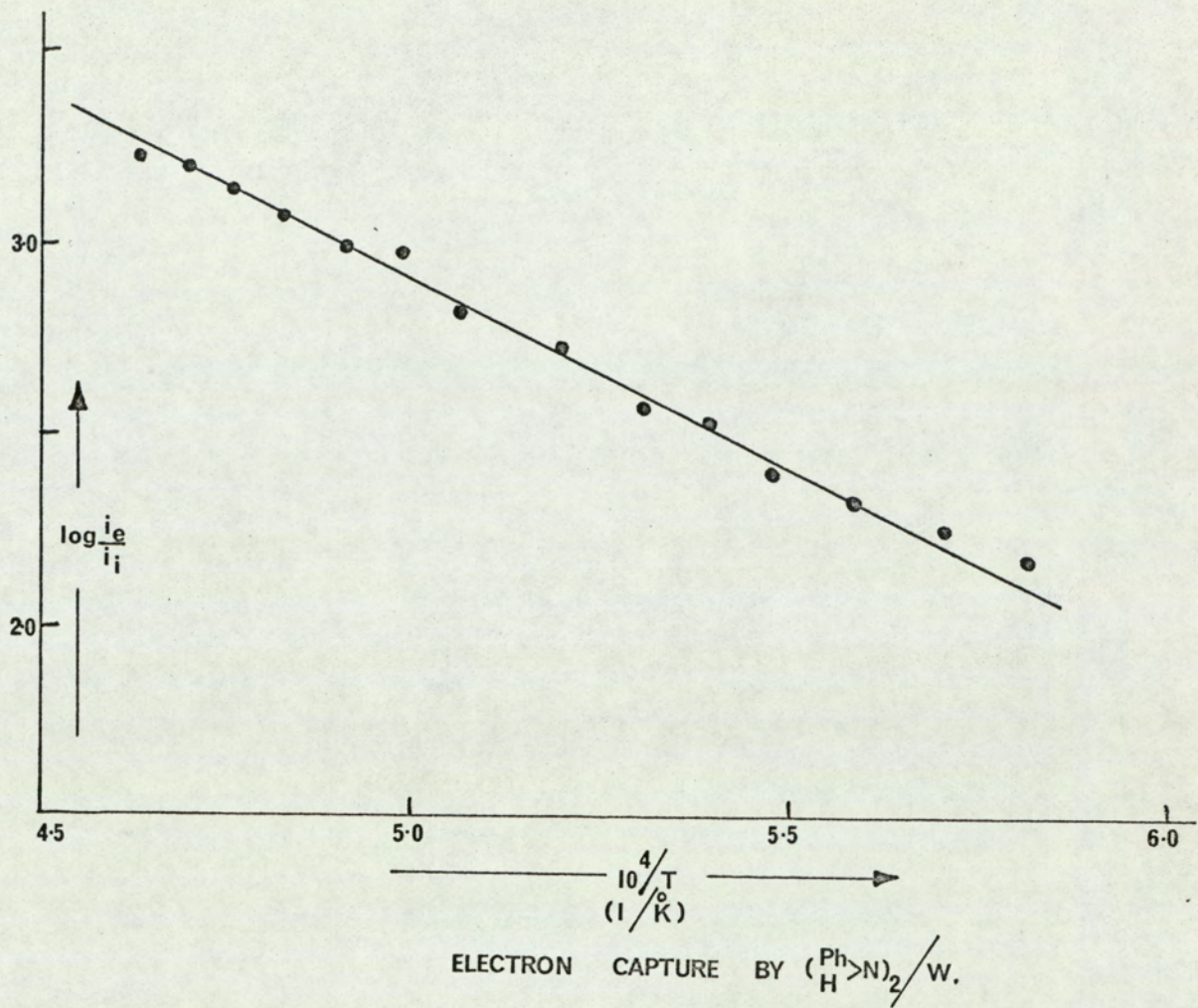


FIG. 22.

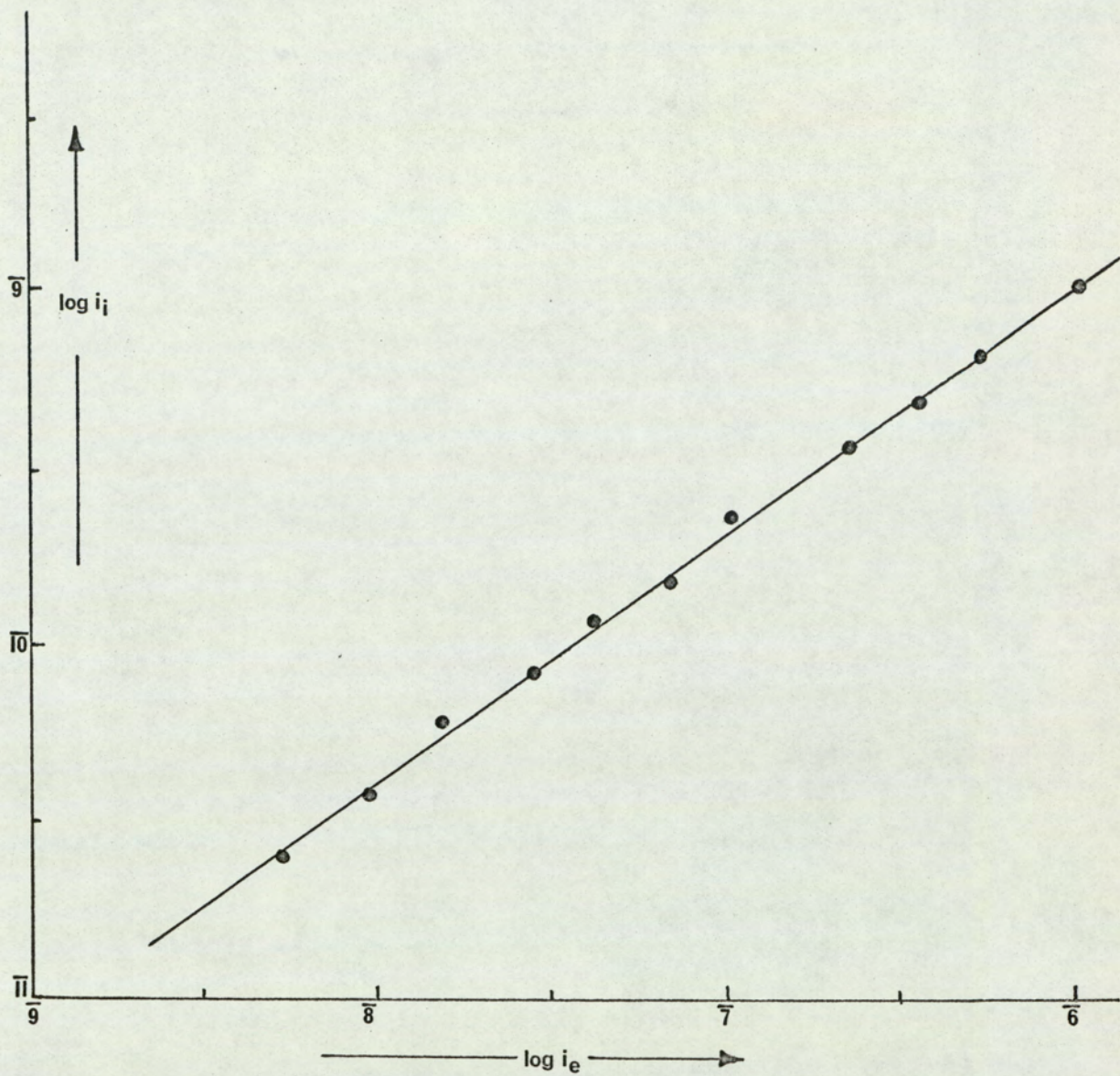
sample inlet system and the Magnetron bottle were kept at 80°C. As the sample pressure was too small to read accurately the runs were done as rapidly as possible so that fluctuations in the pressure were minimised, and it was found to be more convenient to use log-log plots to determine the apparent electron affinity. The work function of the tungsten surface was 110 kcal/mole and at a mean temperature of 1800°K the values obtained for the apparent electron affinity were 39.0, 34.5, 29.3, 36.7, 42.2, 32.0, 32.4, 28.8 and 41.5, which gives a mean value for E_T of 35.2 ± 5.0 kcal/mole. A typical graph is shown in figure 23.

Diphenyldimethyl tetrazene

The $(\text{PhMeN}_2)_2$ was supplied by Dr. J.C. McGowan, I.C.I. Plastics Division, Welwyn Garden City, the filament used was tungsten and the sample pressure was $\approx 1.0 \times 10^{-4}$ Torr. As with tetraphenyl hydrazine the low volatility of diphenyldimethyl tetrazene required the magnetron bottle and sample inlet system to be kept at 80°C and again log-log plots were used to determine the apparent electron affinity. The work function of the surface was 108.0 kcal/mole and the values obtained for the apparent electron affinity were 36.7, 37.8, 47.6, 34.6, 38.9 and 42.1 kcal/mole at a mean filament temperature of 1750°K. Omitting the value of 47.6 kcal/mole gives a mean value for E_T of 38.0 ± 2.8 kcal/mole. A typical graph is shown in figure 24.

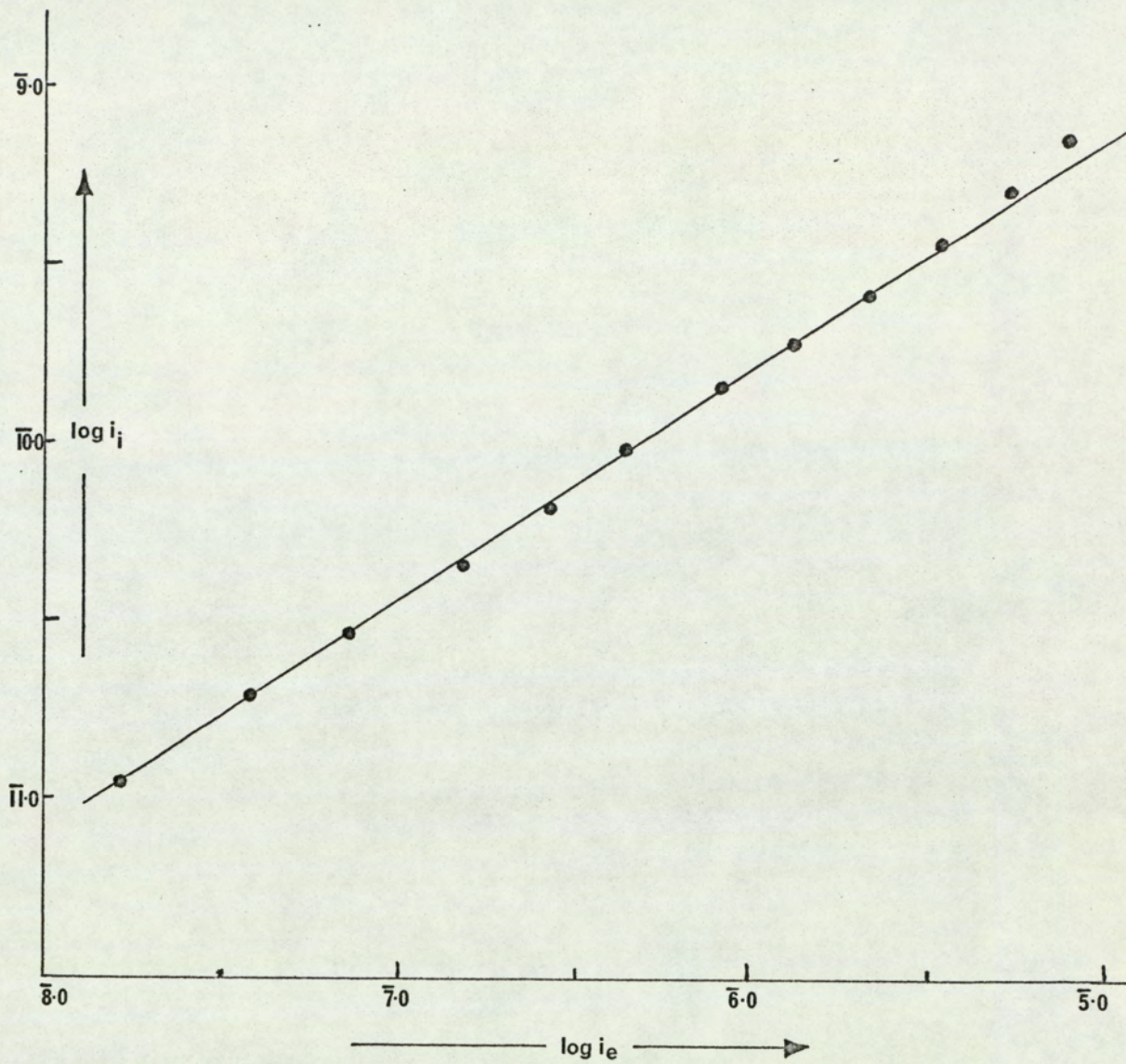
Tetramethyl tetrazene

The $(\text{Me}_2\text{N}_2)_2$ was supplied by Dr. J.C. McGowan, the filament used was tungsten and the sample pressure was approximately $1.1 \times$



ELECTRON CAPTURE BY $(\text{Ph})_2\text{N}^{\cdot}/\text{W}$.

FIG. 23.



ELECTRON CAPTURE BY $(\text{Ph}_2\text{N-N})_2/\text{W}$.

FIG. 24.

10^{-3} Torr. The values obtained for the apparent electron affinity, at a mean filament temperature of 1600°K , were 29.4, 26.3, 26.8, 28.9, 29.4 and 29.4 kcal/mole, giving a mean value for E_{T} of 28.4 ± 1.20 kcal/mole. A typical graph is shown in figure 25.

Aniline

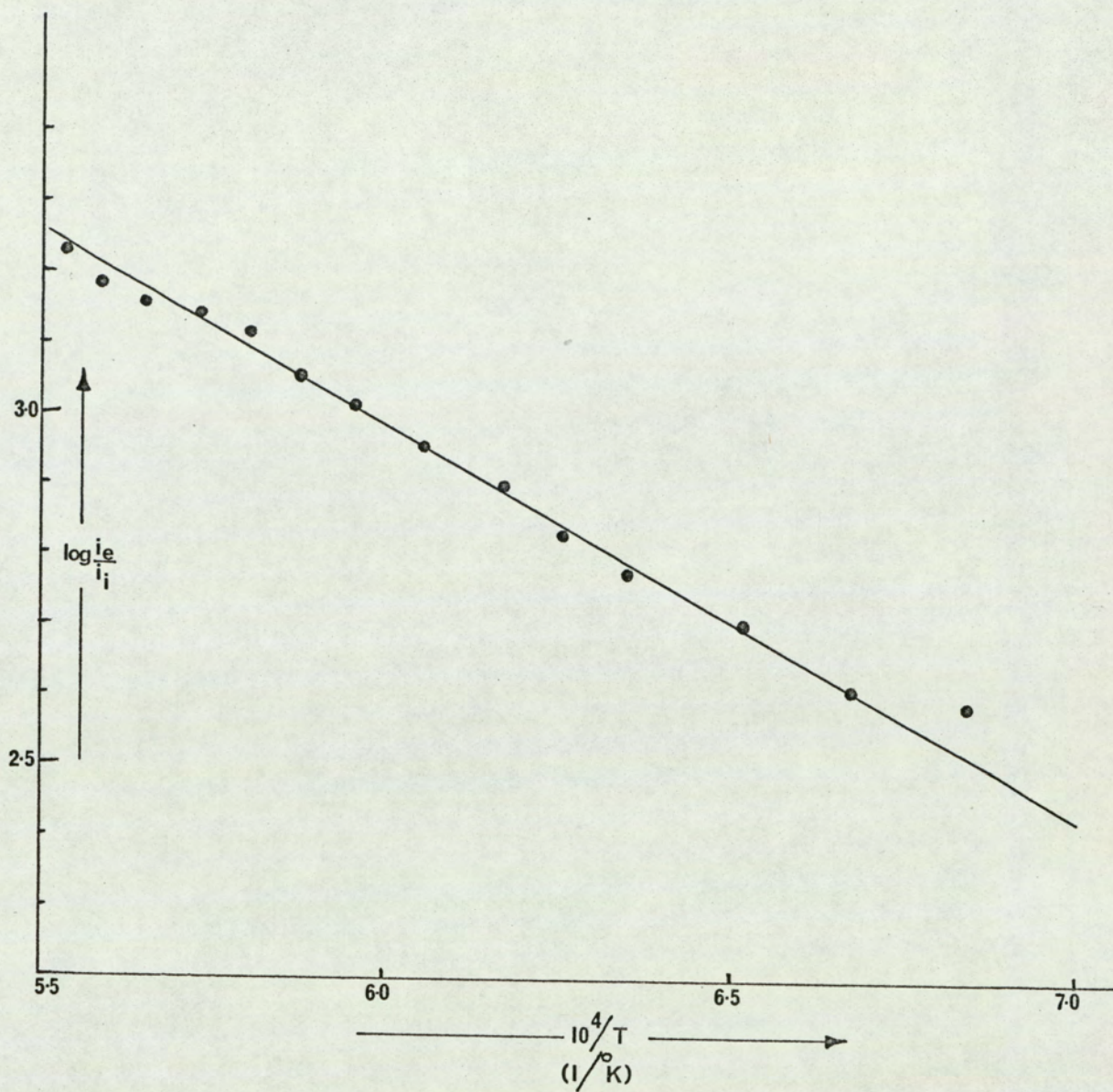
The filament used was iridium and the sample pressure was 1.3×10^{-3} Torr. Below a temperature of 1500°K the ion current was very erratic and unreproducible, although a plot of $\log i_e$ against $10^4/T$ figure 26(b), showed that the work function was the same over the complete temperature range and identical to the clean surface work function of 96.0 kcal/mole. For temperatures above 1500°K a plot of the logarithm of the ratio of the electron to ion currents against $10^4/T$ gave values for the apparent electron affinity of 11.5, 14.4, 11.5, 8.6, 11.5, 16.2, 11.4, 11.6 and 8.6 kcal/mole at a mean filament temperature of 1613°K . This gives a mean value for E_{T} of 11.7 ± 2.5 kcal/mole. A typical run is shown in figure 26(a).

Pentafluoroaniline

The $\text{C}_6\text{F}_5\text{NH}_2$ was supplied by Dr. C.R. Patrick, Birmingham University, the filament used was iridium and the sample pressure was 2.4×10^{-3} Torr. The values obtained for the apparent electron affinity at a mean filament temperature of 1450°K were 14.6, 9.6, 15.9, 11.8, 14.2, 13.1 and 10.2 kcal/mole, which gives a mean value for E_{T} of 12.8 ± 2.3 kcal/mole. A typical graph is shown in figure 27.

Diphenylamine

The filament used was iridium and the sample pressure was approximately 2.5×10^{-3} Torr. As with aniline, the ion current measurement



ELECTRON CAPTURE BY $\left(\begin{array}{c} \text{Me} \\ \text{N-N} \\ \text{Me} \end{array} \right)_2 / \text{W}.$

FIG. 25.

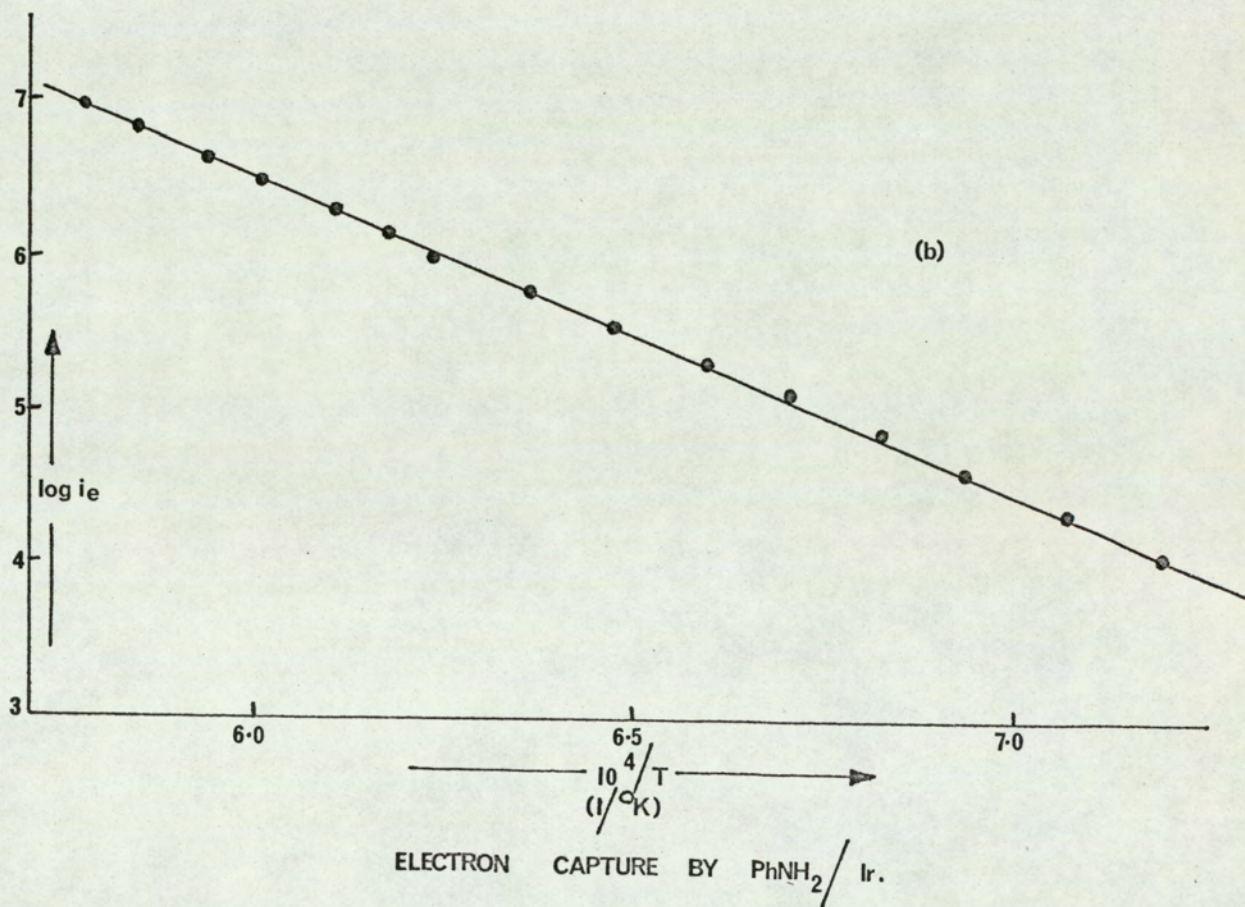
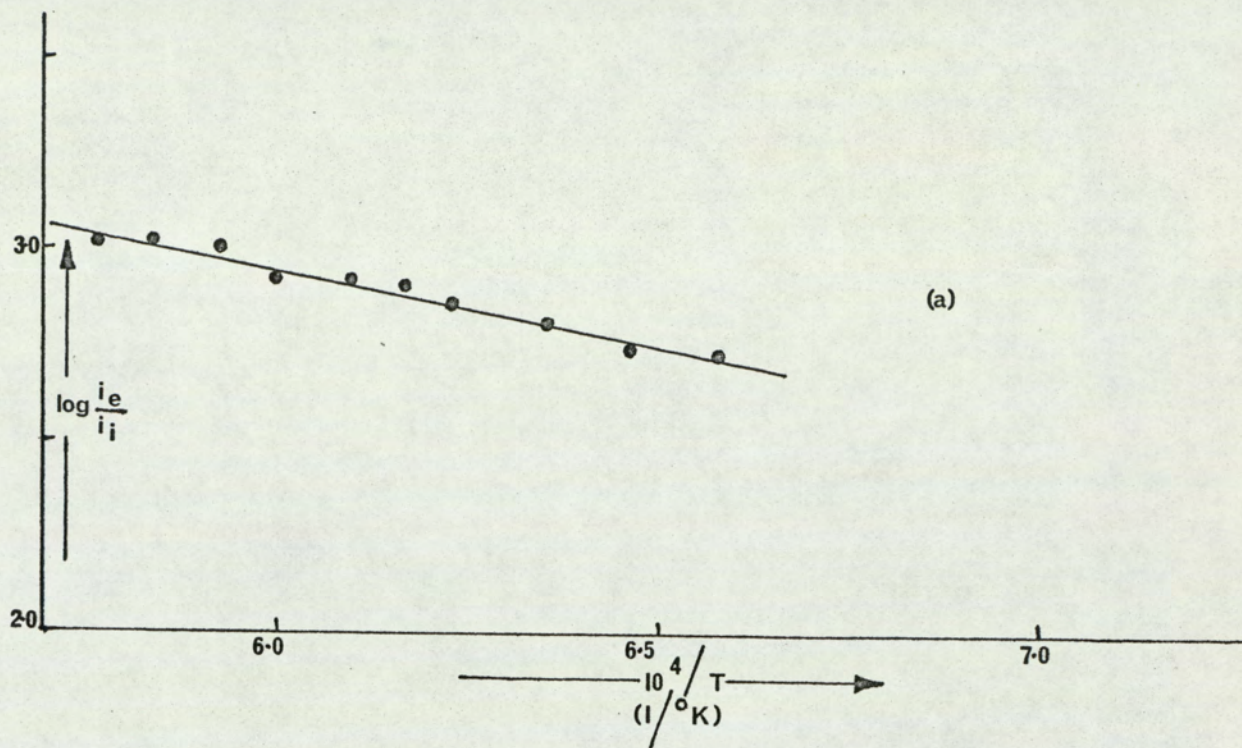


FIG. 26.

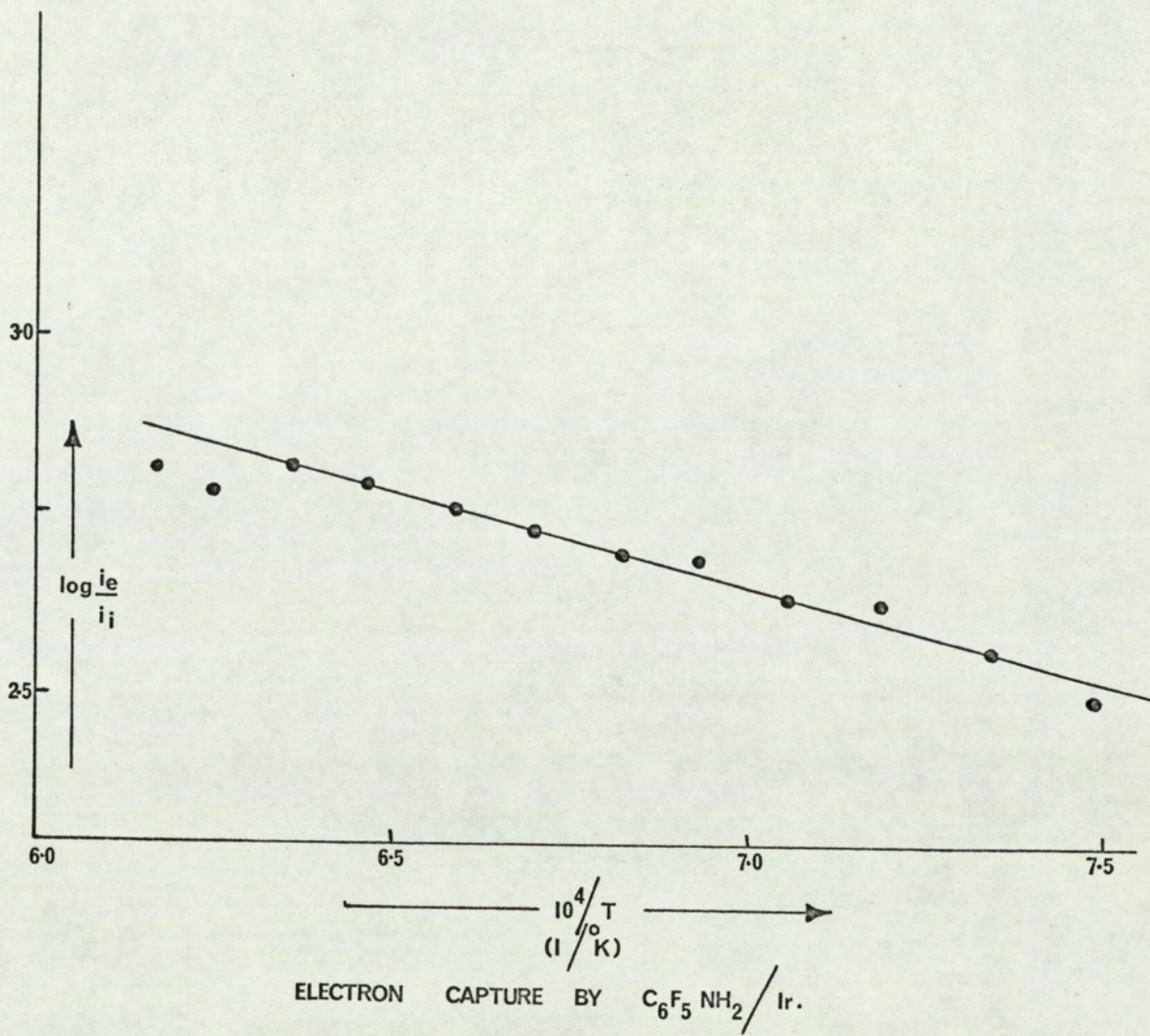


FIG.27.

in diphenylamine were unreproducible below 1550°K, although the work function of the surface was 96.5 kcal/mole over the whole temperature range and identical to the clean surface work function. As shown in figure 28(b), for temperatures above 1550°K the values obtained for the apparent electron affinity at a mean temperature of $T = 1653^{\circ}\text{K}$ were 10.6, 10.0, 12.4, 14.6 and 12.4, which gives a mean value for E_T of 12.0 ± 1.8 kcal/mole. A typical graph is shown in figure 28(a).

Methylaniline

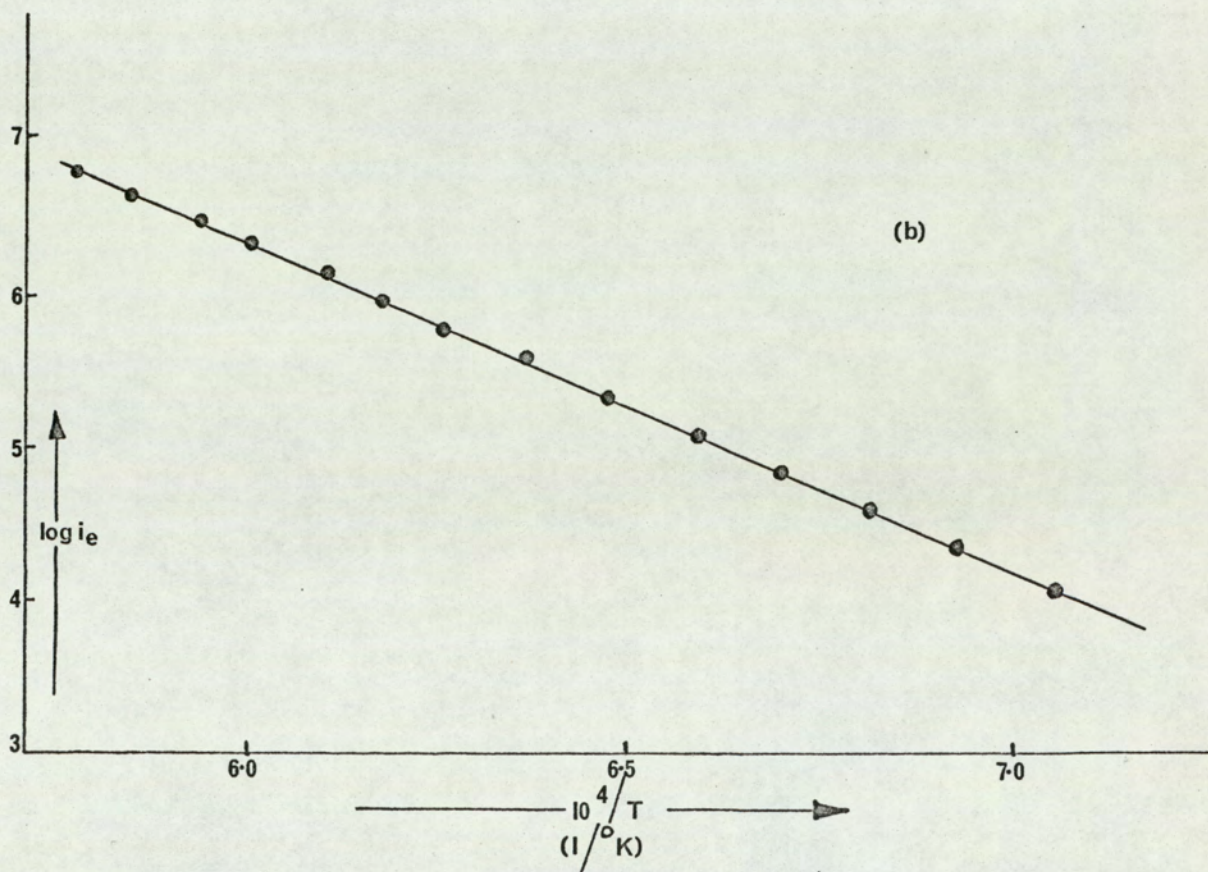
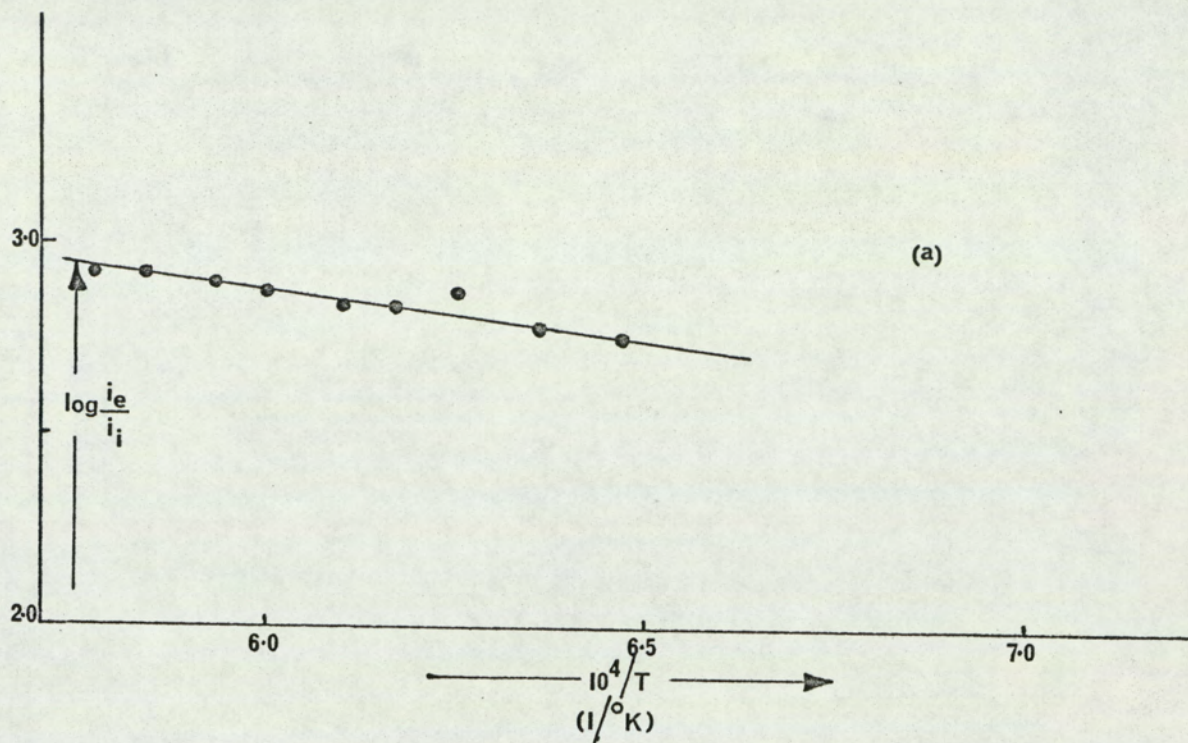
The filament used was iridium, the sample pressure was 1.4×10^{-3} Torr and the apparent electron affinity values obtained at a mean filament temperature of 1515°K were 12.8, 20.5, 18.7, 22.3, 11.4, 22.3, 27.8, 16.9 and 20.5. Omitting the value of 27.8 kcal/mole gives a mean value for E_T of 18.2 ± 4.2 kcal/mole. A typical graph is shown in figure 29.

Dimethylamine:

The filament used was tungsten, the sample pressure was approximately 1.4×10^{-3} and the apparent electron affinity values at a mean filament temperature of 1639°K were 12.3, 6.6, 11.3, 9.5, 7.6, 8.5 and 10.4, giving a mean value for E_T of 9.5 ± 2.0 kcal/mole. A typical graph is shown in figure 30.

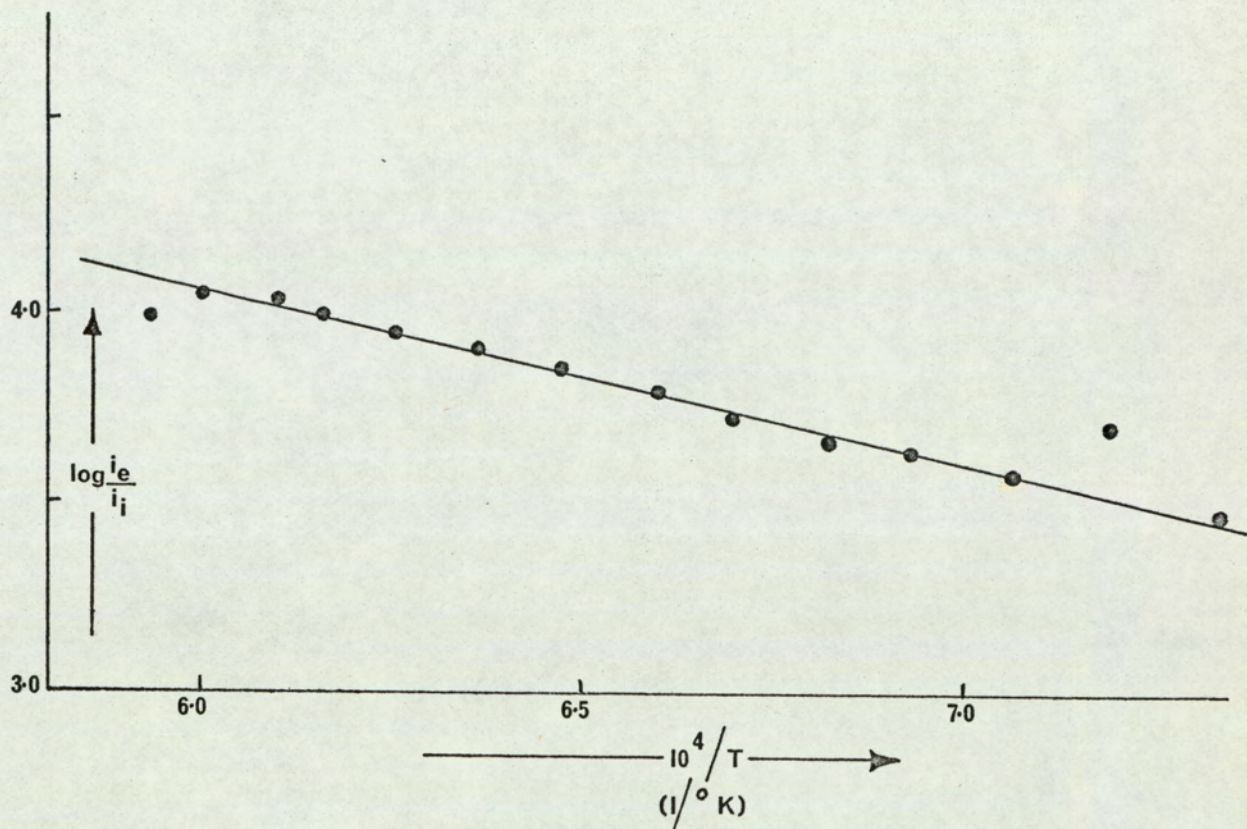
Diphosphine

The diphosphine was prepared by the neutral hydrolysis of commercial calcium phosphide, following the method of Evers and Street¹⁴⁴. It was found to be more satisfactory to employ nitrogen as a sweep gas rather than to pump the apparatus continuously and to surround the first trap with an ice/salt mixture rather than by liquid ammonia.



ELECTRON CAPTURE BY $\text{Ph}_2\text{NH} / \text{Ir.}$

FIG. 28.



ELECTRON CAPTURE BY $\text{Ph}_2\text{NH} / \text{Ir}$
 Me

FIG. 29.

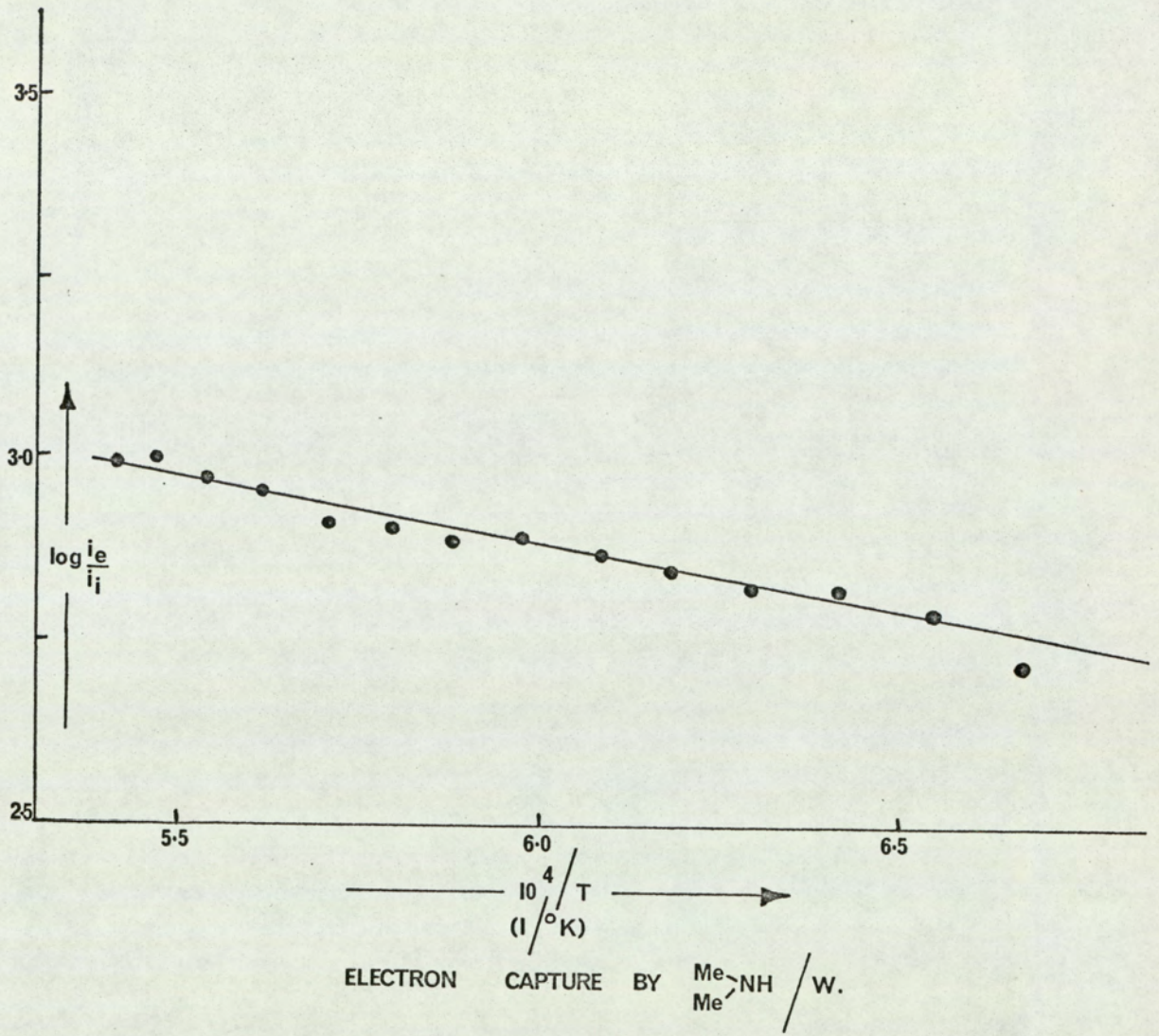


FIG.30.

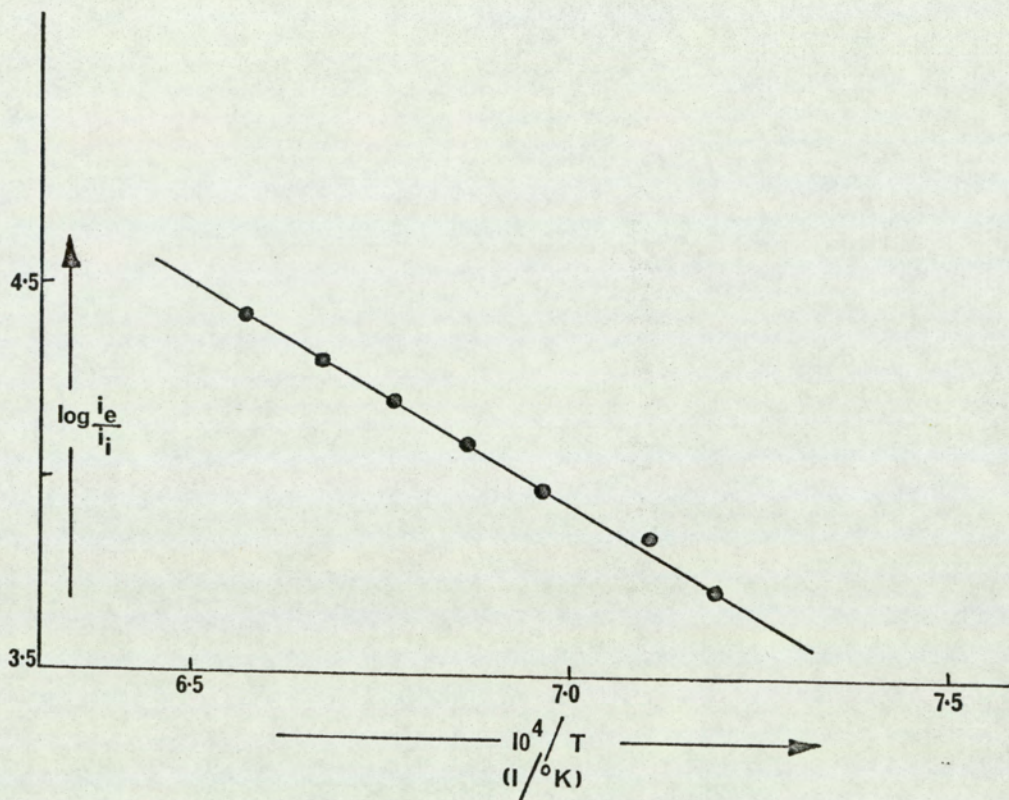
The purified diphosphine was stored at dry-ice temperatures and during a run the sample inlet system and the magnetron bottle were kept as near dry-ice temperatures as possible, to prevent decomposition of the diphosphine into phosphine and lower hydrides.

The filament used was platinum, the sample pressure was approximately 1.2×10^{-3} Torr and the apparent electron affinity values at a mean filament temperature of 1462°K were 49.9, 47.9, 42.5 and 41.4 kcal/mole, giving a mean value for E_T of 45.4 ± 4.1 kcal/mole. A typical graph is shown in figure 31.

Phosphine

The phosphine was produced by the neutral hydrolysis of a mixture of calcium and magnesium phosphides supplied by Albright and Wilson, Oldbury. The product gases were swept out of the reaction vessel by a steady stream of nitrogen gas and passed through four traps; the first two were cooled with a dry-ice/isopropanol slush to remove excess water and the last two were surrounded with liquid nitrogen to freeze out the phosphine. When the reaction was complete the last two traps were isolated, and attached to a clean, evacuated trap surrounded by liquid nitrogen. The two traps containing the phosphine were allowed to warm up to dry ice/isopropanol temperatures and the gaseous phosphine transferred to the liquid nitrogen trap, which was then isolated and transferred to a vacuum line. After repeated degassing of the phosphine the sample was considered pure enough for use.

The filament used was tungsten, the sample pressure was 2×10^{-3} Torr and the apparent electron affinity values obtained at a mean filament temperature of 1515°K were 31.5, 27.1, 30.4, 30.6, 33.7,



ELECTRON CAPTURE BY $\text{P}_2\text{H}_4/\text{Pt}$.

FIG. 31.

33.0, and 27.0 which gave a mean value for E_T of 30.5 ± 2.6 kcal/mole. A typical graph is shown in figure 32.

Diphenyl phosphine

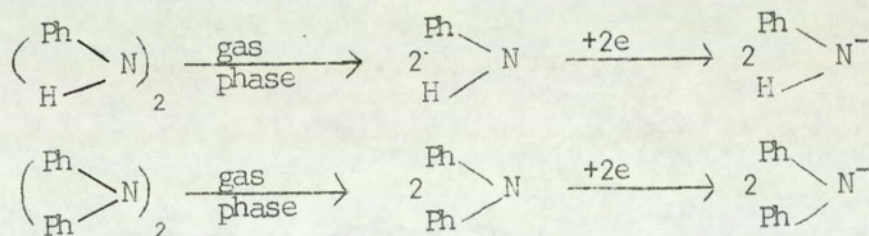
The diphenyl phosphine was supplied by Albright and Wilson, Oldbury, the filament used was iridium, the sample pressure was approximately 1.9×10^{-3} Torr and the apparent electron affinity values at a mean filament temperature of 1567°K were 28.9, 25.6, 45.8, 16.2, 22.1, 27.1, and 31.6 kcal/mole. Omitting the values 45.8 and 16.2 kcal/mole gives a mean value for E_T of 27.1 ± 4.1 kcal/mole. A typical graph is shown in figure 33.

5.4.3. Discussion

5.4.3.1. Electron Capture by R_1R_2N

1.2. Diphenylhydrazine and Tetraphenylhydrazine:

ΔS is calculated to be 90.2 eU and 86.0 eU for, respectively $(\text{PhHN})_2$ and $(\text{Ph}_2\text{N})_2$, which is typical of a type 1 or 2 mechanism. Since direct capture is unlikely by either compound a type 2 process is postulated, analogous to negative ion formation in hydrazine, that is



where $E_T = E + 2RT$. Since for $(\text{PhHN})_2$, $E_T = 42.0 \pm 2.6$ kcal/mole and $T = 1905^\circ\text{K}$ the value for the electron affinity of PhHN is 34.4 ± 2.6 kcal/mole and for $(\text{Ph}_2\text{N})_2$, $E_T = 35.2 \pm 5.0$ kcal/mole and $T = 1800^\circ\text{K}$ the value for the electron affinity of Ph_2N is 28.1 ± 5.0 kcal/mole.

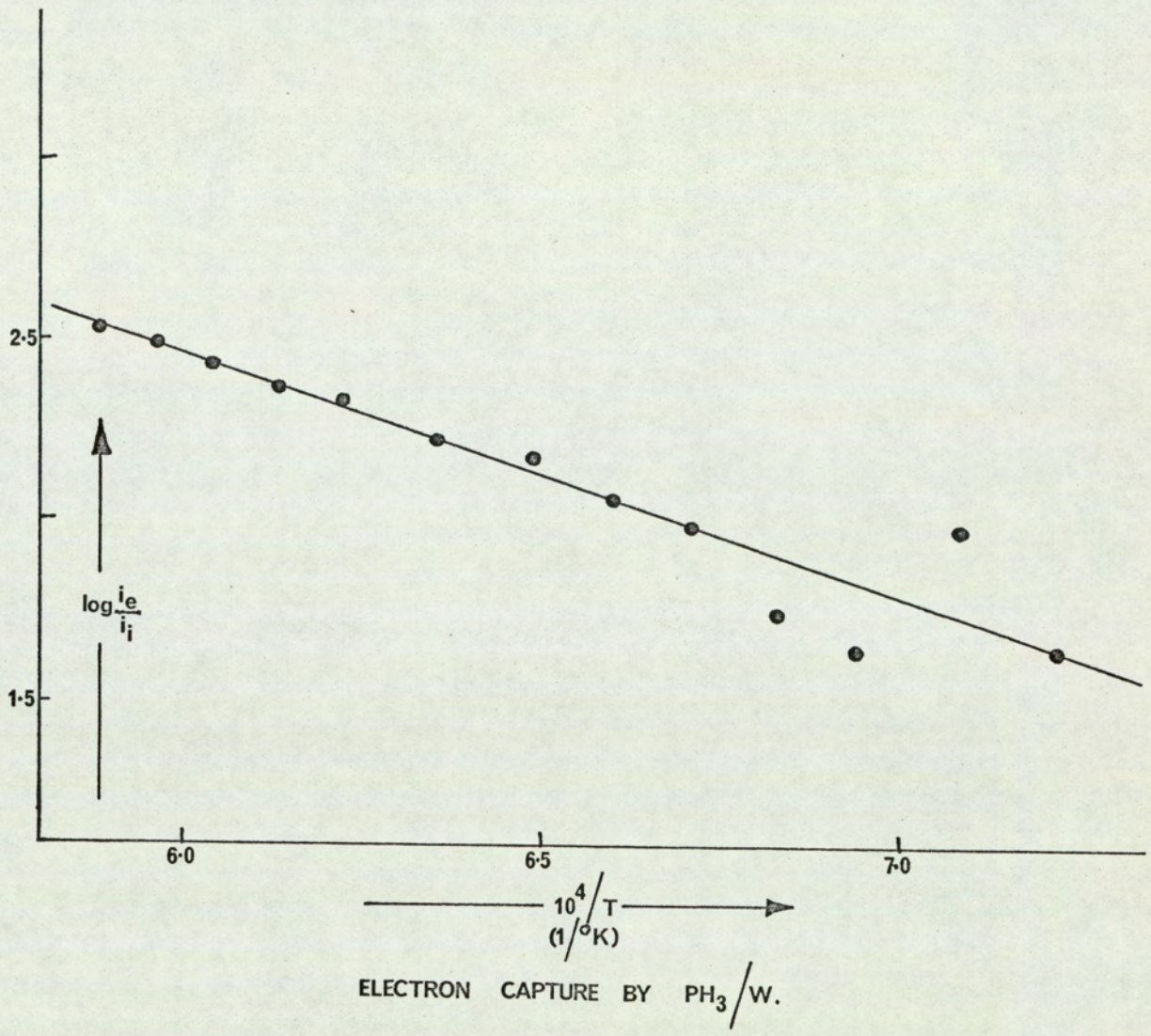


FIG. 32.

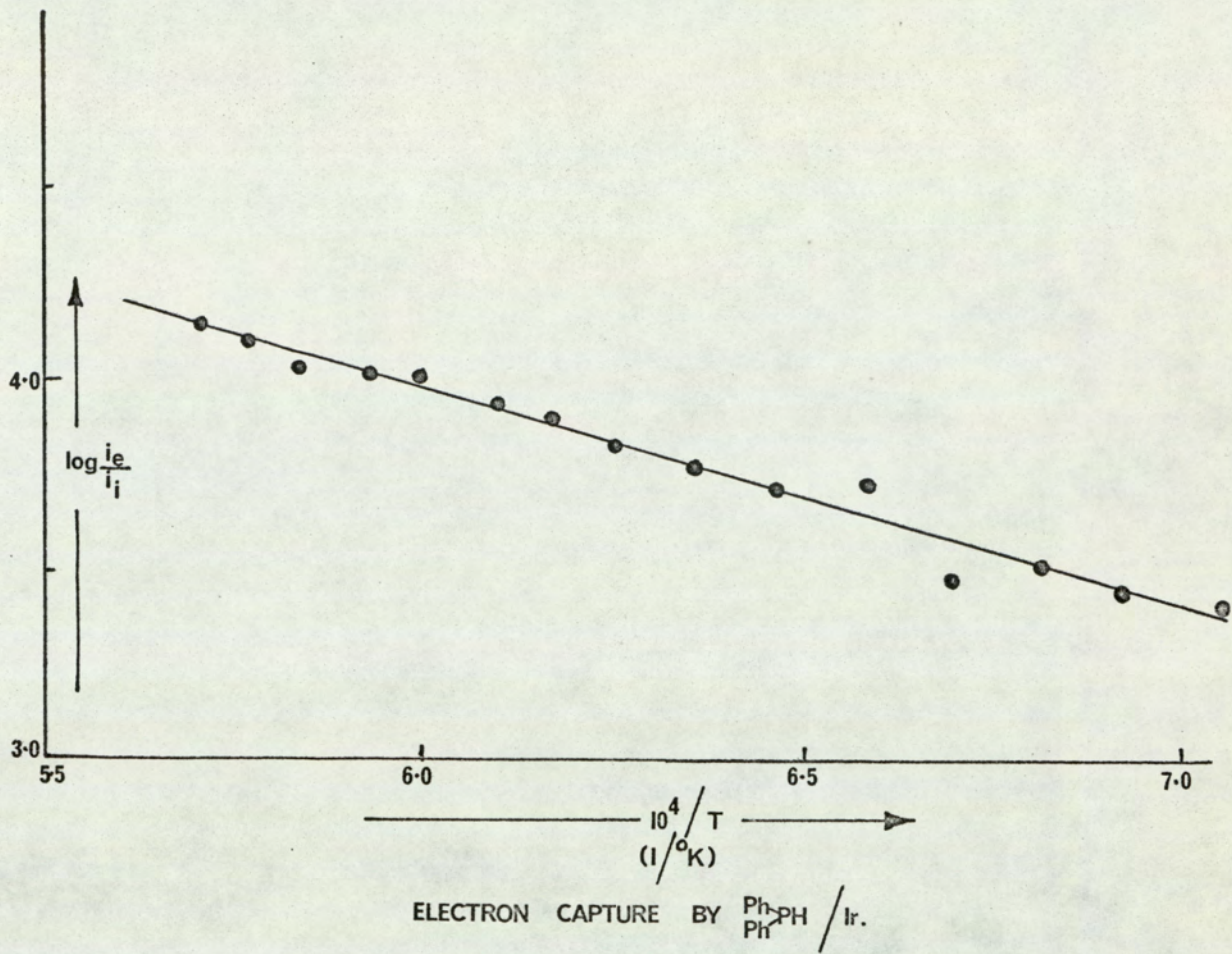
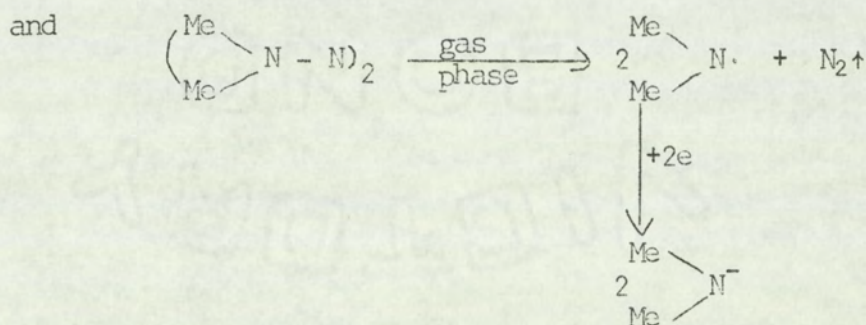
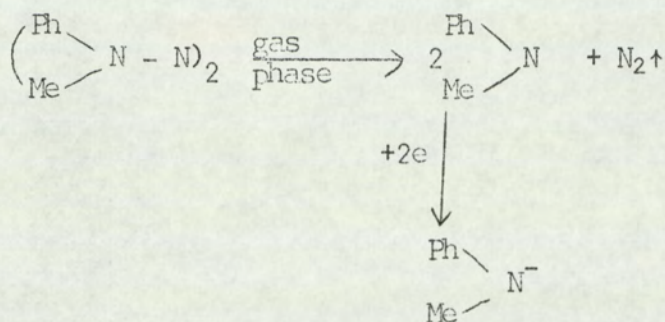


FIG.33.

Diphenyl dimethyltetrazene, Tetramethyltetrazene:

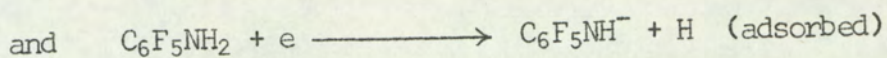
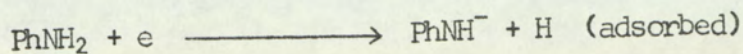
ΔS is calculated to be 90.2 eU and 87.2 eU for $(\text{PhMeN}_2)_2$ and $(\text{Me}_2\text{N}_2)_2$ respectively, which is typical of a type 1 or 2 mechanism. Since Gowenlock¹⁴² has shown that substituted tetrazenes decompose at temperatures greater than 120°C producing amino type radicals, a type 2 process is postulated, that is



where $E_T = E + 2RT$. For $(\text{PhMeN}_2)_2$ $E_T = 38.0 \pm 2.8$ kcal/mole and $T = 1750^\circ\text{K}$ giving the electron affinity of PhMeN as 31.1 ± 2.8 kcal/mole. and for $(\text{Me}_2\text{N}_2)_2$ $E_T = 28.4 \pm 1.2$ kcal/mole and $T = 1600^\circ\text{K}$ giving the electron affinity of Me_2N as 22.1 ± 1.20 kcal/mole.

Aniline and Pentafluoroaniline

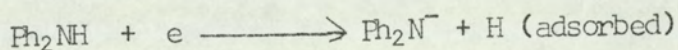
ΔS is calculated as 77.4 eU and 79.3 eU for aniline and pentafluoroaniline respectively, which is typical of type 4 processes and directly analogous to negative ion formation in ammonia. The reactions postulated are:



For a type 4 mechanism $E_T = E + Q - D + 3RT$, where for aniline $E_T = 11.7 \pm 2.5$ kcal/mole, $T = 1613^\circ\text{K}$, $Q_H(\text{Ir}) = 66$ kcal/mole and from the diphenylhydrazine results $E(\text{PhNH}) = 34.4 \pm 2.6$ kcal/mole, giving a value for first N-H bond dissociation energy in aniline of 98.3 ± 5.1 kcal/mole. Similarly for pentafluoro aniline $E_T = 12.8 \pm 2.3$ kcal/mole, $T = 1450^\circ\text{K}$, $Q_H(\text{Ir}) = 66$ kcal/mole and assuming the N-H bond dissociation energy is the same as for aniline gives a value for the electron affinity for $\text{C}_6\text{F}_5\text{NH}$ of 36.4 ± 7.4 kcal/mole.

Diphenylamine

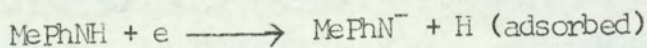
ΔS is calculated as 78.6 eU, which is typical of a type 4 process. The reaction postulated is as for aniline, that is amide formation with the hydrogen atom adsorbed on the filament.



Since $E_T = E - D + Q + 3RT$ and $E_T = 12.0 \pm 1.8$ kcal/mole, $T = 1653^\circ\text{K}$, $Q_H(\text{Ir}) = 66$ kcal/mole and $E(\text{Ph}_2\text{N}) = 28.1 \pm 5.0$ kcal/mole the value for the first N-H bond dissociation energy in diphenylamine is 91.9 ± 6.8 kcal/mole.

Methylaniline

ΔS is calculated as 82.6 eU, which is typical of a type 4 process that is



Substitution of $E_T = 18.2 \pm 4.2$ kcal/mole, $Q_H(\text{Ir}) = 66$ kcal/mole, $T = 1515^\circ\text{K}$ and $E(\text{MePhN}) = 31.1 \pm 2.8$ kcal/mole into the equation for the apparent electron affinity leads to a value for $D(\text{MePhN-H})$ of

88.1 \pm 7.0 kcal/mole.

Dimethylamine

ΔS is calculated as 76.1 eU, which is typical of a type 4 process, and consistent with all the amine results. The reaction postulated is $\text{Me}_2\text{NH} + e \longrightarrow \text{Me}_2\text{N}^- + \text{H}$ (adsorbed), where $E_T = 9.5 \pm 2.0$ kcal/mole, $Q_H(W) = 72$ kcal/mole, $T = 1639^\circ\text{K}$ and $E(\text{Me}_2\text{N}) = 22.1 \pm 1.2$ kcal/mole, which leads to a value for $D(\text{Me}_2\text{N} - \text{H})$ of 94.4 ± 3.2 kcal/mole.

Table 5 summarises the derived electron affinities and gives the value of $\cdot E(\text{NH}_2)$ for comparison.

Table 5

Compound	Information Derived (kcal/mole)
1.2. Diphenyl hydrazine	$E(\text{PhNH}) = 34.4 \pm 2.6$
Pentafluoro aniline	$E(\text{C}_6\text{F}_5\text{NH}) = 36.4 \pm 7.4$
Tetraphenyl hydrazine	$E(\text{Ph}_2\text{N}) = 28.1 \pm 5.0$
Dimethyldiphenyl tetrazene	$E(\text{MePhN}) = 31.1 \pm 2.8$
Tetramethyl tetrazene	$E(\text{Me}_2\text{N}) = 22.1 \pm 1.2$
Hydrazine (86)	$E(\text{NH}_2) = 25.7 \pm 2.0$

and Table 6 gives the derived first N-H bond dissociation energies for the amines studied, and the value for $D(\text{NH}_2 - \text{H})$ for comparison.

Table 6

Compound	Information Derived (kcal/mole)
Aniline	$D(\text{PhHN} - \text{H}) = 98.3 \pm 5.1$
Diphenylamine	$D(\text{Ph}_2\text{N} - \text{H}) = 91.9 \pm 6.8$
Methylaniline	$D(\text{MePhN} - \text{H}) = 88.1 \pm 7.0$
Dimethylamine	$D(\text{Me}_2\text{N} - \text{H}) = 94.4 \pm 3.2$
Ammonia (86)	$D(\text{H}_2\text{N} - \text{H}) = 104.9 \pm 2.0$

The results summarized in table 5 suggest that phenyl substitution at the nitrogen results in an increase in the electron affinity of the radical, whereas methyl substitution results in a decrease in the electron affinity of the radical. Similarly it is found that substitution at the nitrogen in amines has an effect upon the base strength of the amine. Since the base strength of an amine is attributed to the ability of the lone pair electrons on the nitrogen to be shared by electron acceptors there should be a close parallel between the base strength of the amine and the electron affinity of the corresponding amino radical, as the electron affinity will also be very dependent upon the electron density at the nitrogen. That is, the greater the electron density at the nitrogen, as compared to ammonia, the lower the electron affinity of the radical and the greater the base strength of the corresponding amine. The reverse is true for cases where the electron density at the nitrogen is lower than that in ammonia.

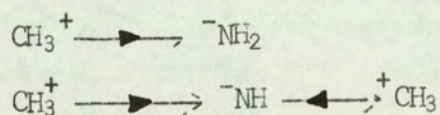
Table 7 gives the values for the electron affinity of the amino radical and the $\text{p}K_b$ value for the corresponding amine.

Table 7

Compound	Ph ₂ NH	PhNH ₂	C ₆ F ₅ NH	PhMeNH	NH ₃	MeNH ₂	Me ₂ NH
E(R ₁ R ₂ N) kcal/mole	28.1 + 5.0 -	34.4 + 2.6 -	36.4 + 7.4 -	31.1 + 2.8 -	25.7 + 2.0 -		22.1 + 1.2 -
pK _b of amine	13.2	9.38			4.74	3.36	3.29

Where pK_b is defined as the logarithm of the reciprocal of the basic dissociation constant K_b given by the equilibrium $B: + HOH \xrightleftharpoons{K_b} B:H^+ + :OH^-$.

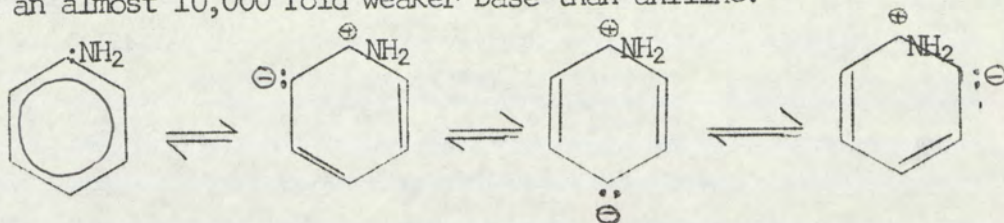
The greater base strength of methylamine over ammonia is thought to result from the greater capability of electron release of the methyl group as compared to hydrogen, which effectively increases the electron density on the nitrogen atom; this is further increased when two methyl groups are present, as in dimethylamine. The effect is shown below



Assuming that the additional electron in the negative ion is localised on the nitrogen as a lone pair then the increase in electron density at the nitrogen should result in the methyl and dimethyl radicals having a lower electron affinity than the unsubstituted species, as is found experimentally.

The vastly lower basicity of aniline as compared to ammonia is attributed to resonance. As shown below the pair of electrons on the nitrogen is distributed over the aromatic ring, and it is, therefore,

less available for sharing in reaction with an acid. Diphenylamine with 2 aromatic rings further reduces the electron density at the nitrogen and is an almost 10,000 fold weaker base than aniline.



Since phenyl substitution reduces the electron density at the nitrogen it should result in phenyl substituted amino radicals having a greater electron affinity than the unsubstituted and methyl substituted radicals, as is in fact found experimentally.

Also electron withdrawing substituents on the aromatic ring will further reduce the electron density at the nitrogen and, therefore, further reduce the basicity of the amine and increase the electron affinity of the amino radical; this effect is illustrated by pentafluoroaniline which has an electron affinity 2.0 kcal/mole greater than that determined for aniline.

The pK_b values quoted in table 7 show that phenyl substitution has a greater effect than methyl substitution upon the electron density at the nitrogen atom, which suggests that the electron affinity of the methyl-phenyl substituted radical should be greater than that for NH_2 but less than that for PhNH or $\text{C}_6\text{F}_5\text{NH}$, as is found experimentally.

Hence, with the exception of Ph_2NH the effect of substitution at the nitrogen atom upon the electron affinity is reasonably small and can be accounted for by simple inductive-resonance effects. However, from a comparison of the base strengths of aniline and diphenyl-

amine the electron affinity of Ph_2N . would be expected to be approximately 40 kcal/mole, which is considerably greater than the experimentally determined value of 28.1 ± 5.0 kcal/mole; a discrepancy which is difficult to account for on resonance grounds since the pK_b value of diphenylamine indicates that the electron density at the nitrogen is much reduced from that in aniline, which should mean that the Ph_2N radical has the greatest electron affinity of all the radicals studied.

It is noticeable that neither of the symmetrical amino radicals, Me_2N . and Ph_2N ., have very different electron affinities from NH_2 ., whereas the unsymmetrical amino radicals have considerably higher electron affinities.

Gaines et. al.¹⁴⁵ have suggested that the substitution of a group into the radical could stabilize the charged state by an amount $\mu e/r^2$, where μ is the dipole moment of the substituent and r is the effective distance from the lone pair, which could provide an alternative explanation for the values of the stabilities of the amide^{no} ions.

Assuming that substitution does not affect the geometry of the amino radical, the electron affinities of the unsymmetrical ions, PhNH ., MeNH . and PhMeN ., should be greater, by an amount $\mu e/r^2$, than the symmetrical ions, NH_2 . Me_2N . and Ph_2N .. An estimate for this stabilization term may be made for aniline since the N-Ph bond moment is about 0.8D^{146} , (0.8×10^{-18} esu), the distance between the nitrogen and the centre of the phenyl group is about 2.9\AA and e is 4.803×10^{-10} esu, which gives a value for $\mu e/r^2$ of about 6.5

kcal/mole. This is in good agreement with the difference between the electron affinities of $\text{Ph}_2\text{N} \cdot$ and $\text{PhNH} \cdot$ of 6.3 kcal/mole. A similar stabilization term will be present for $\text{MeNH} \cdot$ and $\text{PhMeN} \cdot$, which would account for the greater stability of PhMeN over $\text{NH}_2 \cdot$ and $\text{Ph}_2\text{N} \cdot$. In addition Collin¹⁴¹ has determined the electron affinity of MeNH , from mass spectral data as 36.0 kcal/mole as compared to the value for Me_2N of 22.1 kcal/mole, giving a difference of 13.9 kcal/mole, in reasonable agreement with the aniline, diphenylamine results. However, his value may be in considerable error due to the inaccuracies involved in deducing electron affinities from mass spectral data. A study of electron capture by $\text{MeHN} \cdot$ and other mono and disubstituted amino radicals is necessary before an unequivocal description of the effect of substitution at the nitrogen atom upon the electron affinity, can be postulated.

In general, substitution in a molecule affects the bond dissociation energies, and the greater the substitution the greater the effect, as shown by the experimental values given in table 6. The values given in table 6 are to be compared with those determined by other workers, given in table 8.

Table 8

Bond	Bond dissociation energies (kcal/mole)					
$\text{NH}_2\text{-H}$			104 ± 2 ¹⁴⁰			
MeHN-H	92 ± 3 ¹⁴⁷			$98\text{-}99$ ¹⁴⁹	107 ¹⁵⁰	94.8 ¹⁵¹
$\text{Me}_2\text{N-H}$	86 ± 3 ¹⁴⁷			$95\text{-}96$ ¹⁴⁹	110 ¹⁵⁰	89.2 ¹⁵¹
MePhN-H		74.5 ± 3 ¹⁴⁸				
PhHN-H		80 ± 3 ¹⁴⁸				
$\text{Ph}_2\text{N-H}$						

As seen from table 8 the agreement between different workers, and often, therefore, different techniques is not good; the discrepancies probably arise due to the inaccuracies in the various techniques, which are discussed below.

The values given in the first 3 columns^{140,147,148} have been calculated from appropriate heats of formation. This type of calculation gives good values for atom-atom bond dissociation energies as only heats of formation of atomic species are required which are well established. However, in order to calculate atom-radical or radical-radical bond dissociation energies, the heats of formation of radicals are required, which are not so well known and can introduce large errors into the calculations.

The values given in column four¹⁴⁹ are derived from a comparison with the appropriate hydrocarbon R-H and alcohol RO-H, which involves the assumption that R will affect the D(N-H) in an identical manner to the affect it has upon the C-H and O-H bonds, and must be only regarded as speculative values.

The values given in column five¹⁵⁰ are calculated from appearance potential data, derived from electron impact measurements in a mass spectrometer, and the appropriate heats of formation. This type of calculation does not in general lead to very accurate values for bond dissociation energies, mainly due to the difficulty in determining the onset of ion-formation and, therefore, the appearance potential.

The values in column six¹⁵¹ are determined from a kinetic method, where the accuracy depends on the experimental activation energies and experimental heats of formation, which may be in error by more than

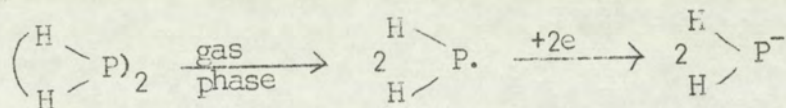
1 kcal/mole. To reduce the errors in their calculations Gray et. al. compared the differences in activation energies for the hydrogen abstraction reaction of ammonia and methylamine, and methylamine and dimethylamine. They obtained values for $D(\text{NH}_2\text{-H}) - D(\text{MeNH-H})$ and similarly $D(\text{MeNH-H}) - D(\text{Me}_2\text{N-H})$ of 11.2 and 5.6 kcal/mole, respectively; these differences are not necessarily subject to the same errors as individual bond dissociation energies, since common terms disappear. They took $D(\text{NH}_2\text{-H})$ as 106 ± 3 kcal/mole which results in $D(\text{MeNH-H}) = 94.8$ and $D(\text{Me}_2\text{N-H}) = 89.2$ kcal/mole.

With the exception of the values quoted by Dibeler et. al.¹⁵⁰ all workers are in qualitative agreement with the Magnetron results; that is both methyl and phenyl substitution reduce the N-H bond energy.

5.4.3.2. Electron Capture by $\text{R}_1\text{R}_2\text{P}$.

Diphosphine

ΔS is calculated to be 106.8 e.U, which is typical of a type 1 or 2 process. As direct capture is unlikely by diphosphine a type 2 process is postulated, analogous to negative ion formation in hydrazine, that is

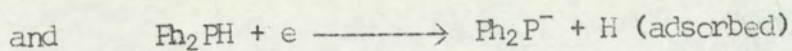
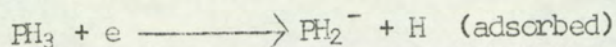


For this type of process $E_T = E + 2RT$ which, substituting the values $E_T = 45.4 \pm 4.1$ kcal/mole and $T = 1462^\circ\text{K}$ gives a value for $E(\text{PH}_2\cdot)$ = 39.6 ± 4.1 kcal/mole.

Phosphine and diphenyl phosphine

ΔS is calculated to be 86.6 eU and 91.9 eU for respectively phosphine and diphenylphosphine. On energetic grounds the only possible

process is a type 4 mechanism, although the calculated entropy values are rather high for this type of process. The reactions postulated are analogous to negative ion formation in ammonia, that is,



For this type of process $E_T = E - D + Q + 3RT$, where for phosphine $E_T = 30.5 \pm 2.6$ kcal/mole, $T = 1515^\circ\text{K}$, $Q_H(\text{W})^{87} = 72$ kcal/mole and from the diphosphine results $E = 39.6 \pm 4.1$ kcal/mole, which gives a value for the first P-H bond dissociation energy in phosphine of 90.2 ± 6.7 kcal/mole. Similarly for diphenyl phosphine $E_T = 27.1 \pm 4.1$ kcal/mole, $T = 1567^\circ\text{K}$ and $Q_H(\text{Ir})^{87} = 66$ kcal/mole, which gives a value for $E - D$ of -48.3 ± 4.1 kcal/mole. To evaluate $D(\text{Ph}_2\text{P} - \text{H})$ it is assumed that $E(\text{Ph}_2\text{P}.) = E(\text{PH}_2) + 2.4$ kcal/mole, analogous to $E(\text{Ph}_2\text{N}) = E(\text{NH}_2) + 2.4$ kcal/mole, which gives a value for $D(\text{Ph}_2\text{P-H})$ of 87.9 ± 8.2 kcal/mole.

The only value quoted for the bond energies in phosphine is the average P-H bond energy of 77 kcal/mole¹⁰⁶, as compared to the average N-H bond energy in ammonia of 93.4 kcal/mole. Since the first bond energy in ammonia is 104 kcal/mole a value of approximately 86 kcal/mole could be expected for $D(\text{PH}_2 - \text{H})$, which is in agreement with the experimental value, whereas from heats of formation¹³³, since $\Delta H_f^\circ \text{PH}_3 = 6.945$, $\Delta H_f^\circ \text{PH}_2 = 30.594$ and $\Delta H_f^\circ \text{H} = 51.645$ the value for $D(\text{PH}_2 - \text{H})$ is calculated to be 75.3 kcal/mole.

5.5. Experimental and Predicted Electron Affinities

The sensitivity of the value of the electron affinity of a radical to the valence state of the accepting centre, as shown by CH ,

CH_3 , C_6H_5 and C_2H_5 , and to the nature of this centre as shown by NH_2 . and PH_2 , and CF_3 and SiF_3 , is good evidence for the theory that the additional electron is localised as a lone pair on the atom where the free valence lay. Although substitution in the radical has a relatively small effect upon the stability of the negative ion, the electron affinity of a radical is basically determined by the nature and valence state of the atom where the free valence lay. Hence, provided the bond energy term in equation 5.2. can be considered to be zero then the electron affinity of a radical will be given by the electron affinity of the atom in the appropriate valence state.

The valence state electron affinity is given by equation 5.3. as ⁵⁶.

$$E_v = E_g + (P_o - P_-)$$

where E_g is the ground state electron affinity P_o , P_- are the promotion energies for respectively the atomic and ionic state.

The promotion energies for C, and C^- , Si and Si^- , P and P^- and N and N^- , are given in table 9 and 10⁵⁶.

In constructing tables 9 and 10 only states of the common multiplicity have been considered, that is for example, neither the state of carbon with 2 singly occupied hybrid orbitals nor the case where all the electrons are in pairs have been included.

The ground state electron affinities of C, Si, N and P are given in table 11.⁴⁵

Table 9

Valence State	C		Si	
	eV	kcal/mole	eV	kcal/mole
s ³ ppp	8.479	195.6	6.223	143.5
di ² di ³ π	7.193	165.9	5.415	124.9
tr ² tr ³ π	6.764	156.0	5.145	118.6
te ² te ³ π	6.549	151.0	5.011	115.6
	C ⁻		Si ⁻	
s ² ppp	0.682	15.7	0.745	17.2
sp ² pp	9.254	213.4	4.867	112.2
di ² di ³ π	4.968	114.6	2.806	64.7
di ² di ² π ²	8.208	189.3	4.674	107.8
tr ² tr ³ π	5.931	136.8	3.408	78.6
tr ² tr ² π ²	7.858	181.2	4.610	106.3
te ² te ³ π	6.326	145.9	3.692	85.1

Table 10

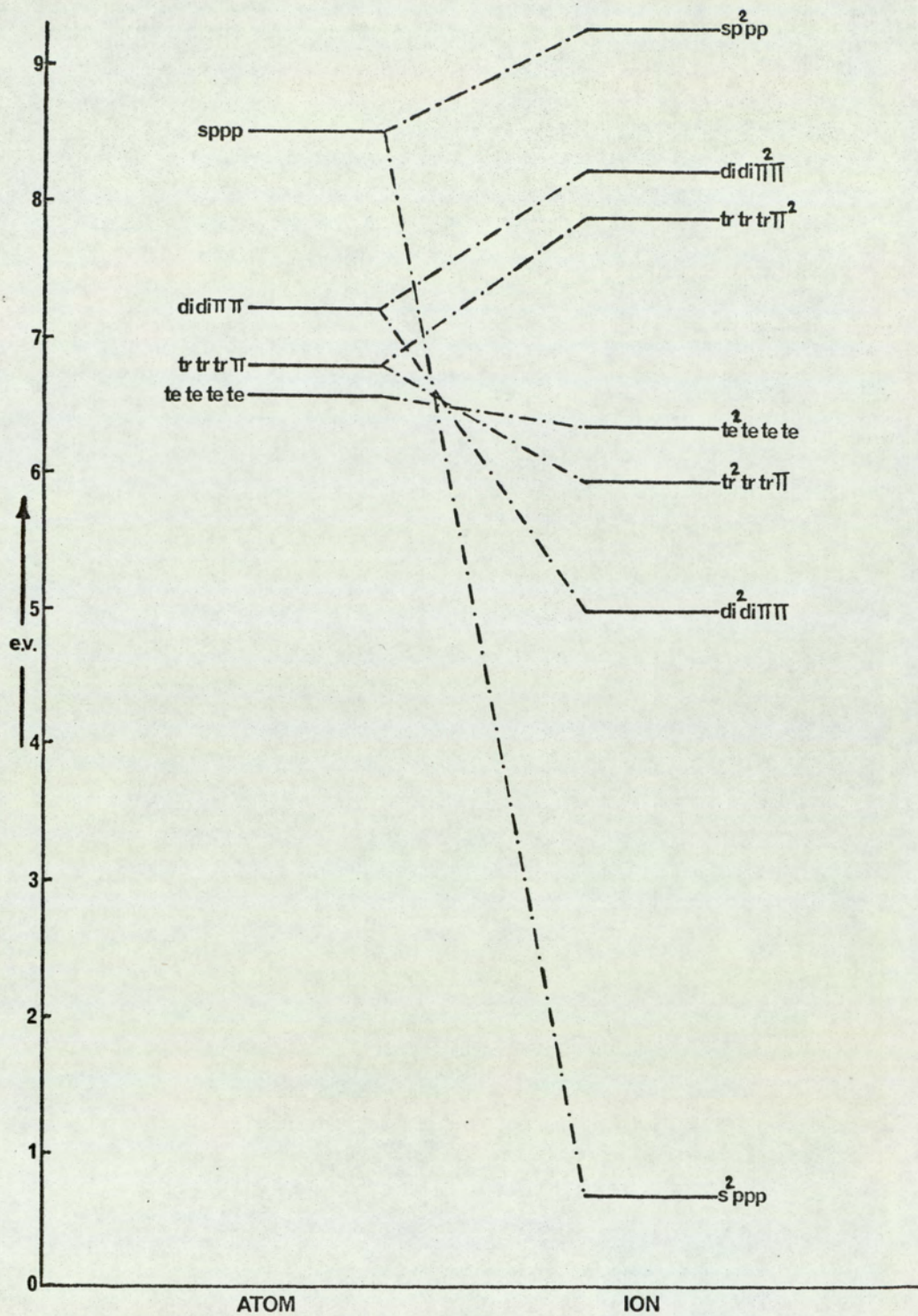
Valence State	N		P	
	eV	kcal/mole	eV	kcal/mole
s^2ppp	1.082	25.0	0.831	19.2
sp^2pp	14.292	329.6	7.891	182.0
$di^2di\Pi\Pi$	7.687	177.3	4.361	100.6
$didi\Pi^2\Pi$	12.867	296.7	7.450	171.8
$tr^2trtr\Pi$	9.255	213.4	5.342	123.2
$trtrtr\Pi^2$	12.392	285.8	7.303	168.4
te^2tete	9.920	228.8	5.795	133.6
	N^-		P^-	
	eV	kcal/mole	eV	kcal/mole
s^2p^2pp	0.350	8.1	0.212	4.9
sp^2p^2p	11.799	272.1	6.686	154.2
$di^2di^2\Pi\Pi$	0.350	8.1	0.212	4.9
$di^2di\Pi^2\Pi$	6.074	140.1	3.449	79.5
$didi\Pi^2\Pi^2$	10.772	248.4	6.203	143.0
$tr^2tr^2tr\Pi$	4.166	96.1	2.370	54.7
$tr^2trtr\Pi^2$	7.526	173.6	4.313	99.5
te^2te^2tete	5.818	134.2	3.328	76.7

Table 11

Atom	Eg kcal/mole
C	28.8 ⁵
N	1.2
Si	33.7
P	17.8

There are a number of possible valence states for both the atom and ion, which suggests that a number of transitions between the atomic and ionic state could occur. However, some transitions between the atomic and ionic states are less likely than others and the most probable are those in which no rehybridisation occurs, the additional electron entering a vacant orbital to form a lone pair. Such transitions for $C \rightarrow C^-$, $Si \rightarrow Si^-$, $N \rightarrow N^-$ and $P \rightarrow P^-$ are illustrated in figures 34, 35, 36 and 37 respectively.

The most probable ground state of a carbon atom in C_2H is $didid\uparrow\uparrow\uparrow$, which suggests that the most probable valence state of the C^- in C_2H^- is $di^2di\uparrow\uparrow\uparrow$, provided the additional electron is localised as a lone pair on the C atom where the free valence lay. Hinze⁵⁶ gives the promotion energies of $C(didid\uparrow\uparrow\uparrow)$ and $C^-(di^2di\uparrow\uparrow\uparrow)$ as 165.9 and 114.6 kcal/mole, respectively; the ground state electron affinity of C is 28.8 kcal/mole⁵. Substitution of these values into equation 5.3. gives a value for the predicted electron affinity of C_2H of 80.1 kcal/mole as compared to the experimental electron affinity of 62.8 ± 4.1 kcal/



PROMOTION ENERGIES FOR VARIOUS VALENCE STATES OF THE CARBON ATOM AND ION.

FIG.34.

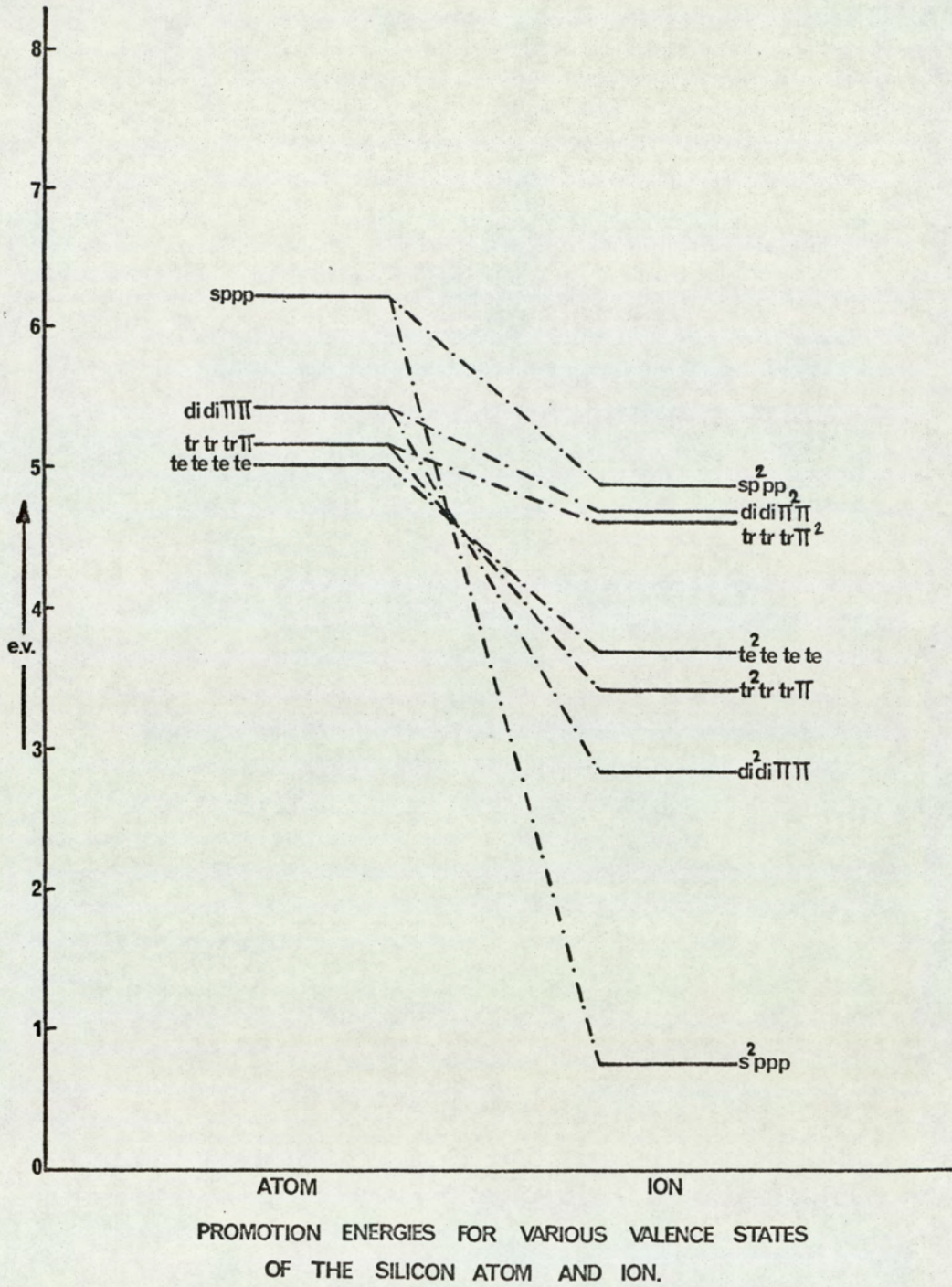
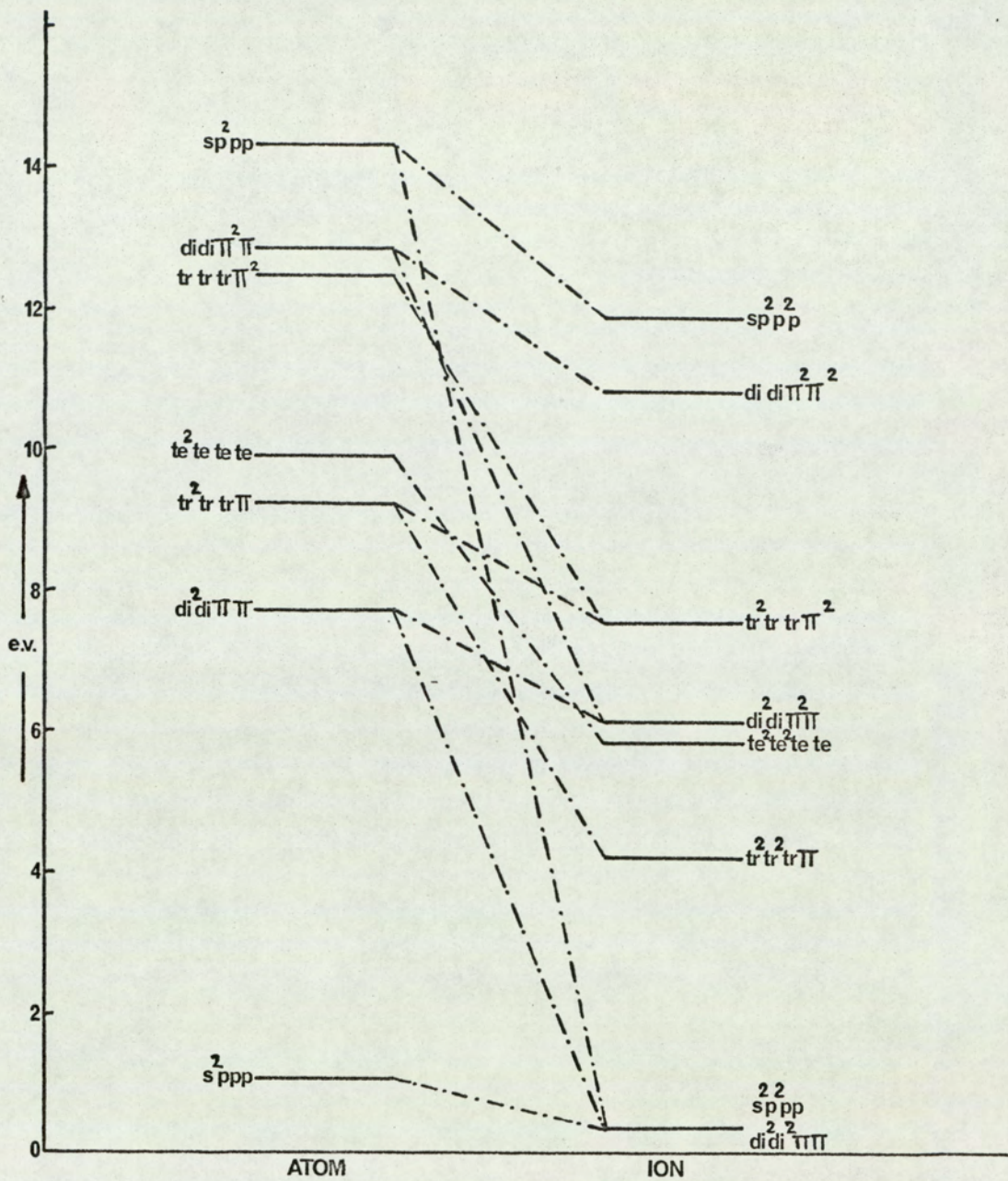
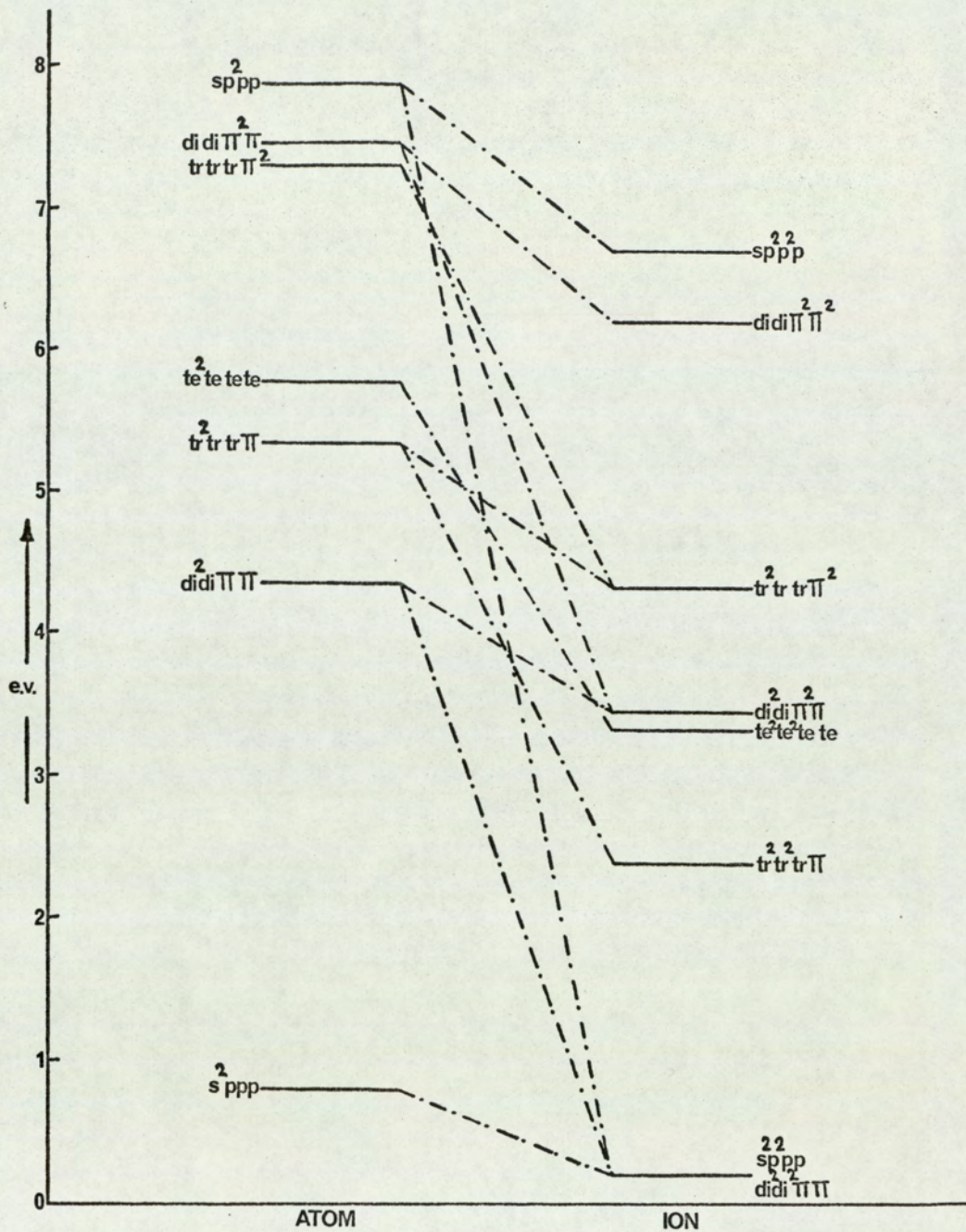


FIG. 35.



PROMOTION ENERGIES FOR VARIOUS VALENCE STATES OF THE NITROGEN ATOM AND ION.

FIG. 36.



PROMOTION ENERGIES FOR VARIOUS VALENCE STATES OF THE PHOSPHORUS ATOM AND ION.

FIG. 37.

mole.

Recent studies of CF_3 by E.S.R.¹⁵² and Infra red spectroscopy¹⁵³ have shown that CF_3 is pyramidal, unlike CH_3 which is planar, which suggests that the most probable valence state of C in CF_3 is tetetete, and the most probable valence state of C^- in CF_3^- is te^2tetete . Hinze⁵⁶ gives the promotion energies of C tetetete and C^- (te^2tetete) as 151.0 and 145.9 kcals/mole, which leads to a value for the predicted electron affinity of CF_3^- of 33.9 kcals/mole, as compared to the experimental value of 42.7 ± 1.8 kcals/mole.

Similarly the ground states of SiF_3 and SiF_3^- are expected to correspond to Si(tetetete) and Si^- (te^2tetete), respectively. The ground state electron affinity of silicon is 33.7 kcals/mole⁴⁵ and Hinze⁵⁶ gives the promotion energies of Si (tetetete) as 115.6 kcals/mole and Si^- (te^2tetete) as 85.1 kcals/mole, which results in a value for the predicted electron affinity of SiF_3 of 64.2 kcals/mole as compared to the experimental value of 78.3 ± 7.0 kcals/mole.

Due to the strong electronegativity of fluorine the bond energy term for CF_3 and SiF_3 may not be zero, and in this case the approximation that the electron affinity of the radical is equal to the electron affinity of the atomic species, in the same valence state is not strictly valid. Although the predicted values for both CF_3 and SiF_3 are lower than the experimental values, the difference in the predicted values of 30.3 kcals/mole is in good agreement with the experimental value of 35.6 kcals/mole, which suggests that even in cases where the radical contains a strongly electronegative group equation 5.3. may be used to predict relative electron affinities.

The prediction of electron affinities for $\text{NH}_2\cdot$ and $\text{PH}_2\cdot$ is complicated as there is a possibility that the lone pair on the nitrogen and phosphorus could be hybridised, which would tend to increase the s character of the orbital accepting the electron and, therefore, increase the electron affinity of the radical. Peters¹⁵⁴ has suggested that the lone pair in ammonia are partly hybridised which could be true of the lone pair in NH_2 and similarly PH_2 .

Since, even the lowest hybridised state, $\text{d}^2\text{d}^2\text{sp}^3$ would require a large promotional energy, as shown in figures 36 and 37, of approximately 150 kcal/mole in the case of nitrogen and 80 kcal/mole in the case of phosphorus, the valence states of NH_2 and NH_2^- are assumed to correspond to $\text{N}(\text{s}^2\text{p}^3)$ and $\text{N}^-(\text{s}^2\text{p}^2\text{pp})$. The ground state electron affinity of nitrogen is 1.2 kcal/mole⁴⁵ and Hinze⁵⁶ gives the promotion energies of $\text{N}(\text{s}^2\text{p}^3)$ and $\text{N}^-(\text{s}^2\text{p}^2\text{pp})$ as 25.0 and 8.1 kcal/mole, respectively, which leads to a predicted electron affinity of 18.1 kcal/mole, as compared to the experimental value of 25.7 ± 2.0 kcal/mole. Similarly PH_2 and PH_2^- are assumed to correspond to $\text{P}(\text{s}^2\text{p}^3)$ and $\text{P}^-(\text{s}^2\text{p}^2\text{pp})$, which leads to a value for the electron affinity of $\text{PH}_2\cdot$ of 32.1 kcal/mole as compared to the experimental value of 39.6 ± 4.1 kcal/mole, since the promotion energies of $\text{P}(\text{s}^2\text{p}^3)$ and $\text{P}^-(\text{s}^2\text{p}^2\text{pp})$ are respectively 19.2 and 4.9 kcal/mole and the ground state electron affinity of phosphorus is 17.8 kcal/mole.

The predicted values for both NH_2 and PH_2 are 7 kcal/mole lower than the experimental values which may be due to partial lone pair hybridisation in these species.

A summary of the predicted and experimental electron affinities is given in table 12.

Table 12

Radical	Transition	Electron affinity (kcal/mole)	
		Predicted	Experimental
C ₂ H	di ² di ² → di ² di ²	80.1	62.8 ± 4.1
CF ₃	tet ² tet ² → te ² tet ²	33.9	42.7 ± 1.8
SiF ₃	tet ² tet ² → te ² tet ²	64.2	78.3 ± 7.0
NH ₂	s ² ppp → s ² p ² pp	18.1	25.7 ± 2.0
PH ₂	s ² ppp → s ² p ² pp	32.1	39.6 ± 4.1

The predicted and experimental values of the electron affinities given in table 12 are in reasonable agreement, considering that both the promotion energies and ground state electron affinities are extrapolated values. Hence, for many species, particularly radicals which have hydrogen as the substituent groups, where effects due to interactions between the substituents and the centre on which the additional electron is localised as a lone pair are minimised, values of the electron affinities for various valence states of the central atom may be predicted, as given by Page and Goode¹⁵⁵.

6. THE IDENTIFICATION OF NEGATIVE IONS USING A QUADRUPOLE MASS FILTER

6.1. Introduction

The disadvantage of the Magnetron technique is that the identification of the ions is only indirect and therefore complex reactions, which give rise to similar numbers of ions of differing mass may be misinterpreted in terms of a simple reaction.

To overcome this disadvantage an all-metal Magnetron assembly was directly mounted onto a Quadrupole Mass Filter. The ions formed at the filament were accelerated towards the anode, in which there was a small hole in line with the axis of the quadrupole field. This allowed a small percentage of the ions to be further accelerated and focussed into the quadrupole field, where they were mass analysed. Although, in theory, this system should have allowed the usual magnetron type measurements of ion current, electron current and filament temperature to be made, in conjunction with the identification of the negative ions present, it was rejected because of experimental difficulties. Due to the attachment of the Quadrupole Mass Filter the solenoid in the simple Magnetron assembly had to be replaced with a pair of Helmholtz coils whose magnetic field strongly interacted with the quadrupole field, and more important the intensity of the negative ions accelerated into the quadrupole field was too low to be detected after mass analysis.

As an alternative, the original electron impact source of the Atlas A.M.P.3. Quadrupole Mass Filter was modified into a surface ionisation source in such a manner that it was possible to determine the

electron and corresponding ion currents for a series of filament temperatures.

The samples studied were bromine and tetracyanoethylene. Bromine was chosen as the first compound to be studied since at filament temperatures in the range 1200-2000°K bromine was completely dissociated into bromine atoms and formed bromide ions by the direct capture of an electron. The apparent electron affinity, determined from the temperature dependence of the ion and electron current was directly related to the electron affinity of the bromine atom by equation 3.33, that is $E_T = E + 2RT$; the experimental value for $E(\text{Br})$ was then compared to the well established spectroscopic value of 77.6 kcal/mole⁷.

Tetracyanoethylene was studied as it was known to readily form negative ions. Page et. al.¹⁵⁶ determined the electron affinity to be 150 kcal/mole, almost twice the value of the electron affinity of chlorine⁷. This was shown to be in error⁸⁷ due to adsorption of the tetracyanoethylene on the tungsten filament, and Farragher⁸⁷ determined the electron affinity as 65.2 ± 1.5 kcal/mole. Since compounds which contain a cyano group usually decompose at the hot filament to produce CN^- it was of interest to determine the relative contributions of the molecular negative ion and of CN^- to the total ion current and thus determine the validity of the value given by Farragher⁸⁷ for the electron affinity of tetracyanoethylene.

6.2. Experimental

The complete apparatus, that is ion source, quadrupole and detection system is shown in figure 38.

The pressure of the gas sample was controlled by an Edwards

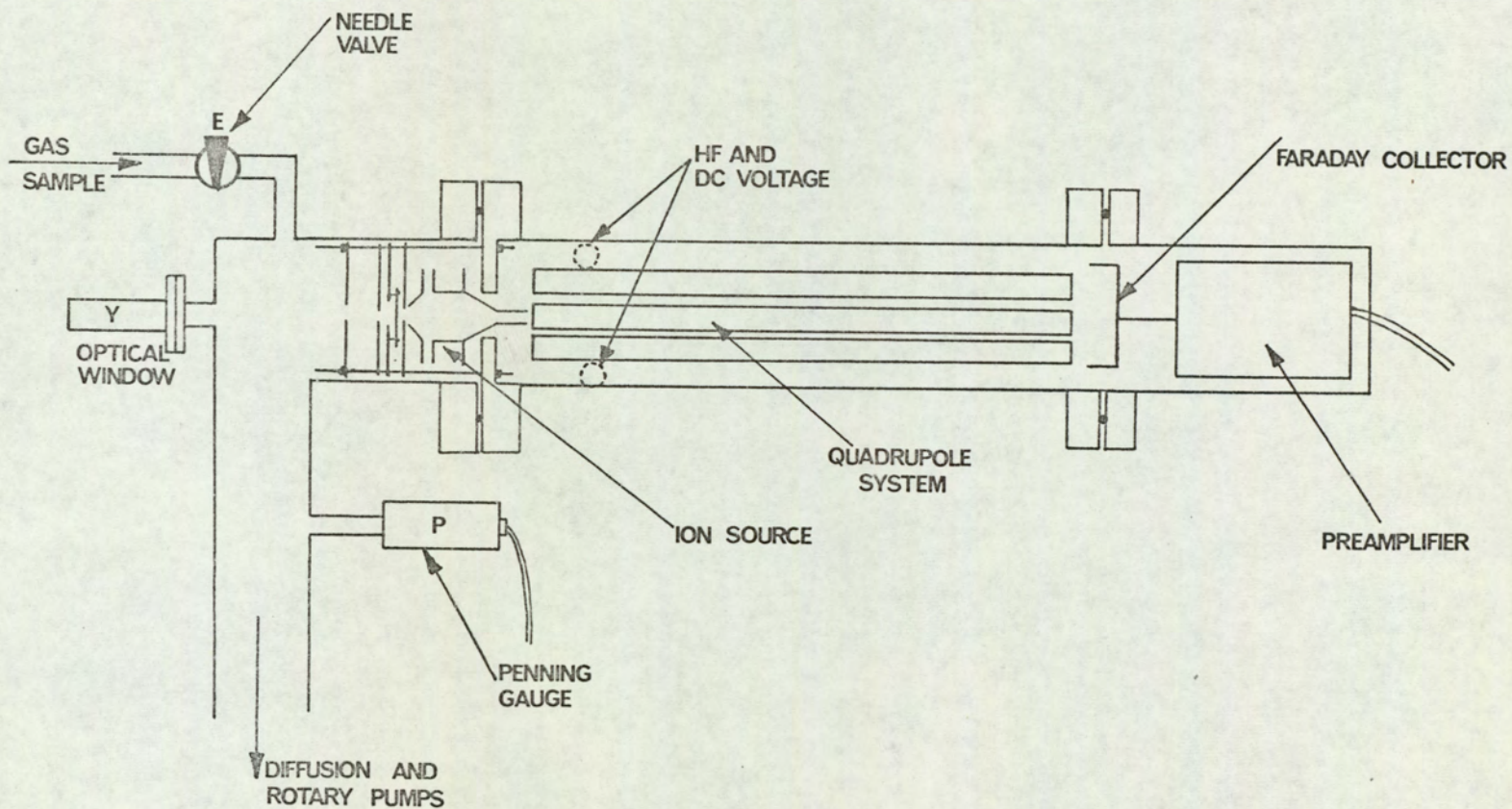


FIG. 38.

needle valve, E, and maintained at approximately 1×10^{-4} Torr; the pressure was measured with the penning gauge, P, supplied with the Atlas Quadrupole Mass Filter.

A $\frac{3}{4}$ " optical window, Y, was mounted via a 'cover' seal and flange to the ion source housing, in direct line with the filament so that the filament temperature could be determined. As in earlier experiments the temperature of the filament was determined by a Leeds and Northrup disappearing filament pyrometer; the experimental temperature was corrected for emissivity and absorption effects as described in 2.3.

The ion source, the quadrupole system and the detection system are discussed below.

Ion Source

The construction of the ion source and filament circuit is shown in figure 39.

All the electrodes were EN 58B polished stainless steel and the ball insulators were alumina. The filament was made as long as possible so that the temperature gradient at the centre of the filament, that is the sampling region, was negligible and the filament was held in position by two 0.01 inch tungsten wire springs, s.

The repeller plate, P, the filament assembly, F, and electrode system were retained in position by means of locating plates L, insulated from each other by glass capillary tubing and mounted on four 10 B.A. stainless steel rods R. The entire ion source assembly was mounted to the Quadrupole housing by the four rods, R, so that the axis of the ion source, BB was located along the centre Z axis of the quadrupole field. The potentials applied to the electrodes were found experimentally to be the optimum values and were supplied by an Exide H1006

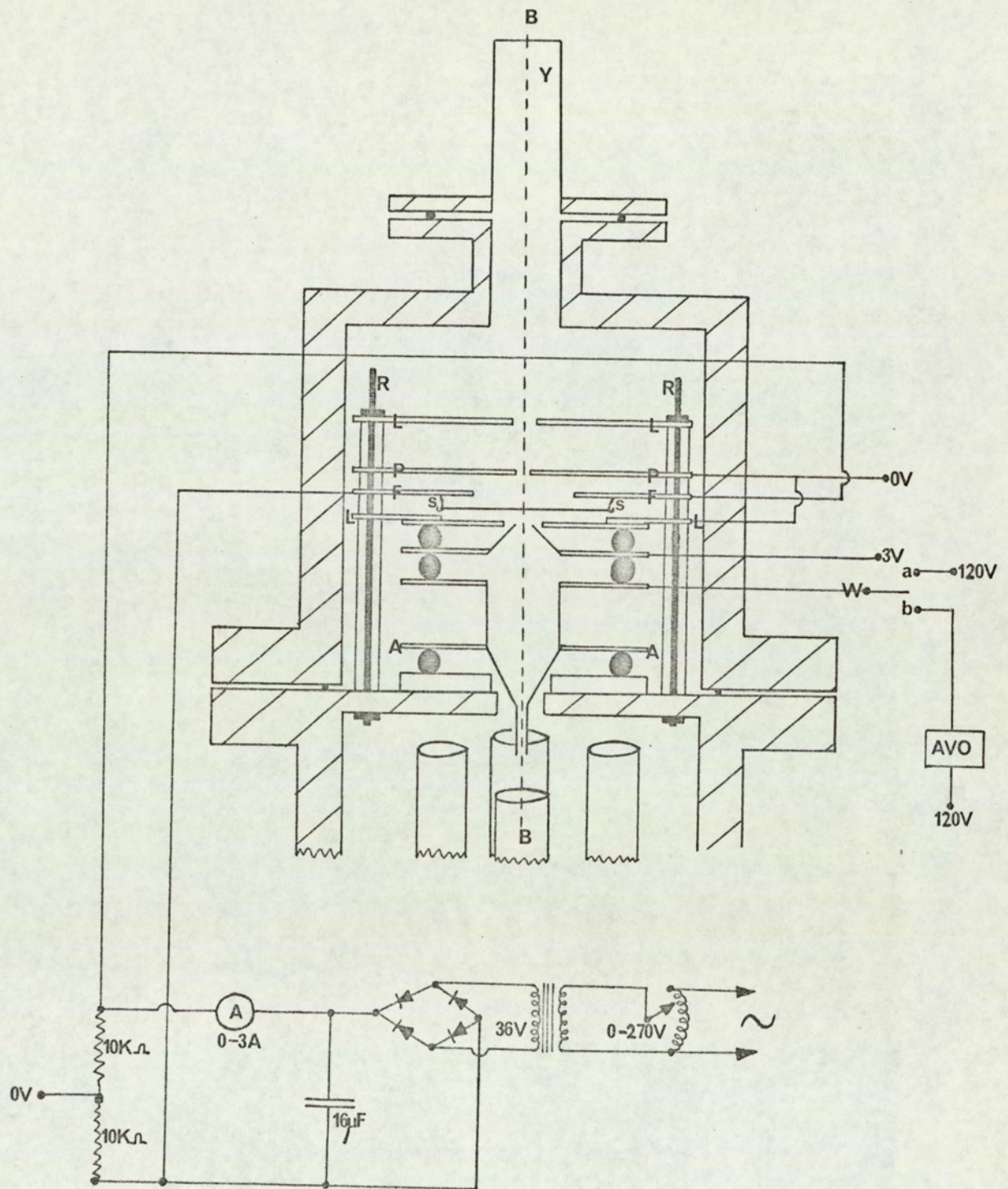


FIG . 39 .

battery.

When the switch, W, was in position b, so that the AVO D.C. amplifier was in circuit and no voltages were applied to the quadrupole rods, the emission current of the filament for a series of filament temperatures was determined. A plot of $\log i_e$ against $10^4/T$, for the case where no gas sample was allowed into the ion source gave a value for the 'clean' work function of the filament surface. The work function of the filament surface in the presence of the gas was then determined in an identical manner.

Whereas when the switch, W, was in position a, that is 120V was directly applied to the final electrode, A, and with the electrical field applied to the quadrupole rods, the ions formed at the filament were accelerated into the quadrupole field and mass analysed.

Quadrupole Mass Filter¹⁵⁷

The construction of the apparatus is as shown in figure 38. The negative ions are formed at the heated filament and are accelerated into the quadrupole field by the electrode system shown in figure 39.

The quadrupole field is generated by four parallel cylindrical rod electrodes to which a direct voltage U, with a superimposed high-frequency, alternating voltage V is applied. In the Quadrupole Mass Filter the ions are situated in an electrical field which is a linear function of its co-ordinates. Such fields are expressed by a potential of the form

$$\phi = \phi_0 (\alpha x^2 + \beta y^2 + \gamma z^2) \quad 6.1.$$

where the x, y and z axes are as shown in figure 40, $\alpha + \beta + \gamma = 0$

when $\Delta\phi = 0$ and in this case $\alpha = -\beta = -1/r_0^2$ and $\gamma = 0$, where $2r_0$ is the

distance between the rod electrodes.

There is a potential $\phi_0 = (U + V \cos wt)$ at the electrodes and the potential ϕ is, therefore, given by

$$\phi = (U + V \cos wt) (x^2 - y^2) / r_0^2 \quad 6.2.$$

The equation of motion for a simply charged ion therefore are

$$m \ddot{x} + 2e (U + V \cos wt) x / r_0^2 = 0 \quad 6.3.$$

$$m \ddot{y} - 2e (U + V \cos wt) y / r_0^2 = 0 \quad 6.4.$$

$$m \ddot{z} = 0 \quad 6.5.$$

Equation 6.5. states that ions injected into the field in the Z-direction will traverse it with uniform velocity in the Z-direction and equations 6.3. and 6.4. describe the oscillations of the ions under the influence of a periodic force. They are known as Mathieu differential equations and by means of the transformations $wt = 2\xi$, $a = 8eU/mr_0^2 \omega^2$ and $q = 4eV/mr_0^2 \omega^2$ they may be simplified to

$$\ddot{x} + (a + 2q \cos 2\xi)x = 0 \quad 6.6.$$

$$\ddot{y} - (a + 2q \cos 2\xi)y = 0 \quad 6.7.$$

The behaviour of the ions is given by the properties of the solutions of these equations of oscillation. Both components of motion obey the same differential equation so that it is sufficient to consider the Mathieu differential equation in its standard form

$$\ddot{x} + (a - 2q \cos 2\xi)x = 0 \quad 6.8.$$

Now, all solutions may be expressed in the form

$$x = \alpha' e^{\mu\xi} \sum_{-\infty}^{+\infty} c_{2s} e^{2is\xi} + \alpha'' e^{-\mu\xi} \sum_{-\infty}^{+\infty} c_{2s} e^{-2is\xi} \quad 6.9.$$

There are consequently two classes of solutions, of which one is considered stable, since for $\xi \rightarrow \infty$, x always remains within a limited

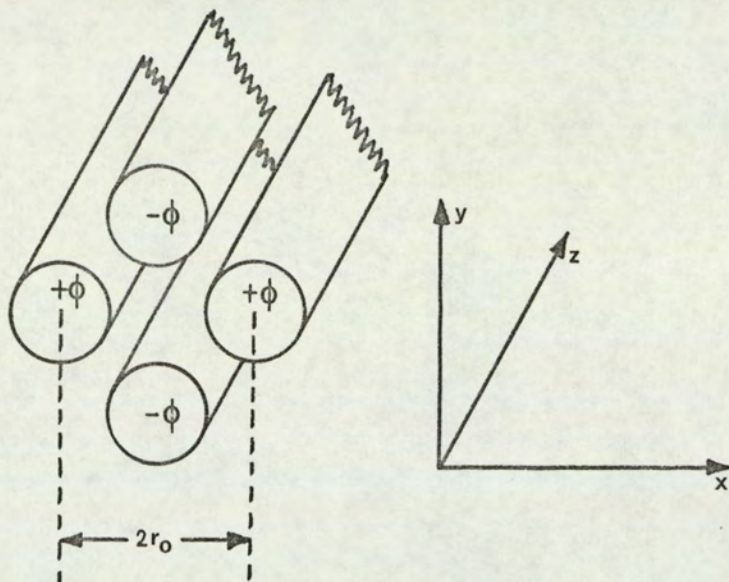


FIG.40.

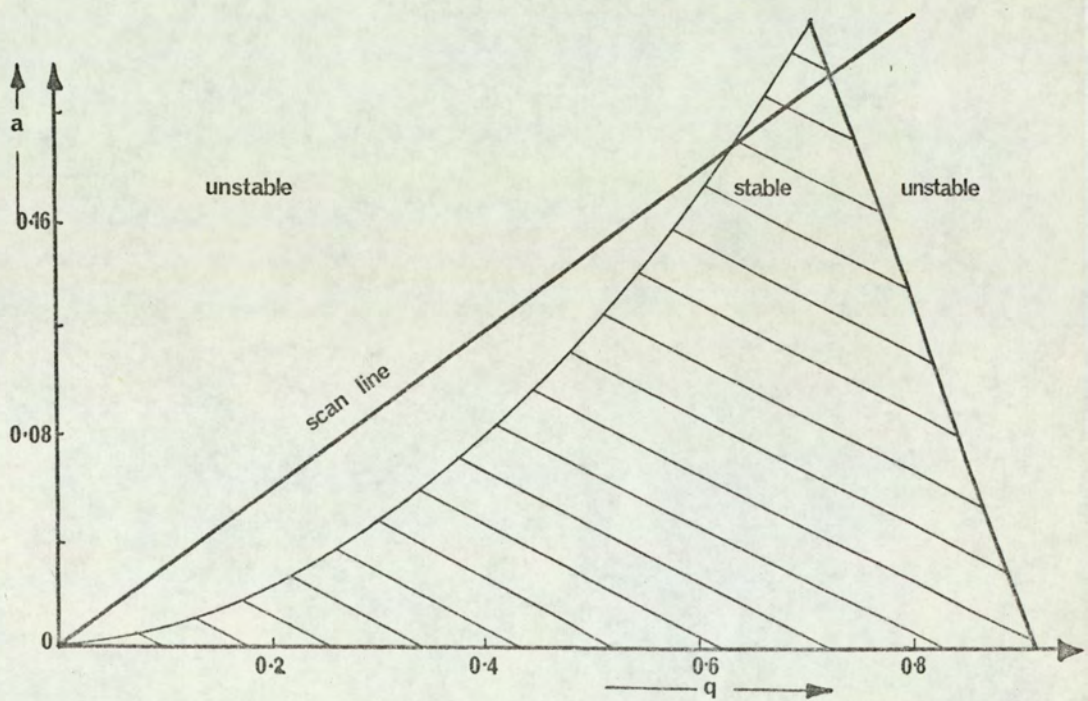


FIG.41.

range, whereas, for the unstable solution with $\xi \rightarrow \infty$, x increases beyond all limits. Which type of solution is given can be judged from the constant μ , which is known as the characteristic exponent and is given unambiguously by a and q . Regions in the (a, q) plane can be given in which all (a, q) values lead to stable solutions and thus the stability diagram shown in figure 41 is obtained for the case of a Quadrupole Mass Filter. The motion of an ion is thus only stable if stable paths are shown for both the x and y components of motion. Hence the working point (a_x, q_x) as well as (a_y, q_y) must lie in the stable region for an ion to be stabilised in the Mass Filter.

All ions of equal mass possess, for the prescribed field values r_0, w, U, V the same working point (a, q) . As the ratio $a/q = 2U/V$ does not depend on the mass, all ions of different mass in the stability diagram lie on a straight line passing through zero, known as the scan line. The gradient of the scan line depends only on the potentials U and V . By increase of the ratio U/V the stable q interval, which corresponds to a definite stable mass interval, may be made so small that only ions of one mass can pass stably through the field. All other ions will move on unstable paths, strike the electrodes and be eliminated.

A mass spectrum is produced by variation of the voltage U and V . If the voltages are increased, the individual mass points run along the scan line in the direction of higher a and q values and traverse the stability region one after another beginning with the small mass numbers.

The ions after mass analysis were detected by a Faraday collector,

the signal was then amplified and the ion current monitored by either an ammeter or recorder.

The experimental procedure followed was to firstly determine the values of the electron current for a series of filament temperatures in the absence and presence of the gaseous sample and hence evaluate the values for the work function of the filament surface in the absence and presence of the gaseous sample. It was found that neither bromine nor tetracyanoethylene had any effect upon the work function of, respectively, tungsten or iridium. Then the instrument was adjusted so that only the ion under investigation was transmitted, and the ion current was determined for a series of filament temperatures. Then from a plot of the logarithm of the ion current against $10^4/T$ the value for $E_T - \chi_T$ was determined since from equation 3.30

$$i_i = (\epsilon dp / 2 \pi M_{AB} K T_g)^{1/2} (Q_i/Q) \exp((E - \chi)/RT)$$

which gave

$$Rd(\log i_i)/d(I/T) = nRT + E - \chi = E_T - \chi_T$$

where the value of n depends on the temperature dependence of Q and Q_i , which in turn is determined by the mode of ion formation as discussed in 3.2.4. However for the special case of a type 1 or type 2 process n is zero and $Rd(\log i_i)/d(I/T) = E - \chi$, which allowed the electron affinity of the species to be calculated as the work function of the surface in the presence of the gas was known.

6.3. Results

Bromine

The filament used was tungsten and the sample pressure was approximately 9×10^{-5} Torr. A negative ion mass spectrum, in the mass range

m/e 0 to 150, gave two peaks of equal intensity at an m/e value of 79 and 81, which were identified as the two isotopes of bromine.

A plot of $\log i_e$ against $10^4/T$ for the tungsten surface, in the presence of bromine gas, gave a work function, χ_T , of 110.0 ± 1.5 kcal/mole, at a mean filament temperature of 1817°K . A plot of $\log i_i/p$ against $10^4/T$ gave values for $E - \chi$ of -29.6, -26.9, -28.3, -29.2, -25.1, -33.3, -29.6, -32.4, -31.0, -26.4, and -30.6 kcal/mole, giving a mean value of -29.3 ± 2.5 kcal/mole, at a mean filament temperature of 1817°K . A typical graph is shown in figure 42.

Tetracyanoethylene

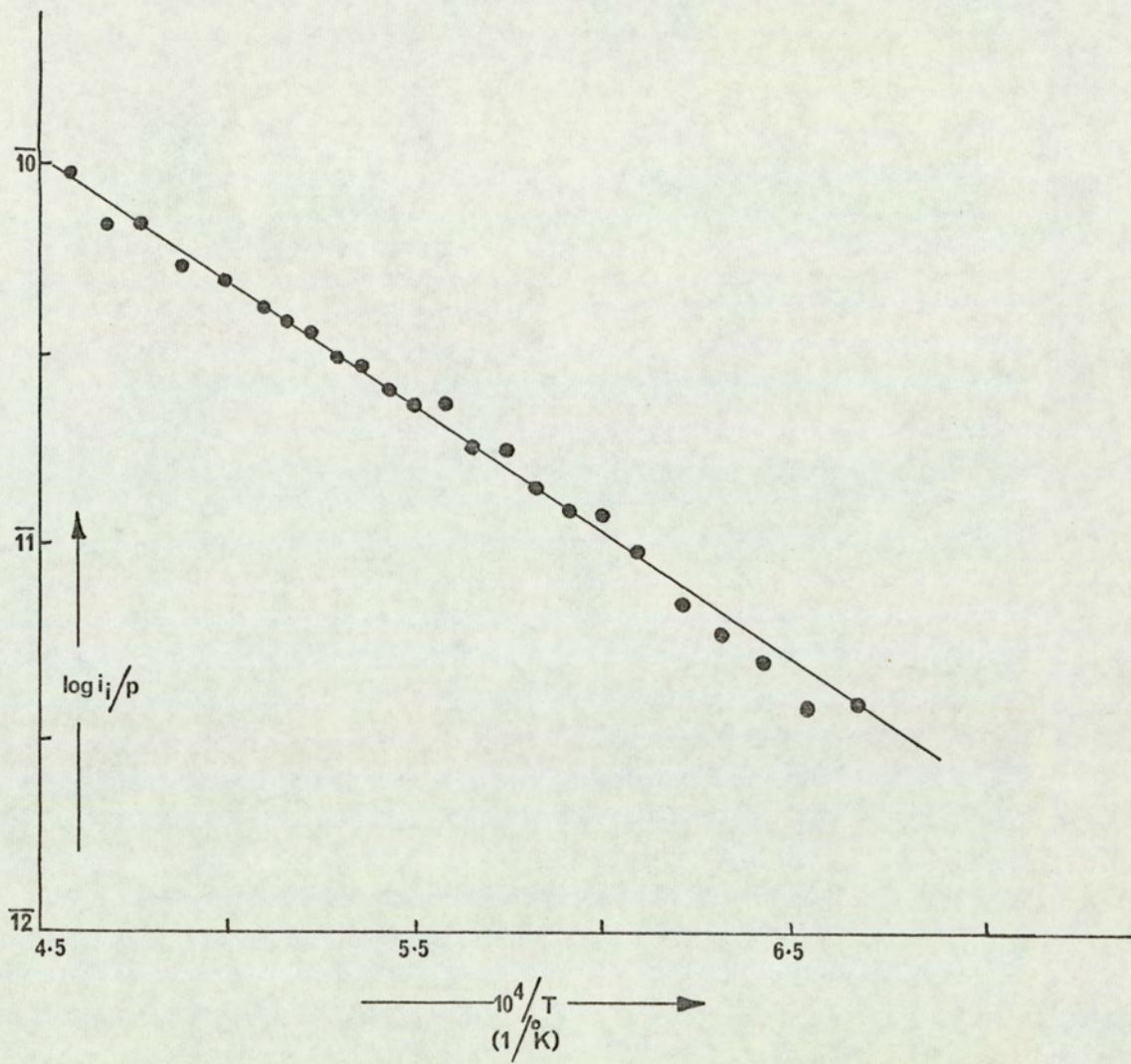
The filament used was iridium and the sample pressure was approximately 1×10^{-5} Torr. A negative ion mass spectrum in the mass range m/e 0 to 150 gave one peak at m/e = 128, which was identified as $\left(\begin{array}{l} \text{CN} \\ \text{CN} \end{array} \right) \text{C} = \text{C} \left(\begin{array}{l} \text{CN} \\ \text{CN} \end{array} \right)^-$. No evidence was found for CN^- or any other fragment ion of tetracyanoethylene in the filament temperature range 1400 - 1800°K .

A plot of $\log i_e$ against $10^4/T$ for the iridium surface in the presence of tetracyanoethylene, at a mean filament temperature of 1640°K gave the work function as 92.0 ± 1.0 kcal/mole. A plot of $\log i_i$ against $10^4/T$ gave values for $E - \chi$ of -15.1, -19.2, -13.9, -15.1, -15.5, -14.2, and -15.5 kcal/mole, which gave a mean value of -15.5 ± 1.7 kcal/mole, at a mean filament temperature of 1640°K . A typical graph is shown in figure 43.

6.4. Discussion

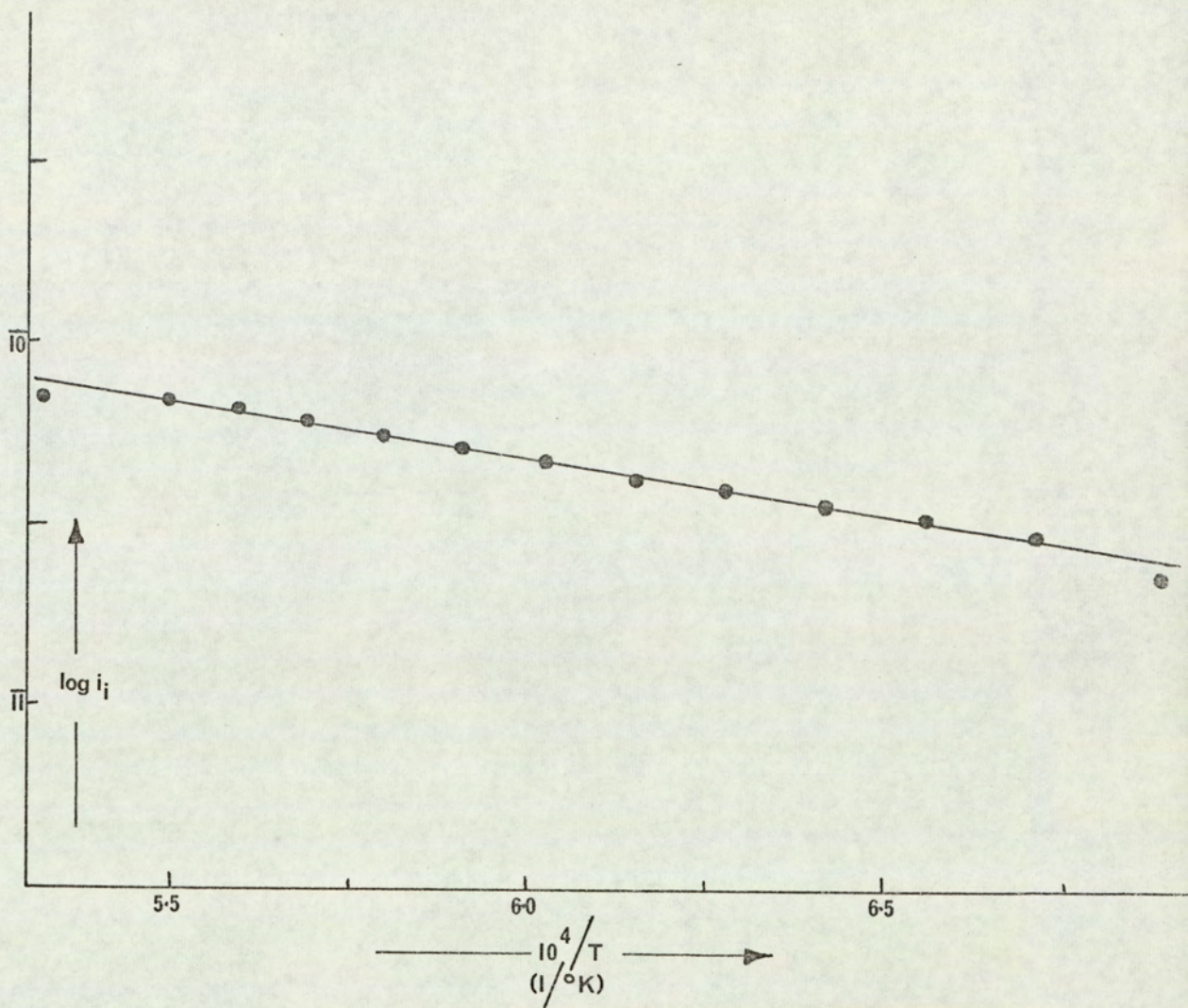
Bromine

From equation 3.17 the experimental work function, χ_T , is given



ELECTRON CAPTURE BY Br_2/W .

FIG. 42.



ELECTRON CAPTURE BY C#N/C=C/C#N / Ir

FIG. 43.

as $\chi_T = \chi + 2RT$. Since χ_T is 110.0 ± 1.5 kcal/mole and T is 1817°K the work function of a tungsten surface in the presence of bromine vapour is 102.8 ± 1.5 kcal/mole.

At filament temperatures in the range $1500\text{--}2200^\circ\text{K}$ bromine is dissociated into bromine atoms and forms bromide ions by the direct capture of an electron. Hence the ion current is given by equation 3.32 as

$$i_i = (A/2) \exp (E - \chi)/RT$$

$$\text{and } Rd (\log i_i)/d(I/T) = E - \chi$$

For bromine, $E - \chi$ is -29.3 ± 2.5 kcal/mole and χ is 102.8 ± 1.5 kcal/mole which gives the value for the electron affinity of a bromine atom as 73.5 ± 4.0 kcal/mole, in good agreement with the spectroscopic value of 77.6 kcal/mole⁷.

Tetracyanoethylene

Since χ_T is 92.0 ± 1.0 kcal/mole and $T = 1640^\circ\text{K}$ the work function, χ , of the iridium surface in the presence of tetracyanoethylene is calculated to be 85.5 ± 1.0 kcal/mole.

The negative ion $\left[\begin{array}{c} \text{CN} \diagdown \\ \text{C} = \text{C} \\ \text{CN} \diagup \end{array} \right]^-$ is formed by the direct capture of an electron by tetracyanoethylene and, therefore, the ion current is given by equation 3.32 as $i_i = (A/2) \exp (E - \chi)/RT$ and $Rd (\log i_i)/d(I/T) = E - \chi$. Since $E - \chi = -15.5 \pm 1.7$ kcal/mole and $\chi = 85.5 \pm 1.0$ kcal/mole the electron affinity of tetracyanoethylene is calculated to be 70.0 ± 2.7 kcal/mole as compared to the value of 65.2 ± 1.5 kcal/mole determined by Farragher.⁸⁷

6.5. Conclusions

The value determined for the electron affinity of a bromine atom of 73.5 ± 4.0 kcals/mole is in agreement, within experimental error, with the spectroscopic value of 77.6 kcals/mole⁷.

Tetracyanoethylene showed no sign of decomposition at filament temperatures in the range 1400-1800°K and only formed the molecular ion. The value determined for the electron affinity of tetracyanoethylene of 70.0 ± 2.7 kcals/mole is in reasonable agreement with the value determined by Farragher⁸⁷ using the Magnetron technique.

In these simple cases, where only one ion is formed by a type 1 or type 2 mechanism the Magnetron technique produces electron affinities in agreement with other workers, and ion formation is well described by the theory postulated by Farragher⁸⁷. However, for more complex systems, where there is a possibility that two or more ions will be formed with similar intensities, a simple "Magnetron" experiment could lead to an oversimplification of the ion-forming reaction. A further study, utilising the Quadrupole Mass Filter as described in 6.2., of all the systems investigated by the Magnetron technique would clarify the mechanisms of the processes occurring and demonstrate the validity of the theoretical models advanced by Farragher⁸⁷.

References

1. Brown, S.C. 'Basic Data of Plasma Physics' (Wiley and Sons Inc. New York 1959).
2. Thomson, J.J. Phil. Mag. 47, 337 (1924).
3. Branscomb, L.M. and Smith, S.J., J.Chem.Phys., 25, 598, (1956).
4. Branscomb, L.M., Burch, D.S., Smith, S.J., and Geltman, S., Phys. Rev. 111, 504 (1958).
5. Seman, M.L. and Branscomb, L.M., Phys. Rev. 125, 1602, (1962).
6. Steiner, B., Seman, M.L. and Branscomb, L.M., J.Chem.Phys., 37, 1200, (1962).
7. Berry, R.S. and Reimann, C.W., J.Chem.Phys., 38, 1540 (1963).
8. Massey, H.S.W. 'Negative Ions' (Cambridge Univ. Press, London and New York, 1950).
9. Farragher, A.L., Page, F.M. and Wheeler, R.C., Disc.Farad.Soc., 37, 203 (1964).
10. Curran, R.K., J.Chem.Phys. 35, 1849 (1961)
Phys.Rev. 125, 910 (1962).
11. Paulson, J.F. 'Ion Molecule Reactions in the Gas Phase' (American Chem.Soc.Pub. Washington 1966).
12. Massey, H.S.W. and Bates, D.R. Astrophys. J. 91, 202 (1940).
13. Chandrasekhar, S. and Minch, G., Astrophys J. 104, 446 (1946).
14. Chandrasekhar, S. and Wildt, R., Astrophys. J., 100, 87 (1944).
15. Mulliken, R.S., J.Chem.Phys. 2, 782 (1934), 3, 573, (1935).
16. Lange, E. Z Electrochem. 56, 94 (1952).
17. Hedges, R.M. and Matsen, F.A., J.Chem.Phys. 28, 950 (1958).
18. Lovelock, J.E., Zlatkis, A., and Becker, R.S., Nature, 193, 540 (1962).
19. Moiseiwitsch, B.L., Adv.Atomic and Mol.Phys. 1, 61 (1965).
20. Born, M., Ber.Deut.Phys.Ges., 21, 13 (1919).
21. Born, M. and Heisenberg, W., Z Physik 23, 388 (1924).

22. Mayer, J.E. and Helmholtz, L., Z Physik, 75, 19 (1932).
23. Verveij, E.J.W. and de Boer, J.H., Rec.Trav.Chim. 55, 431 (1936).
24. Huggins, M.L., J.Chem.Phys. 5, 143, (1937).
25. Kapustinsky, A., Acta Physicochim URSS 18, 370 (1943).
26. Löwdin, P.O., J.Chem.Phys., 18, 365 (1950).
27. Cubicciotti, D., J.Chem. Phys. 31, 1646 (1959)
33, 1579 (1960)
34, 2189 (1961)
28. Hylleraas, E.A., Z Physik 63, 771 (1930)
29. Bichowsky, F.R. and Rossini, F.D. 'The Thermochemistry of the Chemical Substances' (Reinhold New York 1936).
30. Morris, D.F.C. Proc. Roy.Soc. A242, 116 (1957).
Acta Cryst 11, 163 (1958)
31. Sherman, J. Chem. Rev. 11, 93 (1932).
32. Mayer, J.E. and Maltbie, M.M. Z Physik 75, 748 (1932).
33. Baughan, E.C. Trans.Farad.Soc. 55, 736, 2025 (1959).
34. Born, M. and Kornfeld, H. Phys. Z 24, 121 (1923).
35. Kapustinsky, A. Z Physik.Chem. (Leipzig) B22, 257, 261 (1933).
36. Juza, R. Z Anorg. Allgem. Chem. 231, 121 (1937).
37. Nikolskii, G.P., Kazarnovskaya, L.I., Bogda Soryan, Z.A.,
and Kazarnovskii, I.A., Dokl.Akad.Nauk. S.S.S.R.
72, 713 (1950).
38. Yatsimirskii, K.B., J.Gen.Chem. U.S.S.R. (Eng) 17, 2019 (1947).
39. Curran, R.K., Phys.Rev. 125, 910 (1962).
40. Pritchard, H.O., Chem.Rev. 52, 529 (1953).
41. Vedeneyev, V.I., Gurvich, L.V., Kondrat'ev, V.N., Medvedev, V.A.,
and Frankevich, Ye.L. "Bond Energies, Ionization Potentials and Electron Affinities" (Arnold London 1966).
42. Evans, M.G., Hush, N.S., and Uri, N., Quart.Rev., 6, 186 (1952).

43. Burch, D.S., Smith, S.J., and Branscomb, L.M., Phys.Rev. 112, 171, (1958).
44. Glockler, G., Phys. Rev., 46, 111 (1934).
45. Edlén, B., J.Chem.Phys., 33, 98 (1960).
46. Weisner, J.D. and Armstrong, B.H., Proc.Phys.Soc. 83, 31 (1964).
47. Clementi, E. and McLean, A.D., Phys.Rev. 133, A419 (1964).
Clementi, E., McLean, A.D., Raimondi, D.L., and Yoshimine, M., Phys.Rev. 133, A1274 (1964).
48. Pekeris, C.L., Phys.Rev. 126, 1470 (1962).
49. Bates, D.R., Proc.Roy.Irish Acad. A51, 151 (1947).
50. Wu, T-Y. Phil.Mag. 22, 837 (1936).
51. Strotskite, T.D. and Iutsis, A.P., Akad.Nauk Litovskii SSR, Trudy, Ser. B1, 11 (1958).
52. Weiss, A.W., Phys.Rev. 122, 1826 (1961).
53. Eyring, H., Hirschfelder, J.O. and Taylor, H.S., J.Chem.Phys. 4, 479 (1936).
54. McDowell, M.R.C. and Dalgarno, A. Proc., Phys. Soc., A69, 615 (1956).
55. Fischer-Hjalmars, I. Arkiv. Fysik 16, 33 (1959)
J.Chem.Phys. 30, 1099 (1959)
56. Hinze, J.A., Ph.D. Thesis, University of Cincinnati (1962).
Hinze, J.A. and Jaffe, H.H., J.Amer.Chem.Soc. 84, 540 (1962).
57. Knipping, P. Z Physik 7, 328 (1921)
58. Hogness, T.R. and Harkness, R.W. Phys.Rev., 32, 784 (1928).
59. Baker, R.F. and Tate, J.T. Phys. Rev. 53, 683 (1938).
60. Blewett, J.P., Phys. Rev. 49, 900 (1936).
61. Tüxen, O. Z Physik 103, 463 (1936).
62. Dukelskii, V.M. and Ionov, N.I. Doklady Akad. Nauk SSSR 81, 767 (1951).
63. Neuert, H. and Von Trepka, L. Z Naturforsch, 18a, 1295 (1963).

64. Neuert, H., Ebinghaus, H., Kraus, K. and Müller-Duysing, W.,
Z Naturforsch 19a, 732 (1964).
65. Rosenbaum, O., and Neuert, H., Z Naturforsch 9a, 990 (1954).
66. Neuert, H., Z Naturforsch 21a, 501 (1966).
67. Lagergren, C.R. Dissertation Abstr. 16, 770 (1956).
68. Fineman, M.A., and Petrocelli, A.W., J.Chem.Phys., 36, 25 (1962).
69. Craggs, J.D. and Tozer, B.A. Proc.Roy.Soc. A254, 229 (1960).
70. Collin, J. and Lossing, F.P., J.Chem.Phys. 28, 900 (1957).
71. Fox, R.E. J.Chem.Phys., 32, 285 (1960).
72. Randolph, P.L. and Geballe, R. Univ. of Washington. Tech. Rept.
No.6 (1958).
73. Schultz, G.J. and Spence, D., Phys.Rev.Lett. 22, 47 (1969).
74. Rolla, L. and Piccardi, G., Atti acad. Lincei, 2, VI, 29,
128, 173 (1925).
75. Piccardi, G., Atti acad. Lincei, 3, VI, 413, 566 (1926).
76. Piccardi, G., Z Physik, 43, 899 (1927).
77. Rolla, L. and Piccardi, G., Atti acad. Lincei 5, VI, 546 (1927).
78. Dukel'skii, V.M., and Ionov, N.I., J.Exptl. Theoret Phys. U.S.S.R.
10, 1248 (1940)
Ionov, N.I. Compt. rend. acad. sci. URSS 28, 512 (1940).
79. Langmuir, I. and Kingdon, K.H., Proc.Roy.Soc. A107, 61 (1925).
80. Sutton, P.P. and Mayer, J.E., J.Chem.Phys.
2, 145 (1934)
3, 20 (1935)
Doty, P.M. and Mayer, J.E. J.Chem.Phys. 12, 323 (1944).
81. McCallum, K.J. and Mayer, J.E., J.Chem.Phys., 11, 56 (1943).
82. Bernstein, R.B. and Metlay, M., J.Chem.Phys., 19, 1612 (1951).
83. Vier, D.T. and Mayer, J.E., J.Chem.Phys., 12, 28, (1944).
84. Metlay, M. and Kimball, G.E., J.Chem.Phys. 16, 774 (1948).

86. Page, F.M., Trans.Farad.Soc. 56, 1742 (1960)
57, 359 (1961)
57, 1254 (1961)
 Ansdell, D.A. and Page, F.M. Trans.Farad.Soc., 58, 1084 (1962)
 Napper, R., and Page, F.M., Trans.Farad.Soc. 59, 1086 (1963)
87. Farragher, A.L., Ph.D. Thesis, University of Aston in Birmingham, (1966).
88. Burdett, M., Ph.D. Thesis, University of Aston in Birmingham (1968).
89. Parker, P. 'Electronics' (Arnold, London 1963).
90. Tyler, F. 'Intermediate Heat' (Arnold, London 1957).
91. Kaye, G.W.C. and Laby, T.H. 'Tables of Physical and Chemical Constants' (Longmans, Green and Co. Ltd. 1966).
92. Glasstone, S., Laidler, K.J. and Eyring, H. 'The Theory of Rate Processes', (McGraw-Hill, New York, 1941).
93. Dekker, A.J. 'Solid State Physics' (Macmillan and Co. Ltd., London 1963).
94. Fox, R.E. and Hickman, W.M., J.Chem.Phys. 25, 642 (1956).
95. Herron, J.T., Rosenstock, H.M. and Shields, W.R., Nature, 206, 611 (1965).
96. Kay, J. and Page, F.M., Trans.Farad.Soc., 498, 1042, (1964).
97. Gaines, A.F., Kay, J. and Page, F.M., Trans.Farad.Soc. 62, 874 (1966).
98. Kay, J., unpublished work.
99. Hush, N.S. and Segal, G.A., Disc.Farad.Soc., April 1968.
100. Castellan, G.W., 'Physical Chemistry' (Addison-Wesley Reading, U.S.A.).
101. O'Donnell, T.A. and Stewart, D.F., Inorg.Chem., 5, 1434, 1438, (1966).
102. Geichman, J.R., Smith, E.A., Trond, S.S., and Ogle, P.R. Inorg.Chem. 1, 661 (1962).
103. Bartlett, N., Beaton, S.P. and Jha, N.K., Chem.Comm. 6, 168 (1966)
104. Field, F.H. and Franklin, J.L. 'Electron Impact Phenomena' (Academic Press, New York 1957).

105. Johnston, H.S. and Bertin, H.J., J.Amer.Chem.Soc. 81, 6402 (1959).
106. Cottrell, T.L. 'The strength of Chemical Bonds' (Butterworths, London, 1958).
107. Heslop, R.B. and Robinson, P.L., 'Inorganic Chemistry' (Elsevier Pub. Co. Inc., 1963).
108. Cotton, F.A. and Wilkinson, G. 'Advanced Inorganic Chemistry' (Interscience Publishers, 1962).
109. Goddard, W.A., Phys.Rev. 172, 7 (1968).
110. Rohrlich, F., Phys.Rev. 101, 69 (1956).
111. Smith, L.G., Phys.Rev. 51, 263 (1937).
112. Page, F.M., Proc. 8th Symp. Combustion, 57, (1958).
113. Gaines, A.F. and Page, F.M., Trans.Farad.Soc., 59, 1266 (1963).
114. Conant, J.B. and Wheland, G.W., J.Amer.Chem.Soc., 54, 1212 (1932).
115. Bailey, T.L., McGuire, J.M. and Muschlitz, E.E., J.Chem.Phys., 22, 2088, (1954).
116. Melton, C. and Rudolph, P., J.Chem.Phys. 31, 1485 (1959).
117. Green, J.A., AGARD Conf. Proc. c.p. 8 1, 191 (Sept. 1965).
- 117a. Fomenko, V.S. 'Handbook of Thermionic Properties' (Plenum Press Data Division, New York, 1966)
118. Little, L.H., Sheppard, N. and Yates, D.J.C., Proc.Roy.Soc., A259, 242 (1960).
119. Hamilton, W.M. and Burwell, R.L., Proc. 2nd International Congress on Catalysis, 1, 987, (1961).
120. Robertson, A.J.B., Adv. in Mass Spectrometry, P.559 (Ed. Waldron, Pergamon Press 1959).
121. Le Goff, P. Thèse Université de Nancy (1955).
122. Schexnayder, C.J. Nasa Technical Note (May 1963).
123. Tiernan, T.O. and Hughes, B.M., 17th Conf. on Mass Spectrometry and allied topics (Dallas U.S.A. 1969).

124. Neuert, H., private communication.
125. Coulson, C.A., Victor Henri Memorial Volume Liège (1948).
126. Walsh, A.D., Disc.Farad.Soc., 2, 18 (1947).
127. Gaydon, A.G. and Wolfhard, H.G., 'Flames, their structure, radiation and temperature' (Chapman and Hall, 1953).
128. Bibby, M.M. and Carter, G., Trans.Farad.Soc., 59, 2455 (1963).
129. Hickam, W.M. and Berg, D., Adv. in Mass Spectrometry P.458 (Ed. Waldron, Pergamon Press, 1959).
130. Coomber, J.W. and Whittle, E., Trans.Farad.Soc., 63, 1394, (1967).
131. Coomber, J.W. and Whittle, E., Trans.Farad.Soc., 63, 2656, (1967).
132. Coomber, J.W. and Whittle, E., Trans.Farad.Soc., 63, 608, (1967).
133. 'Janaf Thermochemical data' (The Dow Chemical Co., Thermal Laboratory, Michigan).
134. Melton, C.E. and Emmett, P.H., J.Phys.Chem. 68, 3318, (1964).
135. Robertson, A.J.B. and Willhoft, E.M.A., Trans.Farad.Soc., 63, 476 (1967).
136. Apel'baum, L.O. and Temkin, M.I. Russ.J.Physic.Chem. 33, 585 (1959).
137. see reference 64.
138. Szwarc, M., Proc.Roy.Soc. A198, 267, (1949).
139. Ramsay, D.A., J.Phys.Chem. 57, 415, (1953).
140. Altshuller, A.P., J.Chem.Phys., 22, 1947 (1954).
141. Collin, J.E., Hubin-Franskin, M.J. and d'Or, L., Int. Mass Spectrometry Conf. (Berlin 1967).
142. Gowenlock, B.G., Jones, P.P. and Snelling, D.R., Can.J.Chem., 41, 1911, (1963).
143. Gattermann, L., 'Laboratory Methods of Organic Chemistry' P.355 (Macmillan, London 1948).
144. Evers, E.C. and Street, E.H., J.Amer.Chem.Soc., 78, 5726, (1956)
145. Gaines, A.F. and Page, F.M., Trans.Farad.Soc., 62, 3086, (1966).

146. Smith, J.W. 'Electric Dipole Moments' (Butterworths Scientific Publications 1955).
147. Johnson, W.H., Prosen, E.J. and Jaffe, I., J.Res.Natl.Bur.Std., A65, 71, (1961).
148. Kerr, J.A., Trotman-Dickenson, A.F., and Wolter, M., J.Chem.Soc., 3584, (1964).
149. Gowenlock, B.G., Pritchard Jones, P., and Majer, J.R., Trans. Farad.Soc., 57, 23 (1961).
150. Dibeler, V.H., Franklin, J.L. and Reese, R.M., J.Amer.Chem.Soc., 81, 68 (1959).
151. Gray, P., Jones, A. and Thynne, J.C.J., Trans.Farad.Soc., 61, 474, (1965).
152. Fessenden, R.W. and Shuler, R.H., J.Chem.Phys., 43, 2704, (1965).
153. Carlson, G.A. and Pimentel, G.E., J.Chem.Phys., 44, 4053, (1966).
154. Peters, D., J.Chem.Soc., 3, 2901, (1964).
155. Page, F.M. and Goode, G.C. 'Negative Ions and the Magnetron' (John Wiley and Sons, 1969).
156. Kay, J. and Page, F.M., Nature, 199, 483 (1963).
157. Paul, W., Reinhard, H.P. and von Zahn, U Z für Phys., 152, 143, (1958).